



1986

Contaminant migration of oil-and-gas drilling fluids within the glaciated sediments of north-central North Dakota

William A. Beal
University of North Dakota

Follow this and additional works at: <https://commons.und.edu/theses>

 Part of the [Geology Commons](#)

Recommended Citation

Beal, William A., "Contaminant migration of oil-and-gas drilling fluids within the glaciated sediments of north-central North Dakota" (1986). *Theses and Dissertations*. 14.
<https://commons.und.edu/theses/14>

This Thesis is brought to you for free and open access by the Theses, Dissertations, and Senior Projects at UND Scholarly Commons. It has been accepted for inclusion in Theses and Dissertations by an authorized administrator of UND Scholarly Commons. For more information, please contact zeinebyousif@library.und.edu.

CONTAMINANT MIGRATION OF OIL-AND-GAS
DRILLING FLUIDS WITHIN THE GLACIATED SEDIMENTS
OF NORTH-CENTRAL NORTH DAKOTA

By

William A. Beal

Bachelor of Science, Geological Engineering

University of North Dakota, 1983

A Thesis

Submitted to the Graduate Faculty

of the

University of North Dakota

in partial fulfillment of the requirements

for a degree of

Master of Science

Grand Forks, North Dakota

August, 1986

GEO
T1966
B364

This Thesis, submitted by William A. Beal in partial fulfillment of the requirements for the Degree of Master of Science from the University of North Dakota has been read by the Faculty Advisory Committee under whom the work has been done, and is hereby approved.

Alan E. Keher
(Chairperson)

Paul V. Bennett

John R. Reid

This thesis meets the standards for appearance and conforms to the style and format requirements of the Graduate School of the University of North Dakota, and is hereby approved.

Dean of the Graduate School

Title Contaminant Migration of Oil-and-Gas Drilling Fluids
Within the Galciated Sediments of North-Central
North Dakota

Department Geology

Degree Master of Science

In presenting this thesis in partial fulfillment of the requirements for a graduate degree from the University of North Dakota, I agree that the Library of the University shall make it freely available for inspection. I further agree that permission for extensive copying for scholarly purposes may be granted by the professor who supervised my thesis work, or in his absence, by the Chairman of the Department or the Dean of the Graduate School. It is understood that any copying or publication or other use of this thesis or part thereof for financial gain shall not be allowed without my written permission. It is also understood that due recognition shall be given to me and to the University of North Dakota in any scholarly use which may be made of any material in my thesis.

Signature *William A. Beard*

Date June 23, 1986

TABLE OF CONTENTS

	<u>PAGE</u>
LIST OF ILLUSTRATIONS	vi
LIST OF TABLES	xi
ACKNOWLEDGEMENTS	xii
ABSTRACT	xiv
1.0 INTRODUCTION	1
1.1 Description of Problem	
1.2 Drilling Fluid	
1.3 Drilling Fluid Disposal and Pit Reclamation	
1.4 Previous Work	
1.5 Study Sites	
1.6 Geology	
1.7 Groundwater Resources	
1.8 Climate	
1.9 Objectives	
2.0 METHODS	22
2.1 Field Methods	
2.2 Laboratory Methods	
3.0 RESULTS	33
3.1 Local Geologic and Hydrogeologic Setting	
3.1.1 J.J. Winderl No. 1	
3.1.2 Fossum Federal No. 4	
3.2 Sediment Analysis	
3.3 Hydraulic Conductivity	
3.4 Apparent Resistivity	
3.4.1 J.J. Winderl No. 1	
3.5 Groundwater Chemistry	
3.5.1 J.J. Winderl No. 1	
3.5.2 Fossum Federal No. 4	
3.6 Saturated-Paste Extract	
3.7 XRF Experiment	
4.0 DISCUSSION	99
4.1 Characterization of Contaminant	
4.2 Solute Transport	
4.2.1 J.J. Winderl No. 1	
4.3 Geochemical Processes	
4.4 Distribution and Extent of Contamination	
4.4.1 J.J. Winderl No. 1	
4.4.2 Fossum Federal No. 4	
4.5 Evaluation of Disposal Practices	
5.0 CONCLUSIONS	124

TABLE OF CONTENTS (CONT.)

	<u>PAGE</u>
APPENDICES	126
Appendix A. Elevations of Piezometers, depths to screened intervals, and depths of lysimeters	
Appendix B. Slug test procedure	
Appendix C. Textural analysis procedure	
Appendix D. Sample preparation technique for x-ray fluorescence	
Appendix E. Saturated-paste extract analysis procedure	
Appendix F. Driller lithologic log	
Appendix G. Lithologic description of Shelby tube samples	
Appendix H. Results of textural analyses	
Appendix I. Hydraulic conductivity values from slug test data	
Appendix J. Grain size distribution curves	
Appendix K. Apparent and interrupted resistivity profiles at the Winderl and Fossum study sites	
Appendix L. Isoresistivity maps	
Appendix M. Groundwater and pore water chemistry	
Appendix N. Saturated-paste extract chemical analyses	
Appendix O. X-ray fluorescence analyses	
REFERENCES	239

LIST OF ILLUSTRATIONS

	<u>PAGE</u>
Figure 1. The boundaries of the Williston Basin	3
Figure 2. Oil fields in North Dakota	5
Figure 3. Location of the buried drilling fluid disposal sites . .	15
Figure 4. Geologic map of the study area	19
Figure 5. Piezometer and pressure-vacuum lysimeter profiles . . .	24
Figure 6. Configuration of the four electrode array used in the electrical earth resistivity surveys	29
Figure 7. Map view of the Winderl site depicting the location of water sampling instrumentation and Shelby tube holes . .	35
Figure 8. Geologic fence diagram of the Winderl site	37
Figure 9. Water table maps of the Winderl site	40
Figure 10. Map view of the Fossum site depicting the location of water sampling instrumentation and Shelby tube holes . .	42
Figure 11. North-south stratigraphic cross-section of the Fossum site depicting selected water sampling instrumentation .	44
Figure 12. Potentiometric maps of the till unit at the Fossum site.	47
Figure 13. The United States Department of Agriculture textural classification of the till samples from the Fossum site.	50
Figure 14. Map view of the Winderl site showing the locations of the resistivity stations	55
Figure 15. Map view of the Fossum site showing the locations of the resistivity stations	57
Figure 16. Apparent iso-resistivity maps at the Winderl site for electrode spacings of 16 and 40 feet (4.8 and 12.2 m) . .	59
Figure 17. Apparent iso-resistivity maps at the Fossum site for electrode spacings of 12 and 40 feet (3.7 and 12.2 m) . .	62
Figure 18. Concentration profiles of total dissolved solids, chloride, sodium, calcium, chromium, and lead in piezometers WP-1 and WP-4 at the Winderl site	67

LIST OF ILLUSTRATIONS (CONT.)

	<u>PAGE</u>
Figure 19. Concentration profiles of total dissolved solids, chloride, sodium, calcium, chromium, and lead in piezometers WP-8 and WP-14 at the Winderl site	69
Figure 20. Concentration profiles of total dissolved solids, chloride, sodium, calcium, chromium, and lead in piezometers WP-15 and WP-18 at the Winderl site	71
Figure 21. Concentration profiles of total dissolved solids, chloride, sodium, calcium, chromium, and lead in piezometers WP-23 and WP-27 at the Winderl site	73
Figure 22. Piezometer location map and isoconcentration maps of total dissolved solids, chloride, and sodium in groundwater at the Winderl site	76
Figure 23. Isoconcentration maps of calcium, magnesium, chromium, and lead in groundwater at the Winderl site	78
Figure 24. Concentration profiles of total dissolved solids, chloride, sodium, calcium, sulfate, and chromium in groundwater in piezometers FP-1 and FP-3 at the Fossum site	82
Figure 25. Concentration profiles of total dissolved solids, chloride, sodium, calcium, sulfate, and chromium in groundwater in piezometers FP-5 and FP-7 at the Fossum site	84
Figure 26. Concentration profiles of total dissolved solids, chloride, sodium, calcium, sulfate, and chromium in groundwater in piezometers FP-9 and FP-12 at the Fossum site	86
Figure 27. Piezometer location map and isoconcentration maps of total dissolved solids, chloride, and sodium in groundwater at the Fossum site	88
Figure 28. Isoconcentration maps of calcium, magnesium, sulfate, and chromium in groundwater at the Fossum site	90
Figure 29. Concentration profiles of electrical conductivity, chloride, sodium, magnesium, and sulfate from saturated extract analyses of Shelby tube samples FS-2 and FS-3 at the Fossum site	93

LIST OF ILLUSTRATIONS (CONT.)

	<u>PAGE</u>
Figure 30. Concentration profiles of electrical conductivity, chloride, sodium, magnesium, and sulfate from saturated extract analyses of Shelby tube samples FS-5 and FS-6 at the Fossum site	95
Figure 31. Concentration profiles of electrical conductivity, chloride, sodium, magnesium, and sulfate from saturated extract analyses of Shelby tube samples FS-7 at the Fossum site	97
Figure 32. Hypothetical breakthrough curves at the Winderl site for the transport of non-reactive solutes at dispersivities of 1 m, 25 m, and 100 m	105
Figure 33. Northeast-southwest and northwest-southeast cross-sections of Dar Zarrouk interpreted resistivity and isoconcentration map of total dissolved solids in groundwater at the Winderl site	112
Figure 34. Chloride concentrations in porewater and shallow groundwater at the Fossum site	117
Figure 35. Cross-section showing chloride concentrations taken from saturated paste extracts of sediment at the Fossum site	120
Figure 36. Grain size distribution curves for sediments samples from the Winderl site	157
Figure 37. Apparent and interpreted resistivity profiles for stations 1-4 at the Winderl study site	160
Figure 38. Apparent and interpreted resistivity profiles for stations 5-8 at the Winderl study site	162
Figure 39. Apparent and interpreted resistivity profiles for stations 9-12 at the Winderl study site	164
Figure 40. Apparent and interpreted resistivity profiles for stations 13-16 at the Winderl study site	166
Figure 41. Apparent and interpreted resistivity profiles for stations 17-20 at the Winderl study site	168
Figure 42. Apparent and interpreted resistivity profiles for stations 21-24 at the Winderl study site	170

LIST OF ILLUSTRATIONS (CONT.)

	<u>PAGE</u>
Figure 43. Apparent and interpreted resistivity profiles for stations 25-28 at the Winderl study site	172
Figure 44. Apparent and interpreted resistivity profiles for stations 29 and 30 at the Winderl study site	174
Figure 45. Apparent and interpreted resistivity profiles for stations 1-4 at the Fossum study site	176
Figure 46. Apparent and interpreted resistivity profiles for stations 5-8 at the Fossum study site	178
Figure 47. Apparent and interpreted resistivity profiles for stations 9-12 at the Fossum study site	180
Figure 48. Apparent and interpreted resistivity profiles for stations 13-16 at the Fossum study site	182
Figure 49. Apparent and interpreted resistivity profiles for stations 17-20 at the Fossum study site	184
Figure 50. Apparent and interpreted resistivity profiles for stations 21-24 at the Fossum study site	186
Figure 51. Apparent and interpreted resistivity profiles for station 25 at the Fossum study site	188
Figure 52. Location map for resistivity stations and iso-resistivity maps for electrode spacings of 3, 5, and 8 feet (0.9, 1.5, and 2.4 m) at the Winderl site	191
Figure 53. Apparent iso-resistivity maps for electrode spacings of 10, 12, 16, and 20 feet (3.05, 3.7, 4.9, and 6.1 m) at the Winderl site	193
Figure 54. Apparent iso-resistivity maps for electrode spacings of 24, 30, 40, and 50 feet (7.3, 9.1, 12.2, and 15.2 m) at the Winderl site	195
Figure 55. Apparent iso-resistivity maps for electrode spacings of 60, 80, and 100 feet (18.3, 24.4, and 30.5 m) at the Winderl site	197
Figure 56. Resistivity station map and iso-resistivity maps of 3, 5, and 8 feet (0.9, 1.5, and 2.4 m) at the Fossum site	199

LIST OF ILLUSTRATIONS (CONT.)

	<u>PAGE</u>
Figure 57. Isoresistivity maps for electrode spacings of 10, 12, 16, and 20 feet (3.1, 3.7, 4.9, and 6.1 m) at the Fossum site	201
Figure 58. Isoresistivity maps for electrode spacings of 24, 30, 40, and 50 feet (7.3, 9.1, 12.2, and 15.2 m) at the Fossum site	203

LIST OF TABLES

	<u>PAGE</u>
Table 1. Function and general purpose of drilling fluid additives	8
Table 2. X-ray diffraction analyses of clay samples from till at the study sites	51
Table 3. Chemical analyses of groundwater samples from piezometers WP-3 and WP-11 at the Winderl site and the nearby Stevan's farm well	64
Table 4. Chemical analyses of pore water/groundwater from lysimeters FL-1 and FL-9 at the Fossum site	79
Table 5. Chemical analyses of brines from the Madison Formation in the Wylie Field, Bottineau County	100

ACKNOWLEDGEMENTS

This research was supported by North Dakota Water Resources Research Institute Grant No. 5850-4138-6671 through the North Dakota Mining and Mineral Resources Research Institute.

I would like to thank my committee chairman Dr. Alan E. Kehew, and committee members Dr. John Reid and Dr. Gerald H. Groenewold. They were very cooperative and went out of their way to ensure the successful completion of this project.

I especially appreciate the efforts of Edward C. Murphy, the project Principal Investigator. His support, guidance, and friendship were invaluable.

The North Dakota Geological Survey provided vehicle support, including a truck-mounted auger and a geophysical logging van. Mr. Kenneth L. Dorsher, a NDGS employee, drafted the diagrams, and Mr. David O. Lechner, also of the NDGS, helped with the field work and conducted the textural analyses.

I would like to thank Mrs. Marie Weber for allowing me to study the Winderl site. I also wish to thank Mr. Roy Johnson of the North Dakota State University Development Foundation for allowing access to the Fossum Farm, and Mr. Randy Brant, who is renting the area around the Fossum study site. I would also like to acknowledge the cooperation of Chevron, U.S.A., Inc.

I would like to thank Dr. Eugene C. Doll and Dr. Nyle Wollenhaupt for analyzing sediment samples at the North Dakota State University Land Reclamation Research Center in Mandan.

Finally, I express my deepest thanks to my parents and family.
Without their support and encouragement, I never would have been able to
obtain my graduate degree.

ABSTRACT

A common practice during oil and gas well-site reclamation in North Dakota is to bury the drilling muds in shallow trenches near the borehole. These muds are saltwater based (between 100,000 and 300,000 mg/L of NaCl) and can contain high concentrations of chromium, lead, and other toxic trace metals.

Two reclaimed oil and gas well sites were chosen for study in north-central North Dakota: the Winderl site in southeastern Renville County, and the Fossum site in west-central Bottineau County. The Winderl oil well was drilled in 1959, and the drilling fluids were disposed of in a shallow pit excavated in Pleistocene glaciofluvial deposits. The Fossum oil well was drilled in 1978 and the drilling fluids were disposed of in trenches excavated in Pleistocene till.

A total of 41 shallow piezometers (maximum depth is 62 feet (18.9 m)) and 13 pressure-vacuum lysimeters were installed in and around the two disposal sites to obtain groundwater and pore-water samples. Vertical electrode sounding resistivity profiles were conducted at both sites utilizing 14 electrode spacings down to a depth of 100 feet (30.5 m). Sediment samples were obtained with Shelby tubes for x-ray fluorescence and x-ray diffraction analyses. Additional chemical analyses were performed on saturated-paste extracts from the Shelby-tube samples.

The results of chemical analyses of pore water, groundwater, saturated-paste extracts, and the earth resistivity surveys indicate that leachate is being generated from buried drilling fluid at both study

sites. At the Winderl site, contaminants have migrated beyond 400 feet (122 m), the extent of the monitored area, which has resulted in degradation of the Spring Coulee Creek Aquifer. A one-dimensional analytical solute transport equation was utilized to illustrate the potential for contaminant migration at the site. The equation predicts high concentration of contaminants over 3300 feet (1000 m) from the source area.

Contaminant migration within the till at the Fossum site is believed to occur along fractures directly below the water table. The estimated groundwater velocity through these fractures is 3.8 m/day (12.8 ft/day) compared to 7.2×10^{-7} (2.4×10^{-6} ft/day) estimated for the till matrix. However, it has been reported that molecular diffusion is an important retardation mechanism that reduces the concentration of contaminants along these fractures with distance from the source. Also, the fractures constitute a small volume of pore space; therefore, the quantity (or flux) of water flowing along the fractures is small.

Disposal of drilling fluids in glaciofluvial sediments is not recommended. The study at the Winderl site is evidence of the adverse environmental impact such disposal can lead to. The impact of drilling fluid disposal in till is dependent upon the geologic setting. Migration of the drilling fluid constituents will occur along fractures in the till; widespread contamination could result if these contaminants intersect permeable lenses. A subsurface investigation is necessary at the disposal sites in till to identify these permeable lenses and to determine if any nearby aquifers exist.

1.0 INTRODUCTION

1.1 Description of Problem

North Dakota's oil and gas production comes from the Williston Basin--a structural and sedimentary basin located in North Dakota, South Dakota, Montana and southern Canada (Figure 1). Since oil was first discovered in North Dakota in 1951, approximately 10,000 wells have been drilled in the western and north-central portions of the state (Figure 2). During the 1981-83 biennium, taxes collected on oil and gas production became North Dakota's single most important tax revenue (Anderson and Bluemle, 1984).

A problem inherent to the oil industry is the disposal of wastes associated with the drilling process. One such waste is drilling mud, a viscous fluid used during well drilling. A common practice during well-site reclamation is to dispose of drilling muds in shallow trenches and pits near the borehole. Murphy and Kehew (1984) conducted a study of the subsurface migration of drilling-fluid waste components beneath these buried disposal pits. The results of that study indicate that most of the hazardous constituents are attenuated within the unsaturated zone. However, other contaminants such as Na, Ca, and Cl move rapidly through the unsaturated zone and into the groundwater flow system (Murphy and Kehew, 1984).

The disposal sites monitored by Murphy and Kehew (1984) are in western North Dakota and underlain by poorly indurated clayey bedrock or sediments derived from the bedrock. The lithologic and hydrologic properties of these sediments significantly decrease the potential for

Figure 1. The boundaries of the Williston Basin (from Anderson and Bluemle, 1984).

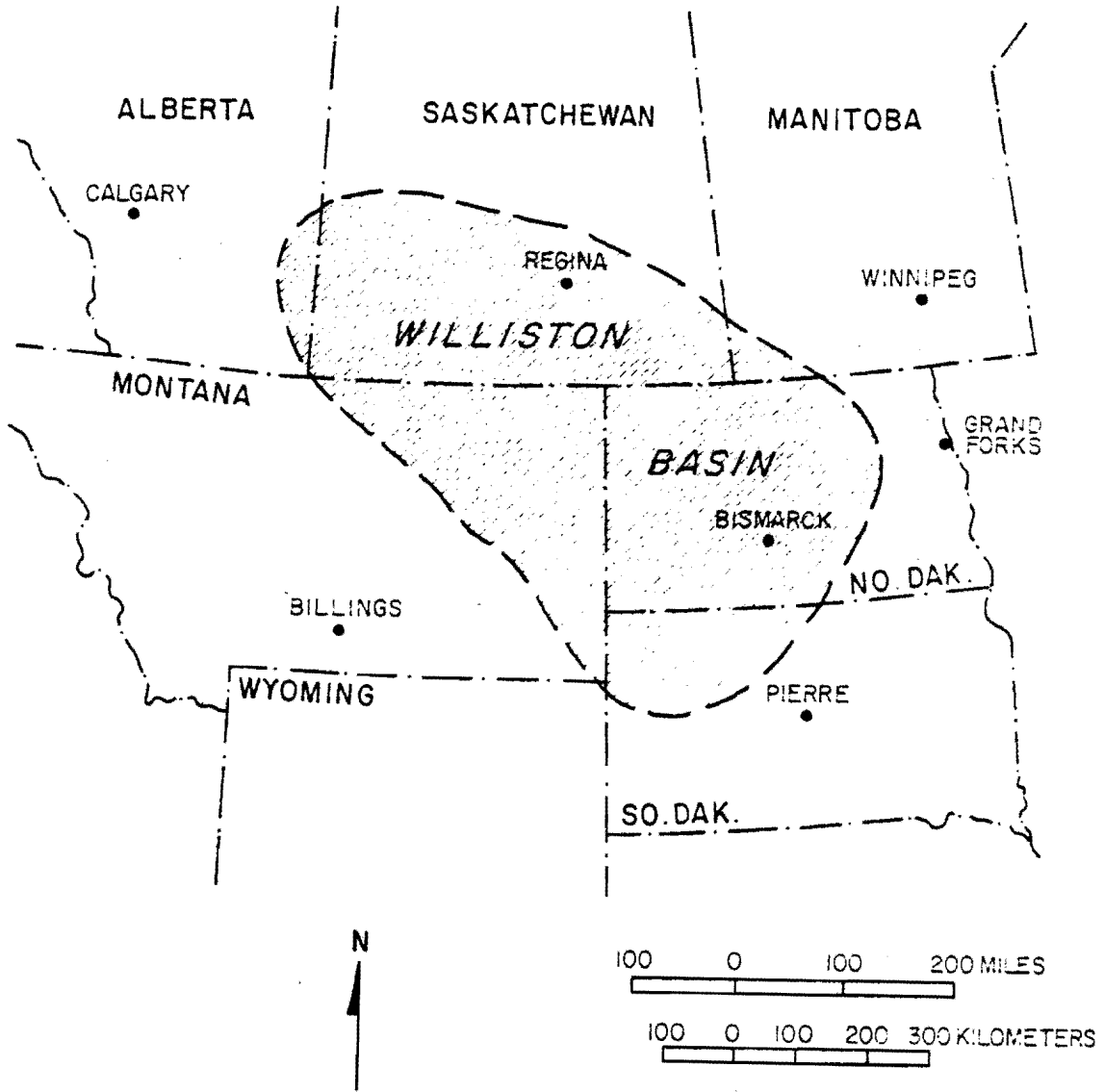
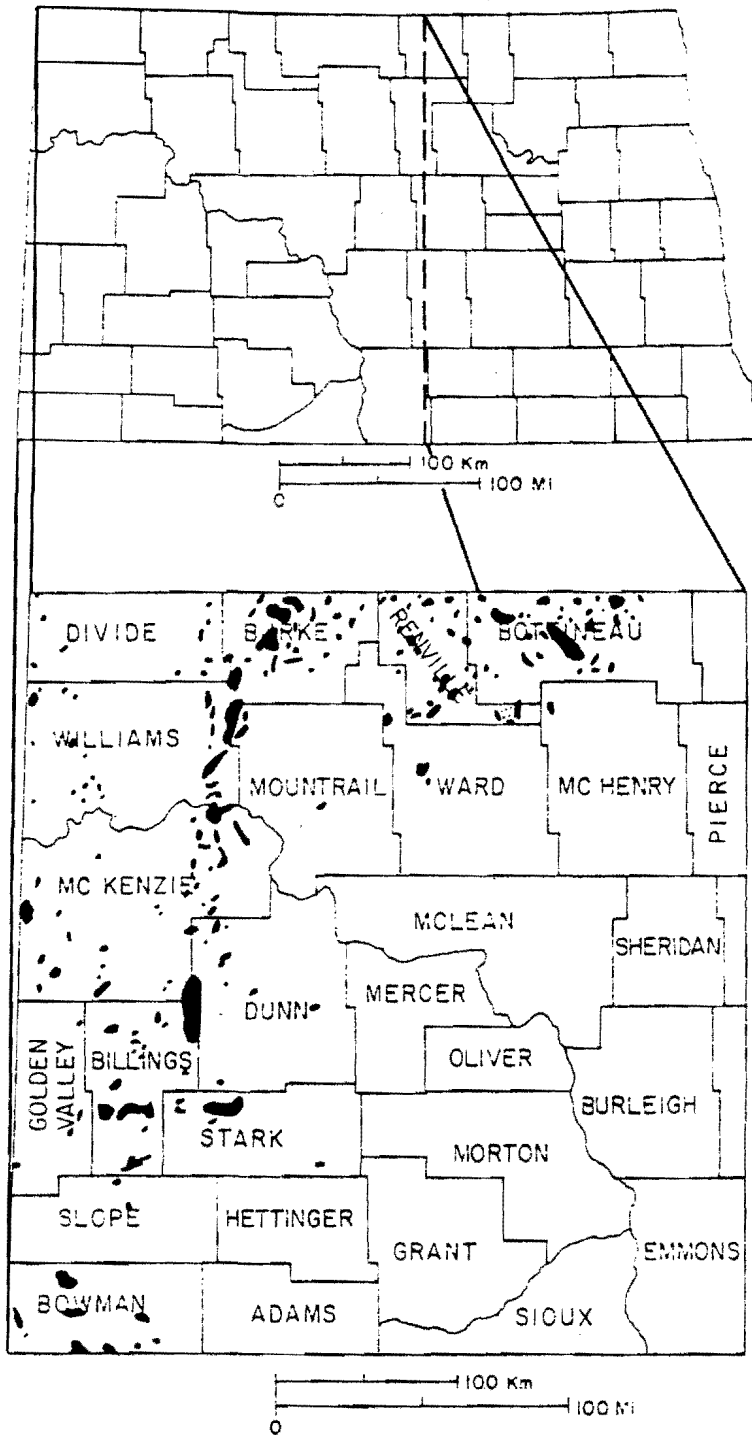


Figure 2. Oil fields in North Dakota (Gerhard and Anderson, 1981).



movement of contaminants in the subsurface. Therefore, the authors suggested further study in areas that have a greater potential for groundwater contamination.

In 1983, the North Dakota Water Resources Research Institute (NDWRRRI) funded a multi-phase study of the detrimental effects of oil-field brines and drilling fluids on soils and groundwater. One phase of that study, and the subject of this thesis, deals with groundwater contamination from drilling-fluid disposal pits. The study stems from the earlier work of Murphy and Kehew, and focuses the research on the glaciated plains of north-central North Dakota. This area differs hydrogeologically from the western North Dakota sites in the following aspects: (1) higher water table (thinner unsaturated zone), (2) presence of sandy permeable sediments, and (3) higher annual precipitation. The potential for migration of leachate and subsequent degradation of groundwater is much greater in this hydrogeologic setting.

1.2 Drilling Fluid

During the drilling of an oil and gas well, a fluid (drilling mud) is circulated down the center of the drill pipe, through the drill bit, and back up to the surface. Rock cuttings, brought up with the fluid, are separated at the shale shaker and the drilling mud is recirculated down the drill pipe. In addition to transporting the cuttings, the drilling fluid must perform the following functions: (1) control formation pressures, (2) maintain borehole stability, (3) protect productive formations, (4) protect against corrosion, and (5) cool and lubricate the bit and drill stem (Simpson, 1975).

Types of drilling fluid include water-base fluids, oil-base fluids, low-solid polymer fluids, and oil-emulsion fluids. However, 85-95

percent are either fresh- or salt-water based (Mosely, 1983). The fresh-water muds generally are colloidal slurries that contain bentonite clay. If salt water is used, attapulgite clay (Fuller's earth) commonly is substituted for bentonite, because sodium bentonite will flocculate and not form a satisfactory colloid in salt water (Gatlin, 1960, p. 81).

Simple colloidal mixtures of clay and water are usually insufficient if the drilling fluid is to perform all the required functions. Therefore, minerals and chemicals are added to modify fluid properties in response to subsurface drilling conditions. Table 1 lists the common drilling additives and their respective functions.

In the Williston Basin, most of the oil is produced from Paleozoic carbonate units that lie beneath a series of halite beds. Salt (NaCl) must be included in the drilling fluids to prevent dissolution of the halite and subsequent loss of circulation during drilling. A typical well in North Dakota is drilled with fresh water until the surface casing is set. At that time, either salt is added to the mud or fresh water is replaced by produced water (brine) (Murphy and Kehew, 1984). Concentrations of salt in drilling fluids are reported to be between 100,000 and 300,000 mg/L (Murphy and Kehew, 1984; Dewey, 1984). Produced waters commonly contain high concentrations of ions other than sodium and chloride. These ions also will be present in the drilling muds that utilize brines for their salt-water base.

As drilling progresses, chemical and mineral additives are incorporated into the drilling fluids (e.g., starches, NO_3^- , CrO_4^{2-} , see Table 1). Subsurface drilling conditions in North Dakota can vary significantly; as a result, the nature and concentration of these additives will

TABLE 1

Function and General Purpose of Drilling Fluid Additives
(From Murphy and Kehew, 1984)

<u>Function</u>	<u>General Purpose</u>	<u>Common Additives</u>
Weighting Material	Control formation pressure, check caving, facilitate pulling dry pipe, & well completion operations	Barite, lead compounds, iron oxides
Viscosifier	Viscosity builders for fluids, for a high viscosity-solids relationship	Bentonite, attapulgite clays, all colloids, fibrous asbestos
Thinner Dispersant	Modify relationship between the viscosity and percentage of solids, vary gel strength, deflocculant	Tannins (quebracho), polyphosphates, lignitic materials
Filtrate Reducer	Cut the loss of the drilling fluid's liquid phase into the formation	Bentonite clays, sodium carboxymethyl cellulose (CMC), pregelatinized starch, various lignosulfonates
Lost Circulation Material	Primary function is to plug the zone of loss	Walnut shells, shredded cellophane flakes, thixotropic cement, shredded cane fiber, pig hair, chicken feathers etc.
Alkalinity, pH Control	Control the degree of acidity or alkalinity of a fluid	Lime, caustic soda, bicarbonate of soda
Emulsifier	Create a heterogeneous mixture of two liquids	Lignosulfonates, mud detergent, petroleum sulfonate
Surfactant	Used to the degree of emulsification, aggregation, dispersion, interfacial tension, foaming, and defoaming (surface active agent)	Include additives used under emulsifier foamers, defoamers, & flocculators
Corrosion Inhibitor	Materials attempt to decrease the presence of such corrosive compounds as oxygen, carbon dioxide, and hydrogen sulfide	Cooper carbonate, sodium chromate, chromate-zinc solutions, chrome lignosulfonates, organic acids and amine polymers, sodium arsenite
Defoamer	Reduce foaming action especially in salt water based muds	Long chain alcohols, silicones, sulfonated oils
Foamer	Surfactants which foam in the presence of water and thus permit air or gas drilling in formations producing water	Organic sodium & sulfonates, alkyl benzene sulfonates
Flocculants	Used commonly for increases in gel strength	Salt, hydrated lime, gypsum, sodium tetraphosphates
Bactericides	Reduce bacteria count	Starch preservative, para-formaldehyde, caustic soda, lime, sodium pentachlorophenate
Lubricants	Reduce torque and increase horsepower at the bit by reducing the coefficient of friction	Graphite powder, soaps, certain oils
Calcium Remover	Prevent and overcome the contamination effects of anhydrite and gypsum	Caustic soda (NaOH), soda ash, bicarbonate of soda, barium carbonate
Shale Control Inhibitors	Used to control caving by swelling or hydrous disintegration	Gypsum, sodium silicate, calcium lignosulfonates, lime, salt

vary as well. The types of additives will also be dependent upon the availability of mud components to the operators.

Completion and workover fluids are also disposed of with the drilling muds and deserve mention here. These fluids are commonly hydrochloric, formic, or acetic acids used to increase the permeability of the producing carbonate zones. The volume of these acids can vary from 500 to several thousand gallons (>1900 L).

1.3 Drilling Fluid Disposal and Pit Reclamation

Murphy and Kehew (1984) present a detailed description of drilling-fluid disposal and pit reclamation practices in North Dakota. Their work is summarized in this section.

The drilling-fluid pit, or reserve pit, is excavated adjacent to the drilling rig and generally has a volume of between 54,000 and 90,000 ft³ (1500 and 2500 m³). If the pit is constructed in permeable sediment, the Oil and Gas Regulatory Division of the North Dakota State Industrial Commission has the authority to require the operator to install an artificial or synthetic liner. This authority is granted to the Oil and Gas Division by the General Rules and Regulations for the Conservation of Crude Oil and Natural Resources, which went into effect in 1974. Prior to these rules, operators commonly would line the pits with bentonite clay to prevent seepage through permeable sediments.

During most of the drilling period, the fluid is circulated in a closed system that does not include the reserve pit. However, cuttings containing fluid coatings are deposited in the pit along with fluids that are periodically flushed out of the settling tanks. The amount of fluid permanently disposed of in the reserve pit varies. If the well is produced, all of the fluid generally will be removed from the borehole

during cementing procedures and pumped into the pit for disposal. On the other hand, if the well is plugged, it is common practice to remove only the drilling fluid displaced by the cement plugs, leaving the remainder in the borehole.

Pit reclamation begins with removal of the low viscosity portion of the fluid for use at another drilling site or disposal in an injection well. In the 1950's and 60's, reserve pits were reclaimed by simply pushing sediment into the pits from the sides. Reclamation took anywhere from a month to a year because the fluids were contained within a small area and could not desiccate rapidly. The most common reclamation procedure today incorporates a trenching method. A series of trenches is excavated on one side of the reserve pit, and sediment is pushed in from the other side forcing the drilling fluid into the trenches. The result is that fluid is spread out over a large area and reclamation can be completed in a few days simply by backfilling and leveling the pit and trenches. However, for reserve pits with synthetic liners, trenching forces the fluid out of the lined pits, and increases the chances of migration of contaminants into the groundwater flow system.

1.4 Previous Work

The U.S. Environmental Protection Agency (EPA) held a conference in 1975 on the environmental effects of chemical use in well drilling (Fisher, 1975). The purpose of this conference was to identify the potential environmental problems that could result from the increase in oil-well drilling that was occurring in the 1970's. Talks were presented on the drilling process and the purpose and nature of drilling fluids. Attention was also given to the toxicity of drilling-fluid additives,

along with the potential for groundwater contamination resulting from drilling-fluid disposal.

Drilling fluids were the subject of much concern in 1976 when Congress passed the Resource Conservation and Recovery Act (RCRA) regulating the generation and disposal of hazardous wastes. The status of drilling fluids and other low volume "low hazardous" wastes was uncertain until addressed in 1980 by the Solid Waste Disposal Act Amendments. These amendments exempted drilling fluids from RCRA until such time as EPA could show need for stricter regulation (Mosely, 1983). The American Petroleum Institute (API), in an attempt to justify the exemption, contracted the engineering consulting firm of Dames and Moore to study the hydrogeologic effects of drilling-fluid disposal across the United States.

Dames and Moore monitored six reserve pits; one site is located in western North Dakota. Chemical analyses were performed on water samples from three wells around each disposal area--an upgradient background well and two downgradient wells. They also analyzed chemical extracts from surface and subsurface soil samples, and analyzed vegetation for chemical uptake. Results indicate that Na^+ and Cl^- are the most mobile ions leached from the pits. However, chloride levels are below drinking water standards within several hundred feet of the disposal areas. Rates of migration of heavy metals were determined to be very slow and not to constitute a health hazard (Dames and Moore, 1982).

The API also sponsored three related studies, which are listed below:

- 1) 1974-1978 "Effects of Drilling Fluid Components and Mixtures on Plants and Soils," Dr. Raymond Miller, Utah State University.

- 2) 1979-1982 "Plant Uptake and Accumulation of Metals Derived from Drilling Fluids," Dr. Darrell Nelson, Purdue University.
- 3) 1981, "Water Base Drilling Mud Land Spreading and Use as a Site Reclamation and Revegetation Medium," James Whitmore, Forsgren-Perkins Engineering.

A single API document summarizes these three studies in addition to the investigation conducted by Dames and Moore (Mosely, 1983).

Drilling-fluid disposal research in North Dakota began with a master's thesis by Edward Murphy that was later published by the North Dakota Geological Survey (Murphy, 1983; Murphy and Kehew, 1984). Four reclaimed disposal sites were monitored in western North Dakota in an attempt to encompass the different hydrogeologic variables of the area. At two of the sites there are thick unsaturated zones and the saturated zone was not monitored. Nevertheless, water analyses from the unsaturated zones support the conclusion that attenuation prevents significant downward migration to the groundwater beneath the water table.

The other two sites are in hydrogeologic settings more conducive to leachate migration (i.e., more permeable sediments and higher water table). Chloride levels indicate that fluid disposal at these two sites affects the groundwater 60 to 90 metres downgradient of the buried pits. In addition, the recommended maximum permissible drinking water standards were exceeded for Cd, Pb, and Se in the shallow groundwater beneath the disposal pits.

Another study of drilling-fluid disposal was recently conducted in the Williston Basin of western North Dakota and eastern Montana (Dewey, 1984). This study incorporated groundwater-chemistry analyses and extensive earth resistivity surveys at two buried disposal sites. Five other sites were evaluated with one to four resistivity soundings.

plumes of leachate were identified in the downgradient direction at the two sites where the groundwater was monitored. Furthermore, resistivity surveys indicated subsurface contamination at three of the other five sites; however, at these sites testing was not extensive enough to determine if buried drilling fluids were the contaminant source.

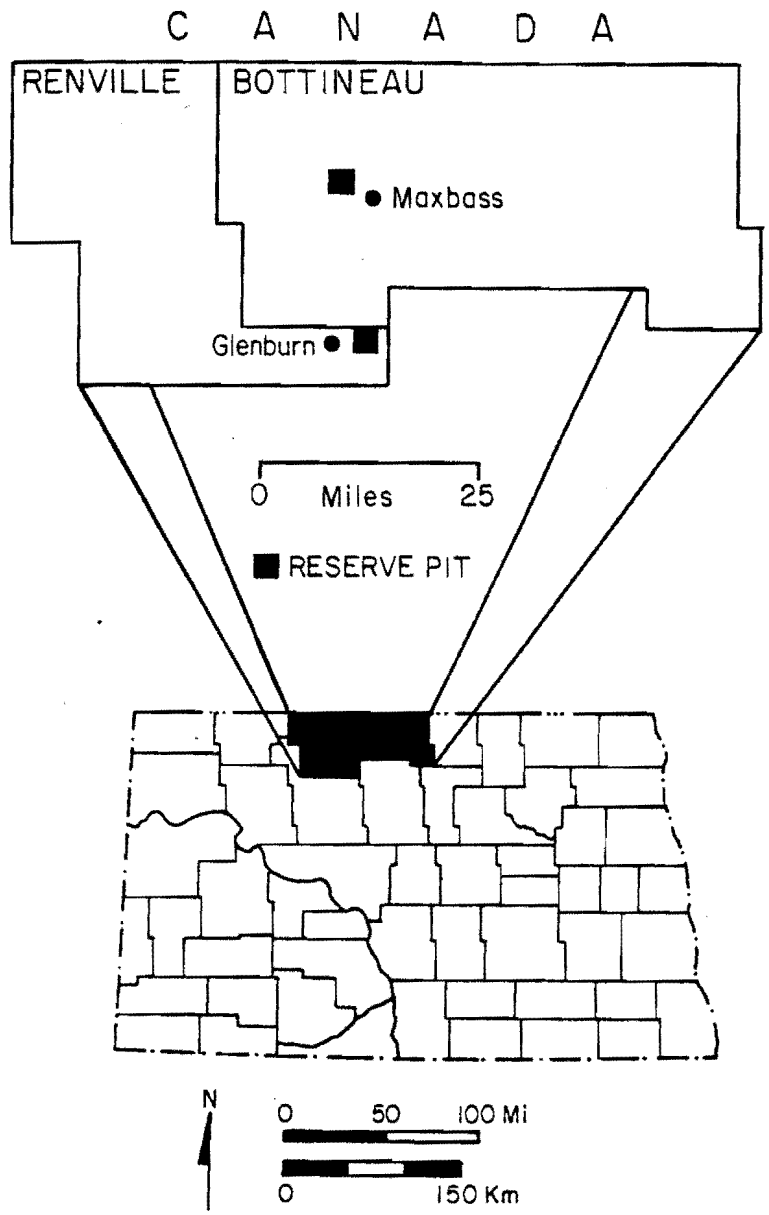
1.5 Study Sites

Two buried reserve pits were selected in north-central North Dakota for the purposes of this study. The objective of site selection was to locate pits situated in two different hydrogeologic settings: one in till, the most common sediment in the area, and the other in sand and gravel, the worst-case situation from a disposal standpoint. Location, accessibility, and land ownership were also considered in the selection process. The two sites chosen are the Fossum Federal no. 4 well in west-central Bottineau County near Maxbass, and the J.J. Winderl no. 1 well in southeastern Renville County near Glenburn (Figure 3).

The Fossum well is situated in the Wiley oil field on land owned by North Dakota State University. This well was selected because of its location and also because it is known to be underlain by a thick layer of till. Chevron USA Inc. drilled the well in 1978 to a depth of 4200 feet (1200 m). The well was treated with 1500 gallons (5700 L) of acid and produces from the Mission Canyon Formation (Mississippian). The buried reserve pit is unlined and was reclaimed by the trenching method.

A reconnaissance study was conducted to locate a suitable buried disposal pit in sand and gravel. The Winderl well in the Glenburn oil field was selected by examining the geologic map of North Dakota (Clayton and others, 1980a) for surface exposures of sand in areas close to the Fossum site, which had already been selected. The Winderl well was

Figure 3. Location of the buried drilling fluid disposal sites.



drilled in 1959 by the California Company to a depth of 4478 feet (1365 m) and treated with 500 gallons (1900 L) of acid. Like the Fossum well, it also produces from the Mission Canyon Formation. The reserve pit was not lined and probably was reclaimed by pushing sediment into the pit from the sides.

In 1980, the Winderl well was deepened to 4597 feet (1402 m) and acidified again with 2300 gallons (8700 L) of HCl. A second pit was excavated. It is not known whether this pit was lined; however, the trenching method probably was used for reclamation.

1.6 Geology

Approximately 8000 feet (2400 m) of sedimentary rocks overlie Precambrian metamorphic rocks in western Bottineau and southeastern Renville Counties. Overlying the sedimentary deposits are between 100 and 300 feet (30 and 90 m) of glacial drift (Bluemle, 1971). Surface and near-surface stratigraphy consists primarily of Pleistocene glacial sediment of Late Wisconsinan age--either deposited directly by the glacier during the last advance, or by water associated with the glacier.

The bedrock-surface lithology varies as successively younger units subcrop below the glacial cover toward the center of the Williston Basin. Near Maxbass (Figure 3), the underlying bedrock includes massive to interbedded sandstones, siltstones, claystones, and shales of the Cretaceous Fox Hills Formation. Overlying the Fox Hills is a lithologically similar sedimentary unit, the Cretaceous Hell Creek Formation, which comprises the bedrock surface for most of the area between Maxbass and Glenburn. Closer to the center of the basin, the subglacial bedrock is a marine silty sandstone, the Cannonball Formation (Tertiary). The subcrop

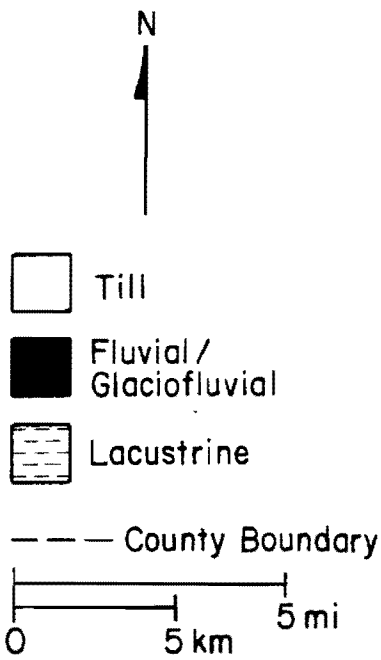
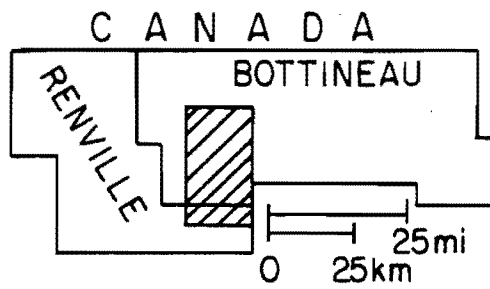
contact between the Hell Creek and the Cannonball trends northwest-southeast through the Glenburn area (Bluemle, 1983).

The glacial drift consists primarily of till interbedded with discontinuous sand lenses and buried glaciofluvial-channel sediments. These deposits are the result of several glacial advances during the Pleistocene Epoch (Bluemle, 1985). The surficial landscape was shaped by the last Wisconsinan glacier, which receded from the area about 12,000 years ago. In western Bottineau and eastern Renville counties, the glacier receded to the northwest, and meltwater from the diminishing glacier formed Lake Souris. At its maximum extent, this glacial lake covered 6,000 km² of north-central North Dakota, including much of Bottineau County (Kehew and Clayton, 1980). Meltwater flowing from the glacier toward Lake Souris incised the till plain with numerous glaciofluvial channels. Many of these channels have since been incorporated into the present-day drainage system.

The surficial geology of the study area is divided into the following three units: till, fluvial and glaciofluvial sediments, and lacustrine deposits (Figure 4).

Till exposed at the surface generally forms gently undulating topography interpreted to indicate collapse of supraglacial sediment associated with melting of the underlying ice (Clayton and others, 1980b). Some areas also show evidence of post-glacial erosion by fluvial and lacustrine processes (Moran and others, 1985). The till contains varying amounts of clay, silt, and sand, as well as some pebbles, cobbles, and boulders. These sediments were ultimately derived from the bedrock underlying the glacier--specifically, igneous, metamorphic and carbonate rocks in Canada, and local bedrock formations (Bluemle, 1985).

Figure 4. Geologic map of the study area (modified from Moran and others, 1985).



The glaciofluvial and fluvial sediments were deposited in channels incised into the till surface. These sediments typically are between 10 and 20 feet (3 and 6 m) thick. However, in the Glacial Lake Souris area, the channels fan out in a "deltaic" pattern and are less than 10 feet (3 m) thick and they cover a wide area (Bluemle, 1985). Sediments associated with the channels are generally subangular to subrounded, moderately well-sorted sands and poorly sorted gravels. Mineralogically, they are similar to the surrounding till (Bluemle, 1985).

The lacustrine deposits were deposited in Glacial Lake Souris. In most surface exposures they are represented by nearshore bedded silts grading to fine sands draped over the till plain. However, in the northwest corner of the study area, a small percentage of the surficial sediments are offshore silts and clays (Moran and others, 1985).

1.7 Groundwater Resources

Groundwater for stock and domestic purposes is derived from both glaciofluvial and bedrock aquifers in the area. According to county groundwater studies (Pettyjohn and Hutchinson, 1977; Randich and Kuzniar, 1984), the Fox Hills and Hell Creek Formations are the primary bedrock aquifers. These studies further indicate that water obtained from the bedrock typically has sodium as the dominant cation and chloride or sulfate as the dominant anion. The total dissolved solids are generally greater than 2000 mg/L, making this water undesirable for most domestic purposes. Nevertheless, some areas are devoid of any other water source, and these bedrock aquifers are utilized.

Glaciofluvial deposits, either buried or exposed at the surface, are the primary source of groundwater in the area. These deposits yield large amounts of high-quality water that is suited for both domestic and

stock purposes. The dominant cation typically is calcium or sodium, and the dominant anion is bicarbonate or sulfate; total dissolved solids are on the average less than 1700 mg/L (Pettyjohn and Hutchinson, 1977; and Randich and Kuzniar, 1984).

1.8 Climate

North Dakota has a semi-arid continental climate, characterized by large seasonal variations in temperature and light to moderate precipitation (Jensen, 1972). Within the study area, the mean annual temperature ranges from 39 to 40°F (3.9 to 4.4°C); approximately 200 days a year are below 32°F (0°C). Mean annual precipitation is around 16 inches (40.64 cm); typically 9 inches (22.86 cm) of that falls between April and July (Jensen, 1972).

1.9 Objectives

To evaluate drilling-fluid disposal in north-central North Dakota, the following objectives have been formulated for this study:

- 1) To determine the characteristics of the contaminant.
- 2) To investigate the chemical attenuation mechanisms.
- 3) To evaluate the distribution and extent of contamination.
- 4) To determine if current drilling-fluid disposal techniques are suitable for the hydrogeologic settings of north-central North Dakota.

2.0 METHODS

2.1 Field Methods

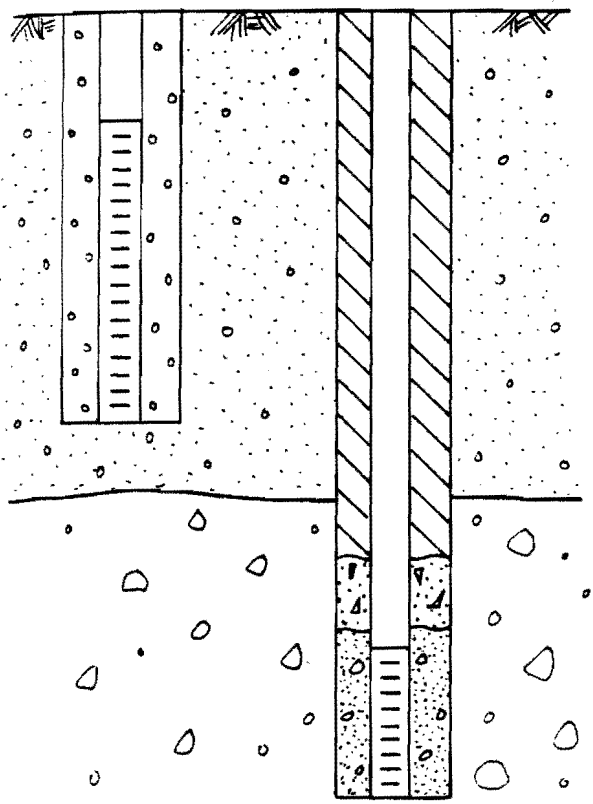
In July of 1984, piezometers were installed at the two study sites to obtain hydraulic data as well as water samples for chemical analysis (Appendix A). These piezometers consist of 2-inch (5.08 cm) diameter PVC pipe connected to a 5 or 10 foot (1.5 or 3 m) section of slotted PVC screen. The piezometer holes were drilled with a rotary rig and a 5.62-inch (14.27 cm) diameter bit. Air was used as the drilling fluid in well indurated or cohesive sediments. In sand and gravel, a mixture of fresh water and bentonite was circulated during drilling to stabilize the borehole. The PVC pipe and screen were placed in the hole and the piezometers were flushed with fresh water until the water coming up at the surface was devoid of any bentonite.

The shallow piezometers at the Winderl site are screened in sand and gravel. The boreholes collapsed after these piezometers were in place and the bentonite was washed out, which formed natural "gravel" packs around the screens. Washed sand or pea gravel was placed in the boreholes of the deeper piezometers at Winderl that are screened in till and all of the piezometers at the Fossum site. The deep Winderl piezometers were sealed with 2 feet (0.61 m) of cement, and backfilled with the available cuttings. At the Fossum site, the holes were filled with cement to the ground surface (Figure 5).

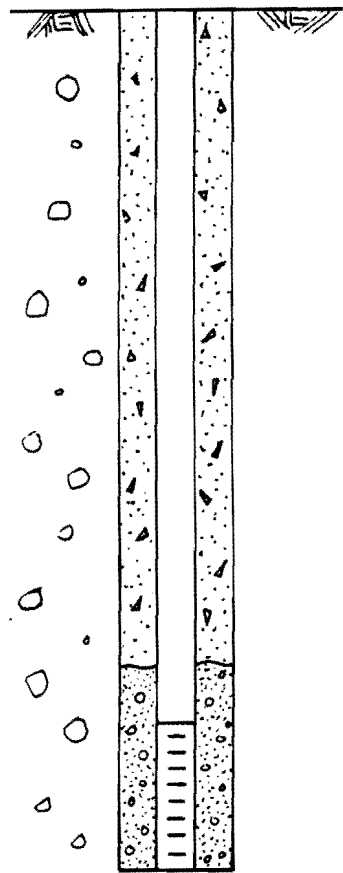
In August of 1984 an air compressor was used as a "gas lift" pump to develop the piezometers. This was accomplished by pumping air into the water, which reduces the fluid density and causes the piezometers to

Figure 5. Piezometer and pressure-vacuum lysimeter profiles.

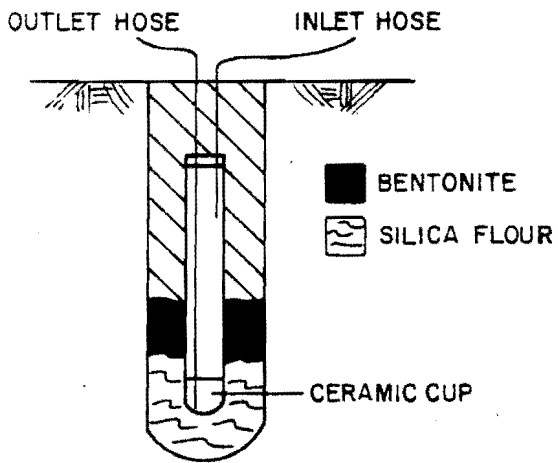
WINDERL PIEZOMETERS










FOSSUM PIEZOMETER



PRESSURE-VACUUM LYSIMETER



-  SAND AND GRAVEL
-  TILL
-  CEMENT
-  FILL
-  SCREEN

-  BENTONITE
-  SILICA FLOUR

flow. Pumping was continued for 30 to 45 minutes or until the water flowing at the surface was relatively clean.

Pressure-vacuum lysimeters were used to sample pore water from the unsaturated zone where the fluid pressure is below atmospheric. Each lysimeter (Soil Moisture Corp. Model 1920) consists of a 1.8-inch (4.57 cm) diameter PVC pipe, 25 inches (63.5 cm) long with a 2.5-inch (6.35 cm) porous ceramic cup at the base; both an inlet and an outlet hose extend from inside the PVC pipe through a sealed rubber stopper at the top.

The lysimeter holes were drilled with a 6-inch (15.24 cm) diameter auger provided by the North Dakota Geological Survey. After each lysimeter was positioned in the hole, silica flour was placed around the ceramic cup to prevent clogging of the pores; a 2-foot (0.61 m) bentonite seal was added and the hole was backfilled with cuttings, leaving only the two hoses exposed at the surface (Figure 5).

During the last week of October 1984, water was sampled from both the piezometers and the lysimeters. To ensure representative samples, the piezometers were bailed until two well volumes had been removed. Each piezometer was allowed to recover, and a bailer was used to obtain enough sample for both major-ion and trace-metal analysis--one litre for majors, one-half litre for trace. The temperature, pH, and electrical conductivity were measured immediately, and the sample was pumped through a 0.45-micron filter into two plastic bottles. After filtering, 5 ml of concentrated nitric acid was added to the one-half litre bottle to lower the pH and prevent precipitation of the trace metals. Both bottles were placed in coolers and later transported to the chemistry lab at North Dakota State University.

Approximately two weeks before sampling, a vacuum was induced in each lysimeter through one of the hoses exposed at the surface. The vacuum reduced the pressure in the lysimeter below the surrounding fluid pressure, causing pore water to migrate in through the ceramic cup. Sampling was accomplished by pumping air into the inlet hose and retrieving the sample from the outlet hose. Commonly, only enough sample was available for either major-ion or trace-metal analysis. The remainder of the sampling procedure was similar to that used for the piezometers.

Stratigraphic data and sediment samples for textural and chemical analysis were obtained from continuous Shelby-tube cores. These relatively undisturbed cores were taken with a truck-mounted, hollow-stem auger (Mobile Drill B-50) provided by the North Dakota Geological Survey. Each Shelby tube is 3 inches (7.62 cm) in diameter and 2.5 feet (0.762 m) long. Approximately 70 tubes were collected from the two study sites. In areas where sand and gravel overlie till, Shelby-tube cores of the till could not be obtained with the hollow-stem auger. Therefore, a split-tube core barrel, attached to a rotary rig, was used to extract the till samples.

Hydraulic conductivity values of the screened intervals were estimated with single-well response, or slug, tests (Appendix B). A slug was dropped down each piezometer, which raised the water level; the head values were recorded at certain time intervals as the water level returned to equilibrium. The unrecovered head differences were plotted against time, and the hydraulic conductivity values were estimated using a method outlined by Hvorslev (1951). Single-well response tests did not work for piezometers screened within sand and gravel because head recovery was too rapid. The hydraulic conductivity values for these

sediments were estimated with a textural analysis technique discussed below in Section 2.2.

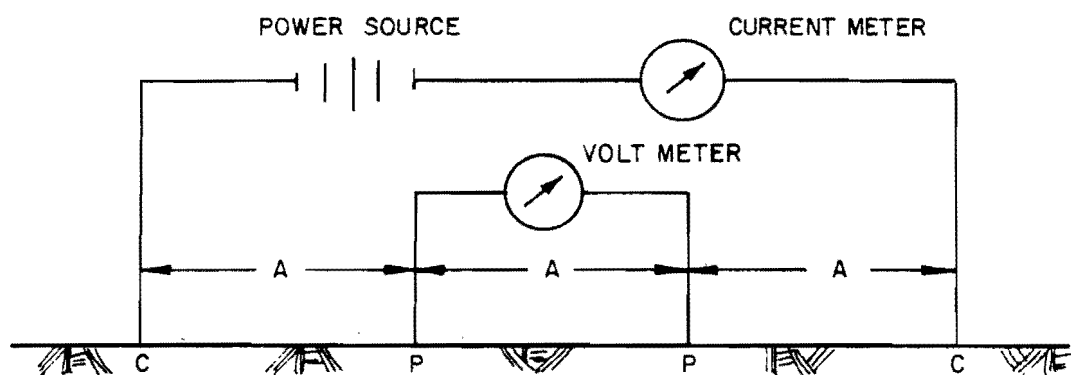
In recent studies, electrical earth resistivity methods have been used successfully to trace contaminant movement in the subsurface (Cartwright and McComas, 1968; Reed and others, 1981; Murphy and Kehew, 1984). These methods are based on the theory that the resistivity of a geologic unit is a function of the conductivity of the pore water as well as the lithology and degree of saturation of the material. Therefore, a resistivity survey accompanied by limited chemical, hydrologic and lithologic data can be an effective means of tracing highly conductive, contaminated groundwater.

Resistivity surveys were conducted around both study sites using a direct-current meter (Soiltest Inc. R50 Stratameter), and the Wenner electrode configuration. Figure 6 illustrates a typical Wenner array. The electrode current travels through the subsurface between the two current electrodes (C). Changes in resistivity are calculated from the voltage difference between the potential electrodes (P), and the magnitude of the induced current. For the Wenner configuration, the electrode spacing is constant across the array, and the equation is reduced to the following:

$$\rho_0 = \frac{2\pi A \Delta V}{I} ,$$

where (ρ_a) is the apparent resistivity, which is equal to the true resistivity only for a homogeneous, isotropic medium; (A) is the electrode spacing; (ΔV) is the voltage difference between the two potential electrodes; and (I) is the current.

Figure 6. Configuration of the four electrode array used in the electrical earth resistivity surveys.



C-CURRENT ELECTRODE P-POTENTIAL ELECTRODE A-ELECTRODE SPACING (A - Spacing)

Apparent resistivity, as a function of electrode spacing, was obtained with vertical electrode sounding (VES) profiles. VES profiles are conducted by expanding the array in increments about a fixed center--the resistivity station. Apparent resistivity is determined for each successive A-spacing. Electrode spacings of 3, 5, 8, 10, 12, 16, 20, 24, 30, 40, 50, 60, 80, and 100 feet were used in this study.

2.2 Laboratory Methods

A major objective of this investigation was to evaluate chemical and lithologic properties of the sediments. To satisfy this objective, the Shelby-tube samples were analyzed with several laboratory techniques--specifically, textural analysis, x-ray diffraction, x-ray fluorescence, and saturated-paste extracts.

The textural analysis consisted of determining sand, silt, and clay percentages of selected samples. A combination of sieve and hydrometer techniques was used; the procedure is outlined in Appendix C.

Adsorption and ion exchange is an important attenuation mechanism in groundwater flow systems. This process is particularly important for clay-size particles because of the large charge to surface-area ratio (Freeze and Cherry, 1979, p 127). A majority of clay-size particles consist of one of several clay minerals--crystalline, hydrous silicates with layer-lattice type structure (Drever, 1982, p 65). The attenuation properties are dependent upon the structure and thus the type of clay (Griffin and others, 1976). Therefore, x-ray diffraction was employed in this study to determine clay mineralogy. This technique is primarily qualitative, although it does give an indication of the relative abundance of the different clay minerals. Sample preparation consisted of mixing the sediment in distilled water and allowing the greater than

2-micron fraction to settle out. A sample of the remaining clay-water solution was placed on a glass disk and dried overnight. Analysis was done with a Phillips x-ray diffractometer for both air-dried and glycolated samples.

Shelby-tube samples were analyzed with a Rigaku wavelength-dispersive x-ray fluorescence (XRF) unit in the Natural Materials Analytical Laboratory (NMAL) at the University of North Dakota. Interaction between the XRF x-ray beam and the sample causes emission of characteristic x-rays. These x-rays are detected and counted for selected elements. A computer software package compares the counts with known standards and determines the elemental composition of the sample in oxide percents (Stevenson, 1985). The chemical analyses included Na, Mg, Al, Si, P, K, Ca, Ti, Mn, and Fe. Sample preparation techniques are outlined in Appendix D.

Some of these Shelby-tube sediment samples were also analyzed for major-ion content by the North Dakota State University Land Reclamation Research Center in Mandan, North Dakota. The sample preparation technique is described in detail in Sandoval and Power (1977) and is summarized in Appendix E.

As discussed in Section 2.1, single-well response tests could not be used to estimate hydraulic conductivity values for the sand and gravel deposits. Therefore, it was necessary to utilize the following relationship between hydraulic conductivity and grain-size distribution presented by Freeze and Cherry (1979, p 350):

$$K = A d_{10}^2,$$

where (K) is the hydraulic conductivity in cm/s; A is equal to 1.0; and d_{10} is the effective grain size in mm. The effective grain size is the

grain-size diameter at which 10% of the sediment is finer. It is obtained from the grain size distribution curve generated from sieve analysis. This technique provides a rough estimate of hydraulic conductivity for sediments in the fine sand to gravel size range.

3.0 RESULTS

3.1 Local Geologic and Hydrogeologic Setting

The subsurface investigations for the two disposal sites are detailed in this section, including the locations of all borings and groundwater monitoring equipment. The results of these investigations are utilized to define the local geologic and hydrogeologic settings of both the Winderl and Fossum sites.

3.1.1 J.J. Winderl No. 1

The ground surface at the Winderl site slopes gently to the south toward a low-lying marshy area adjacent to Spring Coulee Creek. A majority of the piezometers was installed to the south of the buried disposal pit, under the assumption that the equipotential lines mirror the topography and that groundwater flow is in the downslope direction. Approximately 700 feet (213 m) to the north, three piezometers (WP-1, WP-2, and WP-3) were installed to obtain background information (Figure 7).

Figure 8 is a geologic fence diagram that illustrates the three dimensional stratigraphy at the Winderl site. Lithologic logs, which are presented in Appendix F, were used to construct this fence diagram. Till interbedded with discontinuous sand lenses is overlain by sand and gravel from a glacial meltwater channel. The meltwater channel generally is between 14 and 16 feet (4.3 and 4.9 m) thick, increasing to 33 feet (10.1 m) to the northwest. A surface organic layer, up to 2 feet (0.61 m) thick, overlies the meltwater-channel sediments in the low-lying marshy area. The drilling fluid disposal pit is located within the sand

Figure 7. Map view of the Winderl site depicting the location of water sampling instrumentation and Shelby-tube holes. The reserve pit boundaries are approximated by a dashed line near the center of the diagram.

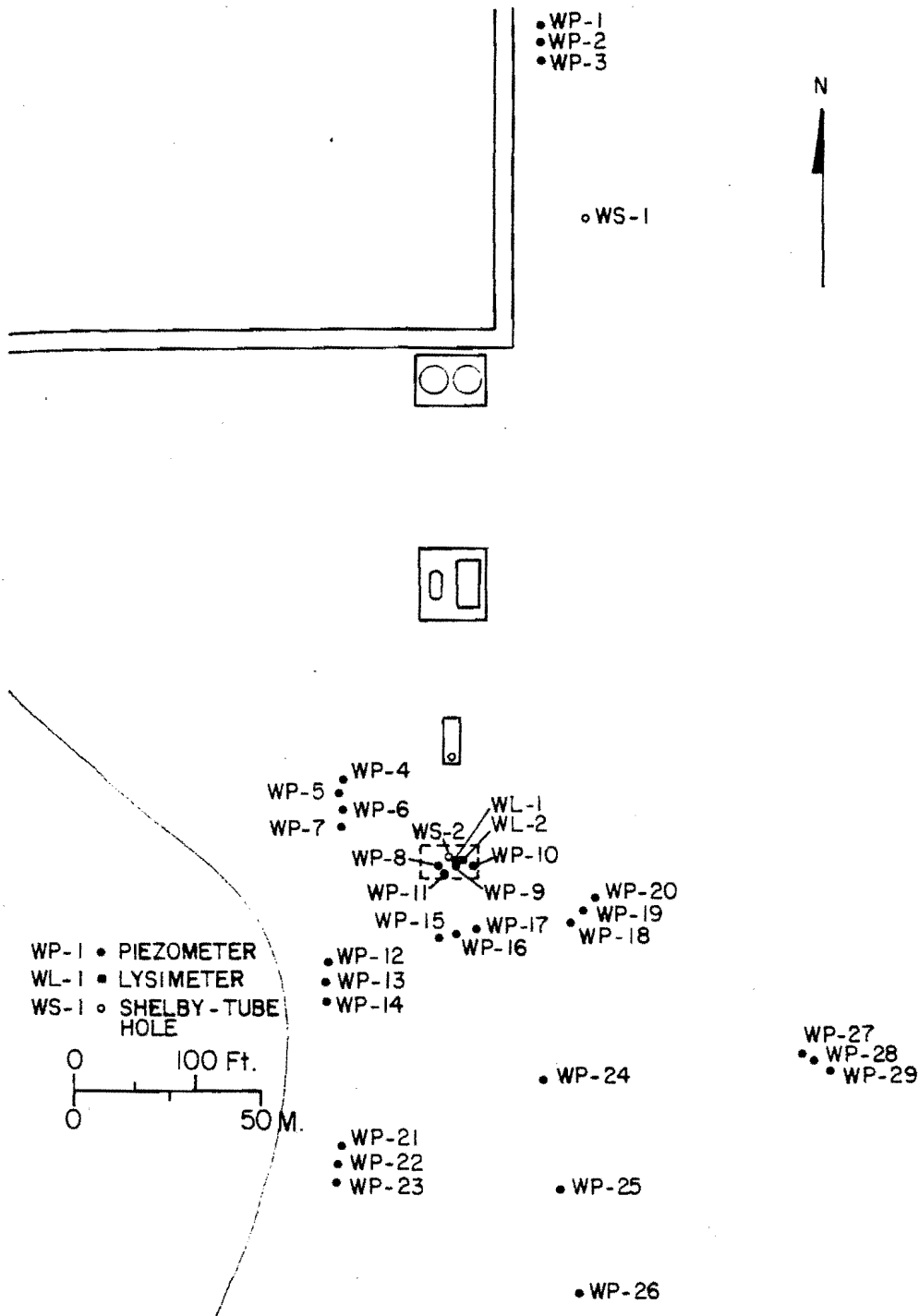
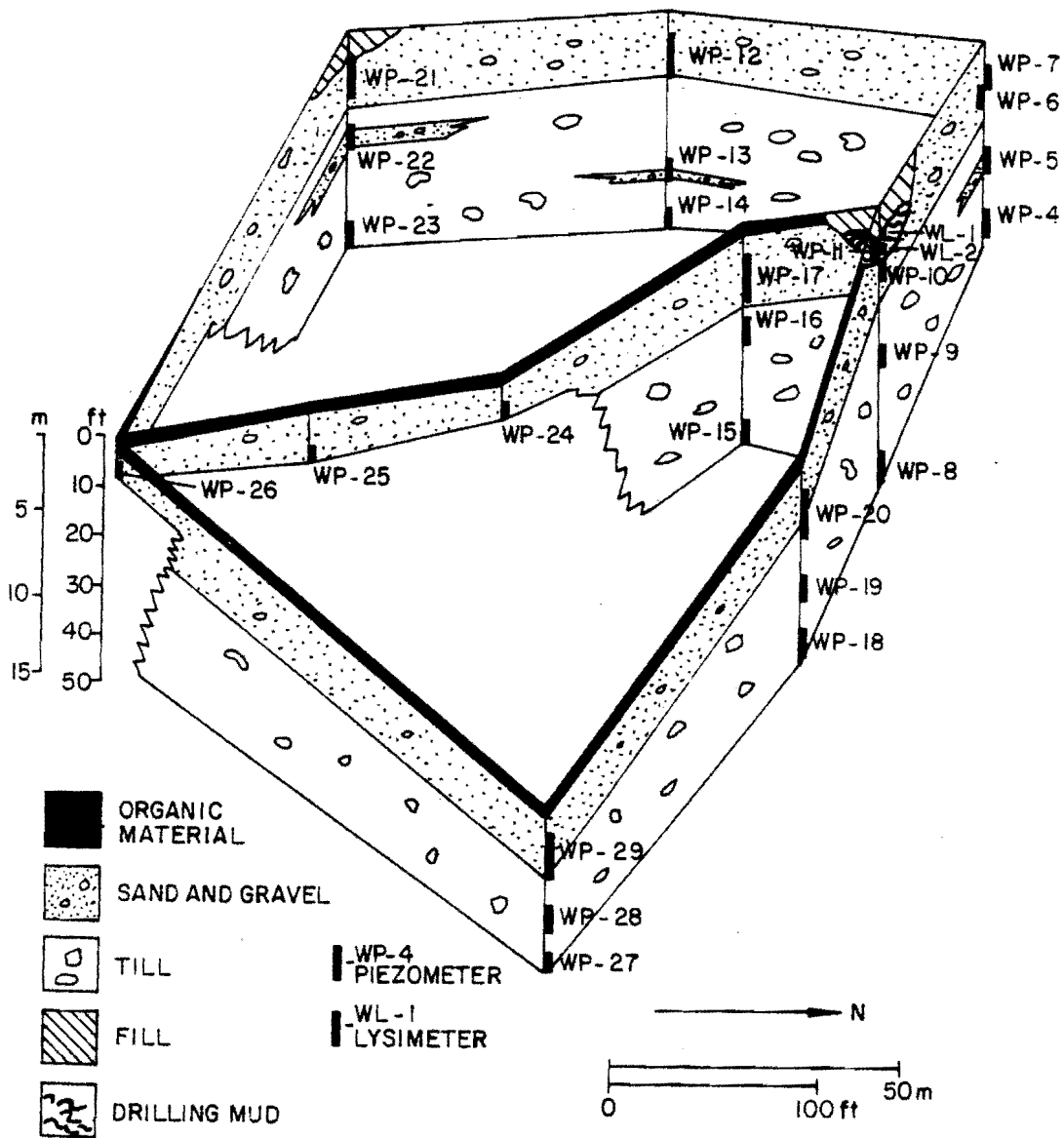
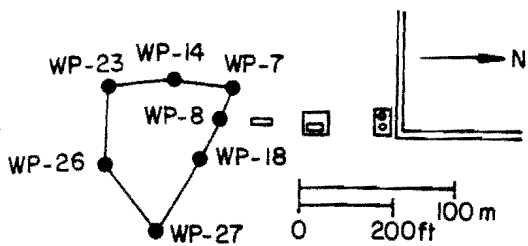


Figure 8. Geologic fence diagram of the Winderl site.



and gravel and is capped by fill material. Nested piezometers were installed at three different stratigraphic horizons, one in the upper sand and gravel and the other two at different depths within the underlying till. In addition, two pressure-vacuum lysimeters were installed within the buried disposal pit.

The upper sand and gravel unit acts as an unconfined system, which has been named the Spring Coulee Creek Aquifer (Pettyjohn and Hutchinson, 1977). The water table was determined from the piezometers screened within these sediments. During the monitoring period (October, 1984 to June, 1985), the depth to the water table varied from less than 2 feet (0.61 m) below the surface in the low-lying marshy area to more than 6 feet (1.8 m) below the surface at the background well (WP-3). Water table maps (Figure 9) indicate that groundwater within this unconfined aquifer generally is flowing to the south, away from the disposal pits. An exception is evident on the January 1985 map, which indicates northeasterly components of flow away from the disposal area.

3.1.2 Fossum Federal No. 4

Piezometer, pressure-vacuum lysimeter, and Shelby-tube hole locations at the Fossum site are depicted in Figure 10. The ground surface slopes gently upward to the north from the disposal pit. The instrumentation was concentrated to the south of the disposal pit because groundwater was assumed to be flowing in the downslope direction. Background information was obtained for piezometers, pressure-vacuum lysimeters, and Shelby-tube holes located approximately 450 feet (137 m) to the north of the pit.

A stratigraphic cross section of the Fossum site is presented in Figure 11. The lithologic logs utilized to construct this cross section

Figure 9. Water table maps of the Winderl site (October, 1984 to June, 1985).

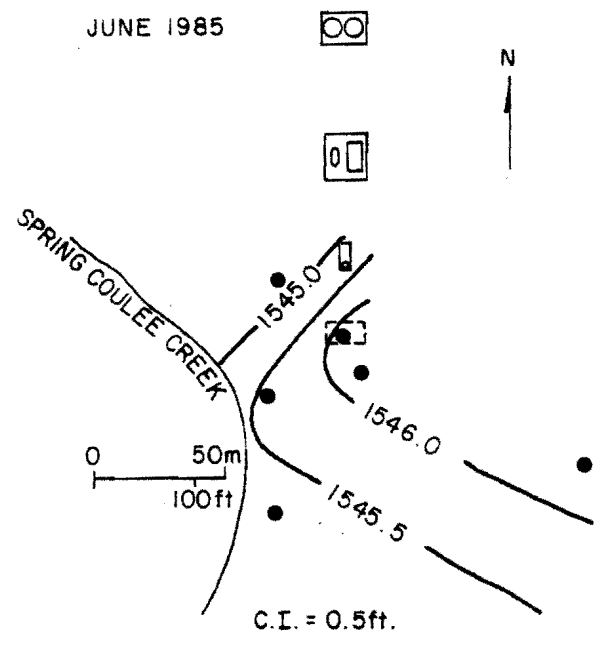
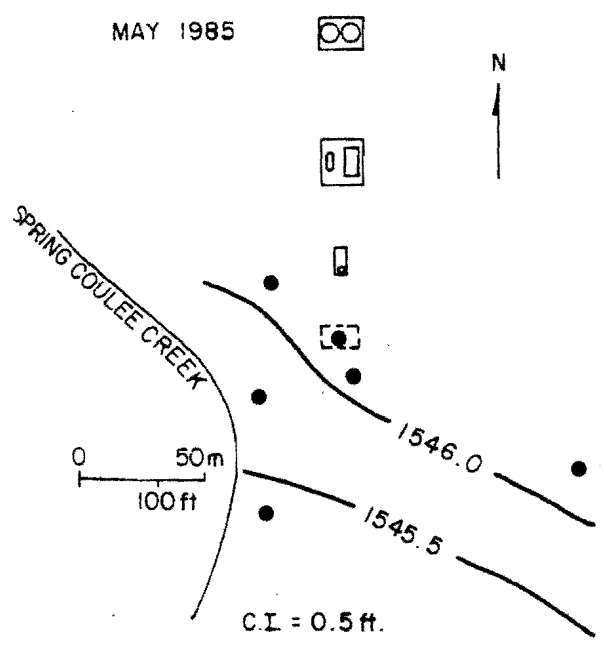
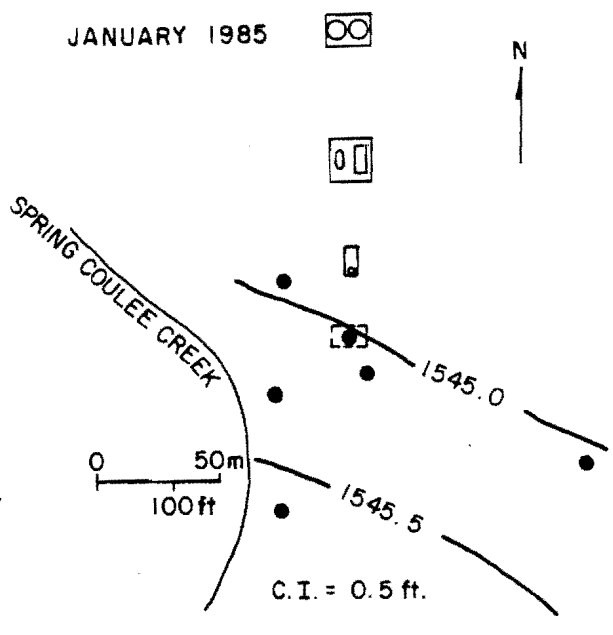
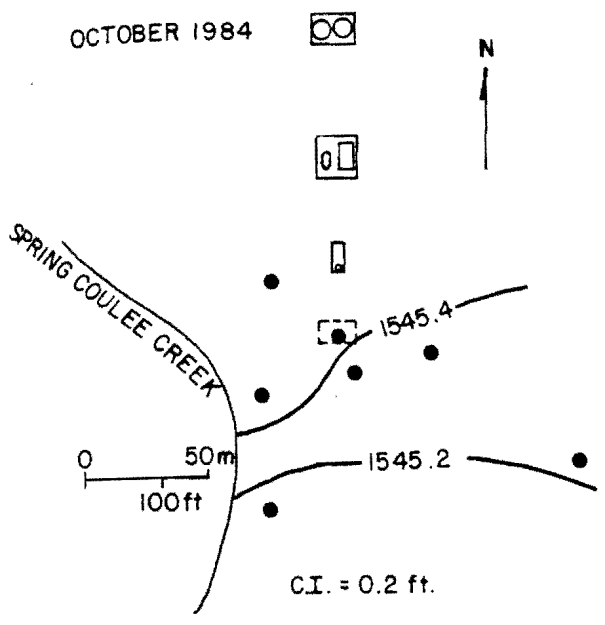


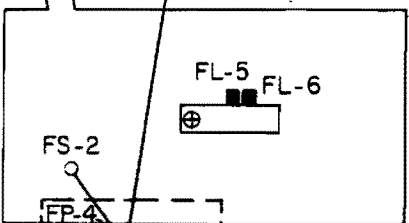
Figure 10. Map view of the Fossum site depicting the location of water sampling instrumentation and Shelby-tube holes. The reserve pit boundaries are approximated by a dashed line near the center of the diagram.

FL-2 FL-3
FL-1 FL-4
○ FS-1

FP-1 FP-2

N

A'

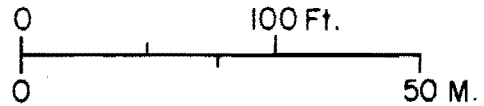


FP-5 FS-4
FP-6

FP-8
FP-7

FS-5 FS-6
FS-7 FL-10
FL-11
FP-10
FP-9

- LYSIMETER
- PIEZOMETER
- SHELBY TUBE

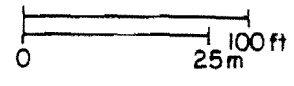
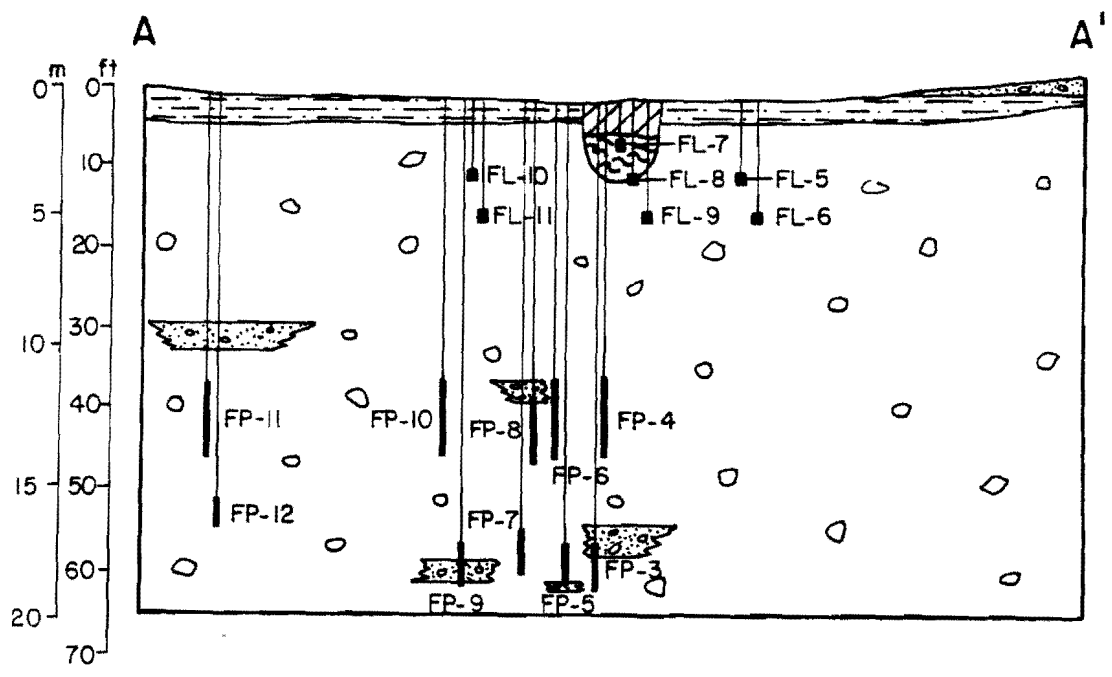


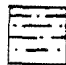






FP-12
FP-11

A



Figure 11. North-south stratigraphic cross-section of the Fossum site depicting selected water sampling instrumentation.



-  SILT AND CLAY
-  SAND AND GRAVEL
-  TILL
-  FILL
-  DRILLING MUD
-  FP-3
PIEZOMETER
-  FL-5
LYSIMETER

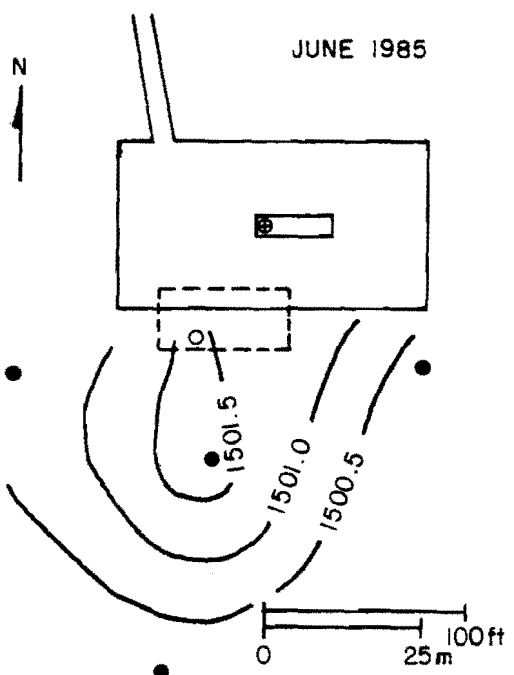
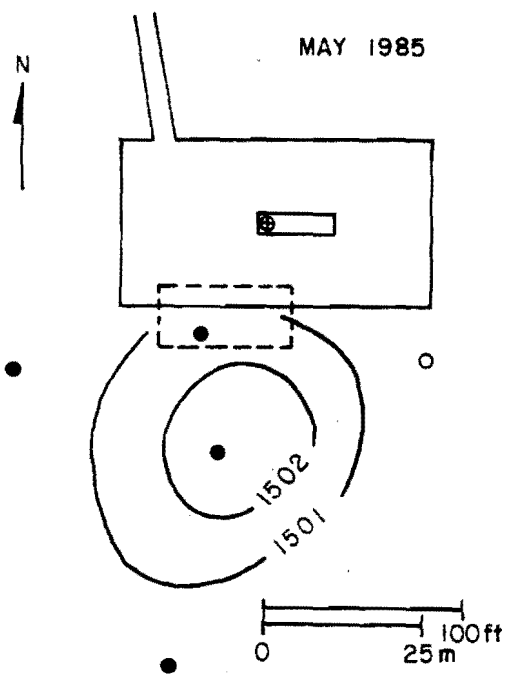
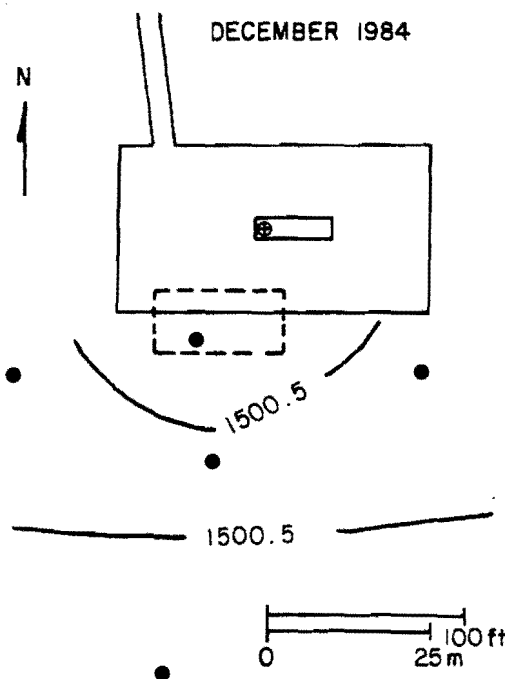
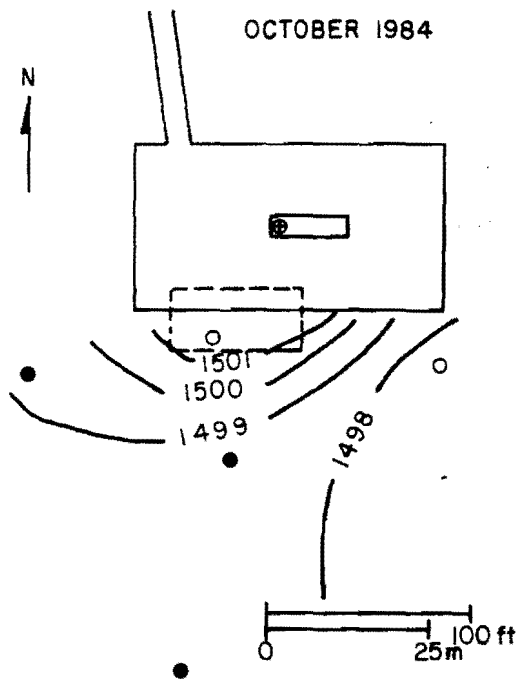
are included in Appendix F. The Fossum site is underlain by till interbedded with discontinuous sand lenses. Overlying the till is 2 to 4 feet (0.61 to 1.2 m) of finely laminated silts and clays. Moran and others (1985) have mapped these sediments as nearshore lacustrine deposits of Glacial Lake Souris. A near-surface sand unit is located to the north of the disposal pit where the ground surface slopes upward. The surficial sediment over much of the area is approximately 1 foot (0.3 m) of well-sorted silt, probably wind-blown sediment from nearby lacustrine deposits.

Nested piezometers were installed at two different depths within the till, and the pressure-vacuum lysimeters were placed at various depths in and around the drilling-fluid disposal pit (Figure 11). An initial hole was drilled at the site and the water level measured in this hole was approximately 40 feet (12.2 m) below the surface. Accordingly, the upper piezometer in each nest was positioned to intersect this interval. However, water levels in these piezometers ranged from 3 to 9 feet (0.9 to 2.7 m) below the land surface during the monitoring period, indicating a much higher water table than previously anticipated. Because the vertical gradient in these nested piezometers is relatively low (<0.009 ft/ft), the potentiometric values from the upper piezometers are used to depict the potentiometric surface of the till unit. Contour maps of these head values show radial flow away from the disposal area in October and December, 1984, and radial flow away from a mound south of the disposal pit in May and June of 1985 (Figure 12).

3.2 Sediment Analysis

Lithologic descriptions of the Shelby-tube samples are presented in Appendix G. Textural analyses were performed on two till samples from

Figure 12. Potentiometric maps of the till unit at the Fossum site (October, 1984 to June, 1985).



the Winderl site, and 12 till samples from the Fossum site (Appendix H). The textural-analysis results are illustrated in Figure 13. Most of the till is either loam or clay loam according to the United States Department of Agriculture classification. At both sites, the pebbles are carbonate and granitic rock fragments, with some dark gray shale and lignite. Horizontal and vertical fractures were evident in both the Shelby-tube samples from the Fossum site, and the split-tube samples from the Winderl site. These fractures are thought to be ubiquitous in the tills of the Great Plains Region (Grisak and others, 1976).

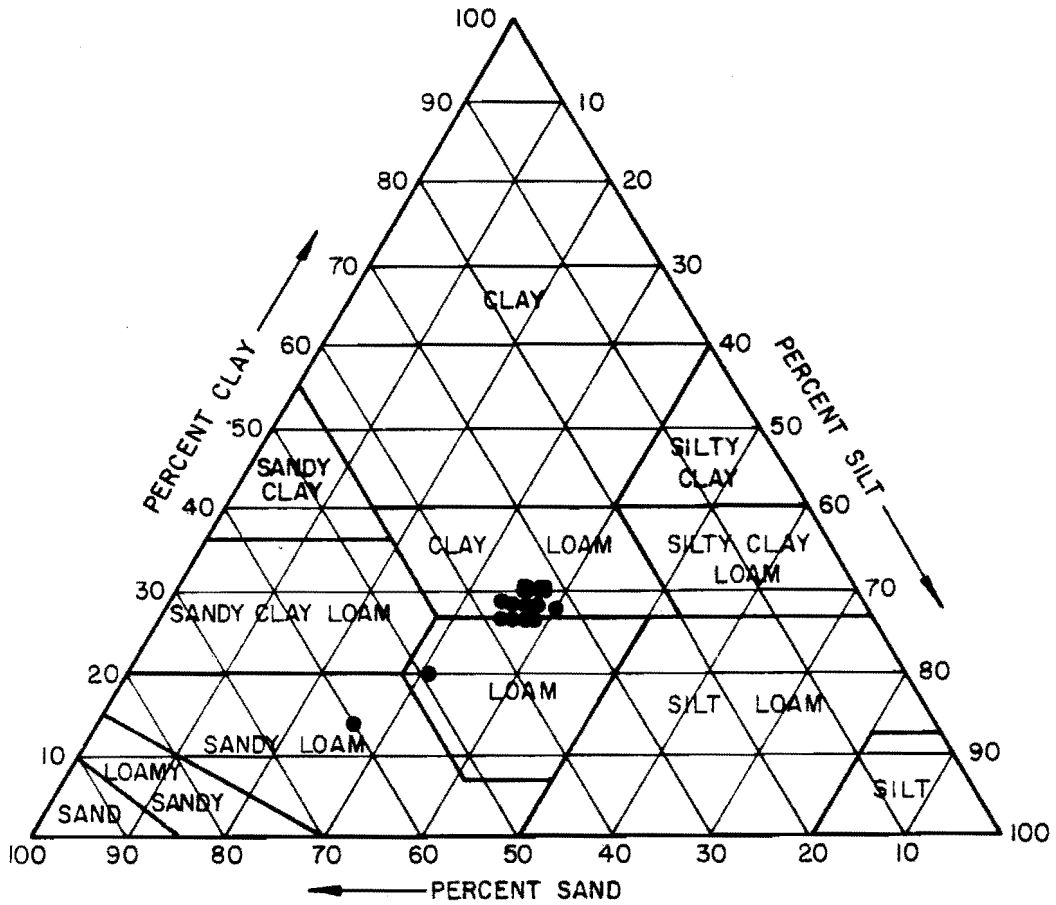
The results of the x-ray diffraction (XRD) analyses of clay samples from the till are presented in Table 2. Peak heights on an x-ray diffractogram are an indication of the relative abundance of the different minerals; therefore, smectite is interpreted as the dominant clay. Further analysis of these clays with an energy-dispersive scanning electron microprobe determined that the smectite is predominantly a Ca-montmorillite.

Textural analyses were also performed on two meltwater-sediment samples from the Winderl site (Appendix H). The following gravel, sand, silt, and clay percentages were calculated from these analyses:

	Gravel %	Sand %	Silt %	Clay %
WP-25 3 ft-6 ft (0.9-1.8 m)	3.2	84.2	9.2	3.4
WS-1 5 ft-8 ft (1.5-2.4 m)	16.9	77.6	5.5	0.0

The sand-size grains are predominantly quartz and granitic rock fragments. The gravels mainly consist of carbonates, shales, and granitic rock fragments.

Figure 13. United States Department of Agriculture textural classification of the till samples from the Fossum site.



- SAMPLES FROM J.J. WINDERL NO. 1
- SAMPLES FROM FOSSUM FEDERAL NO. 4

TABLE 2

X-ray Diffraction Analyses of Clay Samples
From Till at the Study Sites

Location	Depth (feet)	Smectite [001]	Chlorite [001]	Muscovite [001] Illite [001]	Kaolinite [001] Chlorite [002]
<u>Air-Dried</u>		<u>Peak Heights (inches)</u>			
FS-5	10	4.6	---	3.2	2.3
FS-5	20	23.0	9.0	13.0	14.0
FS-5	40	19.6	---	4.0	15.0
WP-2	15	9.0	---	5.6	8.0
WP-9	18.5	10.8	---	6.6	8.6
<u>Glycolated</u>					
FS-5	10	16.0	---	2.8	3.0
FS-5	20	51.0	---	10.8	12.8
FS-5	40	51.0	---	7.4	11.8
WP-2	15	24.0	4.0	5.0	7.0
WP-9	18.5	23.4	---	4.0	7.0

3.3 Hydraulic Conductivity

The hydraulic conductivity of the till at the Winderl site was estimated from 12 single-well response tests (slug tests). These tests yielded values that range from 2.4×10^{-6} cm/s to 5.6×10^{-3} cm/s, averaging 5.6×10^{-4} cm/s. At the Fossum site, similar tests were conducted on 12 piezometers screened within the till; the resulting hydraulic conductivity estimates range from 4.5×10^{-6} cm/s to 5.7×10^{-5} cm/s, with an average of 1.8×10^{-5} cm/s (Appendix I).

The hydraulic conductivity values obtained from these single-well response tests are considerably higher than the grain size indicates. Grisak and Cherry (1975) have estimated intergranular hydraulic conductivity from laboratory consolidation tests on 85 till samples across the Interior Plains Region. They obtained an average of 5×10^{-9} cm/s. The higher values from the slug tests in this study are attributed to secondary permeability from fractures, which is not reflected in laboratory consolidation tests. Evidence of the greater permeability along the fractures can be found in the Shelby-tube samples from the Fossum site (Appendix G). The oxidized zone extends approximately 2 feet (0.61 m) deeper along fracture surfaces than in the till matrix, which is an indication that downward percolating water is moving faster along these fractures.

Grain-size distribution curves were generated from sieve analyses of two samples taken from the upper sand and gravel unit at the Winderl site (Appendix J). The effective grain sizes (d_{10}) from these curves were used to estimate hydraulic conductivities. Values of 1.7×10^{-2} cm/s and 1.5×10^{-1} cm/s were obtained from sample WP-25 and WS-1 respectively. These magnitudes are considered to be within the clean sand to gravel size range (Freeze and Cherry, 1979, p. 29).

4 Apparent Resistivity

Thirty resistivity stations were surveyed at the Winderl site and 25 at the Fossum site (Figures 14 and 15). From these profiles, apparent resistivity values were calculated for each electrode spacing. Apparent resistivity is equal to the true resistivity only in a homogeneous, isotropic medium. With the Wenner electrode configuration, a rule of thumb states that the apparent resistivity is a weighted average over a hemispherical bowl of a radius equal to the electrode spacing (Greenhouse and Harris, 1983). This rule holds true only if the a-spacing is approximately equal to the depth of current penetration. Electrode spacing vs. apparent resistivity curves are plotted in Appendix K. In addition, apparent iso-resistivity maps were generated for the different electrode spacings (Appendix L).

A-spacing vs. apparent resistivity curves, or Wenner sounding curves, resemble or commonly coincide with Dar Zarrouk curves calculated from the modified Dar Zarrouk function (Zhody, 1975). A computer program developed by Zhody and Bisdorf (1975), which incorporates the modified Dar Zarrouk function, inverted Wenner sounding curves from the resistivity survey into layer thicknesses and interpreted resistivities. The interpreted resistivity values are also presented in Appendix L.

4.1 J.J. Winderl No. 1

The 16-foot a-spacing corresponds best to the depth of the sand and gravel-till contact at the Winderl site, assuming that the depth of current penetration equals the electrode spacing. Therefore, the $a = 16$ foot apparent iso-resistivity map, presented in Figure 16, is used to illustrate resistivity variations within this sand and gravel unit. Figure 16 indicates that an abrupt decrease in apparent resistivity

Figure 14. Map view of the Winderl site showing the locations of the resistivity stations. The boundaries of the reserve pit are approximated by the dashed line near the center of the diagram.

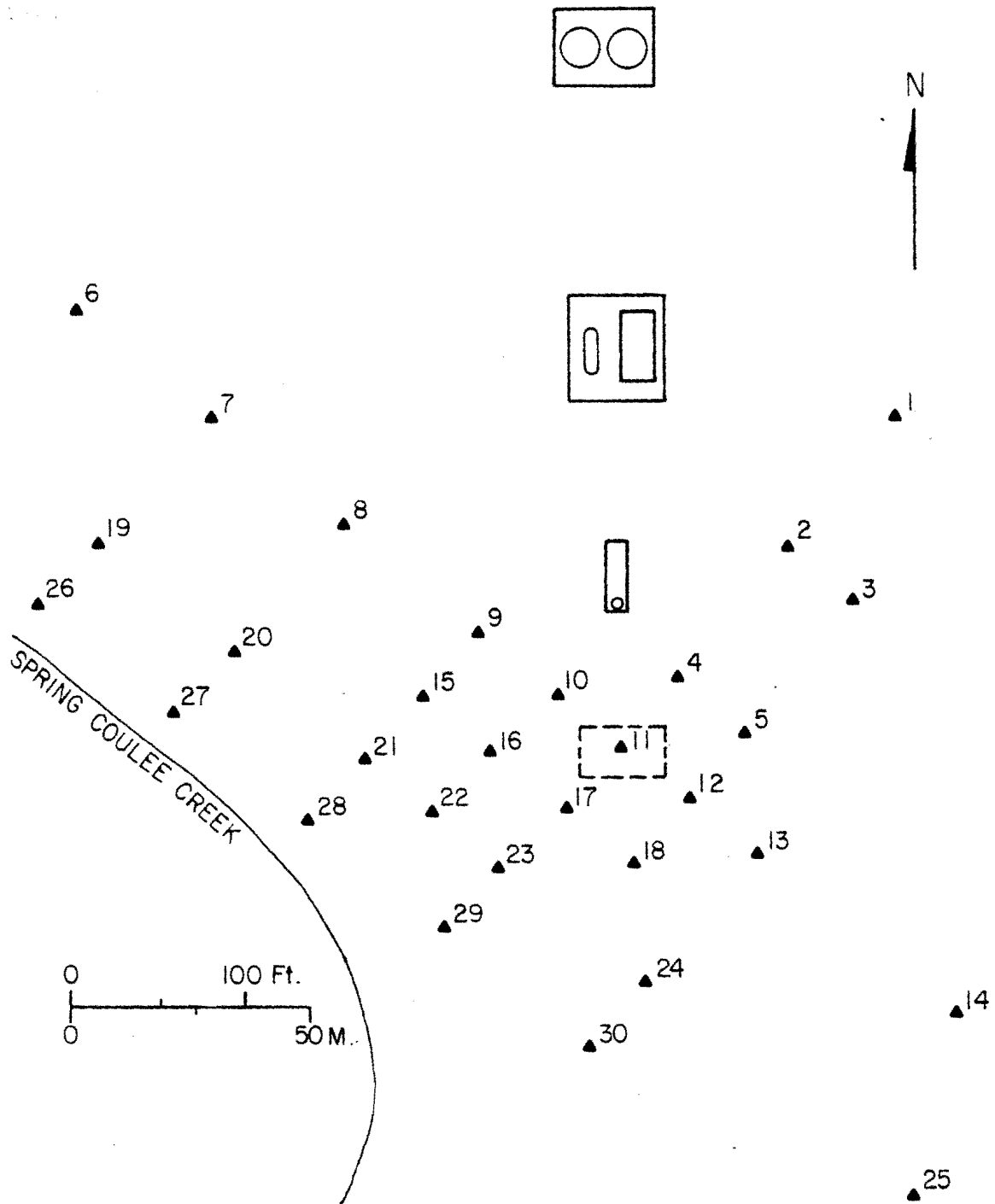


Figure 15. Map view of the Fossum site showing the locations of the resistivity stations. The boundaries of the reserve pit are approximated by the dashed line near the center of the diagram.

Figure 15. Map view of the Fossum site showing the locations of the resistivity stations. The boundaries of the reserve pit are approximated by the dashed line near the center of the diagram.

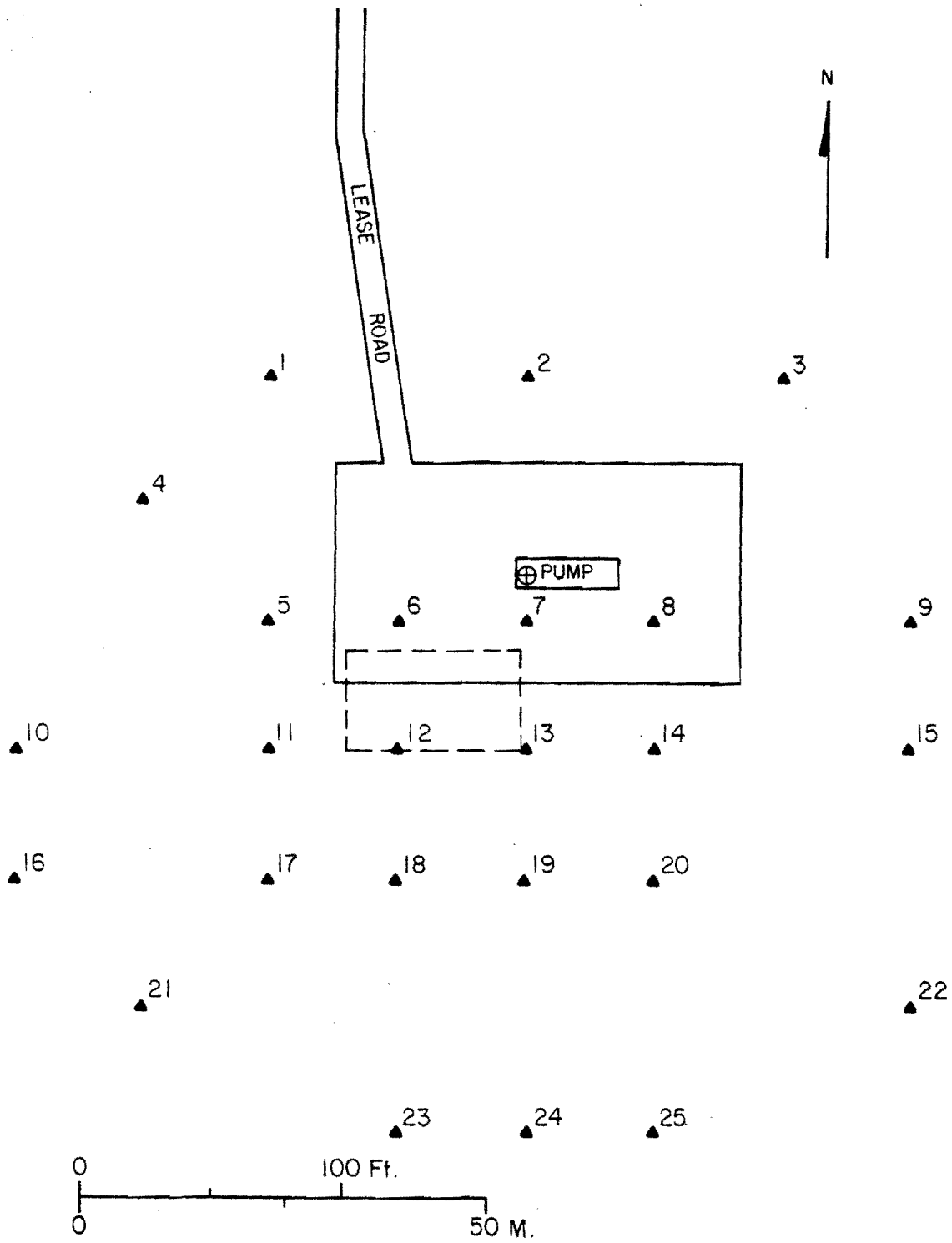
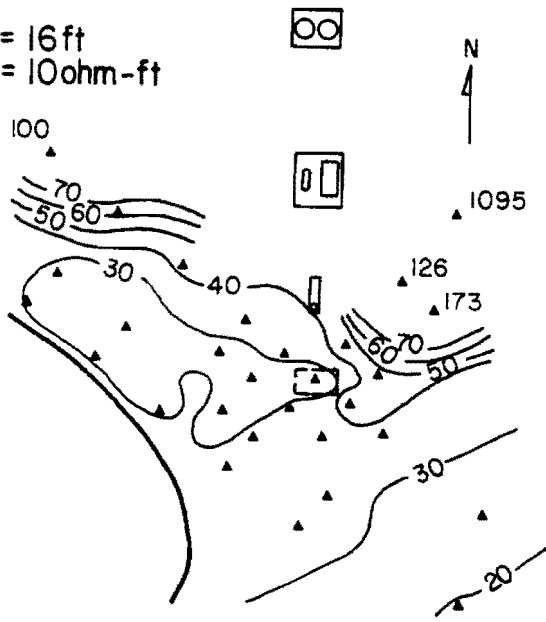
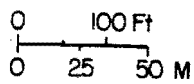
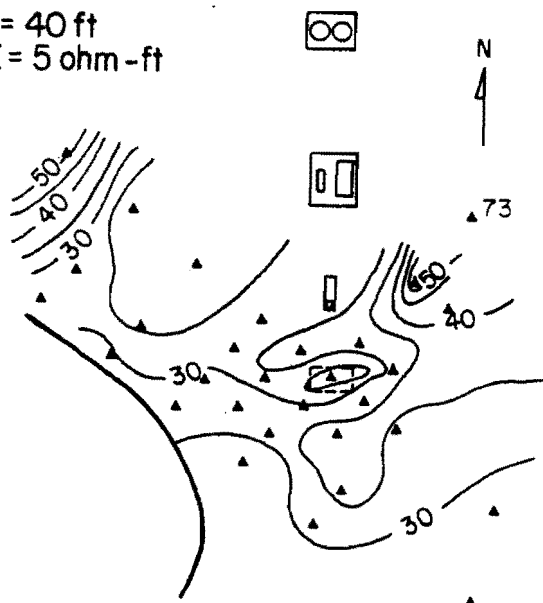


Figure 16. Apparent isoresistivity maps of the Winderl site for electrode spacings of 16 and 40 feet (4.8 and 12.2 m).

A = 16 ft
CI = 10 ohm-ft



A = 40 ft
CI = 5 ohm-ft



occurs from north to south across the study area, with a high of 1696 ohm-feet (517 ohm-m) in the northeast corner. Resistivities directly to the northwest and to the south of the disposal pit are less than 30 ohm-feet (10 ohm-m), with a low of 20 ohm feet (6.1 ohm-m) in the southwest corner. Typical resistivity values for sand and gravel deposits range from 1,000 to 10,000 ohm-feet (300 to 3,000 ohm-m) (Soiltest, 1968).

The apparent isoresistivity map for the 40-foot (12.1 m) a-spacings is also presented in Figure 16. At this a-spacing, apparent resistivity ranges from 73 ohm-feet (22.3 ohm-m) in the northeast to less than 25 ohm-feet (7.6 ohm-m) near the disposal pit and to the northwest.

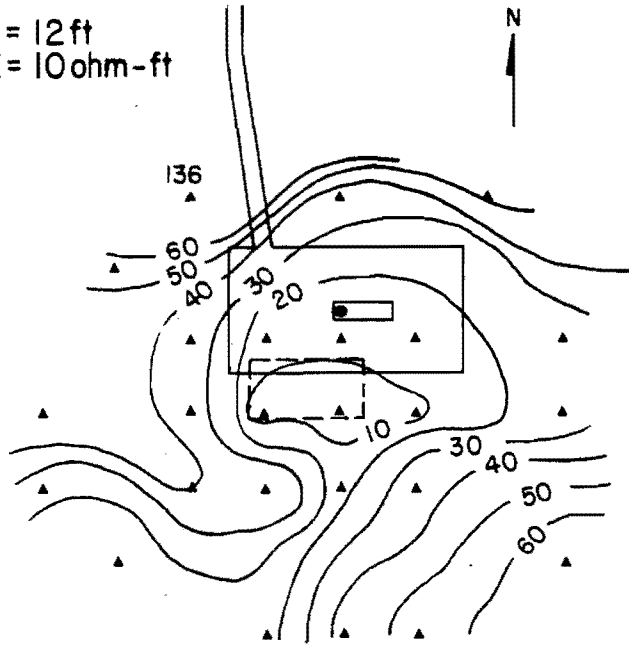
3.4.2 Fossum Federal No. 4

The disposal pit is approximately 5 feet (1.5 m) below ground surface at the Fossum site, and the water table generally is less than 7 feet (3.7 m) below the surface. Accordingly, the a=12 feet isoresistivity map is presented in Figure 17 to delineate areas of low resistivity caused by movement of contaminants from the pit in the upper part of the saturated zone. This map indicates that apparent resistivity is less than 10 ohm-feet (3.0 ohm-m) near the disposal pit and increases toward the periphery of the resistivity study area to a maximum of 136 ohm-feet (41 ohm-m). There is also an area of low resistivity directly to the south of the disposal pit.

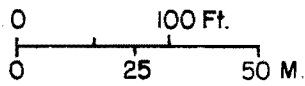
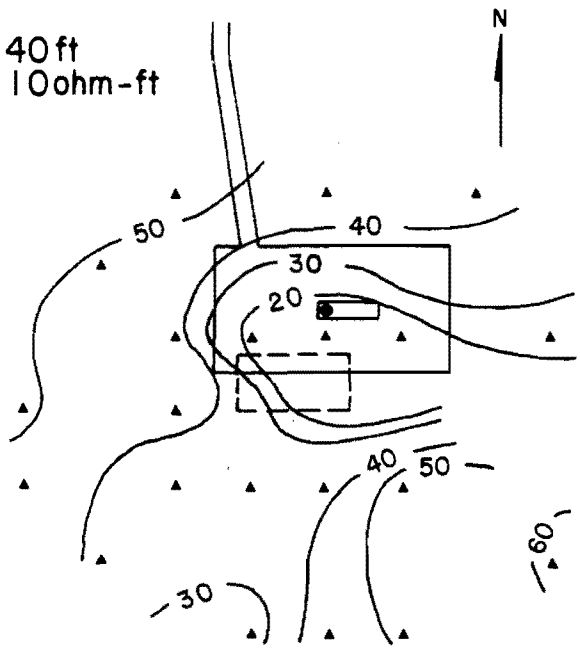
The 40-foot (12 m) a-spacing map is also included in Figure 17 to illustrate resistivity variations at depth. At this a-spacing, the apparent resistivities adjacent to and south of the disposal area are less than 20 ohm-feet (6.1 ohm-m). These values increase radially away from this area to a maximum of 50 ohm-feet (15.2 ohm-m) in the northeast.

Figure 17. Apparent isoresistivity maps at the Fossum site for electrode spacings of 12 and 40 feet (3.7 and 12.2 m).

A = 12 ft
CI = 10 ohm-ft



A = 40 ft
CI = 10 ohm-ft



3.5 Groundwater Chemistry

Results of chemical analyses of the groundwater samples from both study areas are presented in Appendix M. This section summarizes those results and details the effects of leachate generated from the disposal of drilling fluids.

3.5.1 J.J. Winderl #1

Water samples were collected for chemical analysis from 29 wells at the Winderl site (Appendix M). Attempts to collect samples from the two pressure-vacuum lysimeters were unsuccessful.

The chemistry of groundwater directly below the pit (WP-11) is compared to background levels to determine the effects of the buried disposal pit on the groundwater chemistry of the Spring Coulee Creek Aquifer (Table 3). The background wells selected include WP-3, north of the buried disposal pit, and the Stevan's farm well screened in Spring Coulee Creek Aquifer approximately 0.75 miles (1.2 km) southeast of the Winderl site. Also listed in Table 3 are the recommended permissible concentrations (RPC) for total dissolved solids (TDS), sulfate, chloride, iron, and manganese, and the maximum permissible concentrations (MPC) for lead and chromium. Comparison of the chemical analyses in Table 3 suggests that increased hardness, alkalinity and TDS, in addition to elevated concentrations of calcium, magnesium, sodium, potassium, sulfate and manganese, all result from the buried disposal pit. Four of these constituents (TDS, Cl, Na, and Ca), in addition to two trace metals (Cr and Pb), are designated as indicator parameters to further evaluate contamination from the disposal pit.

Three intervals are screened at the Winderl site--one interval in the upper sand and gravel unit and two in the underlying till. Water

TABLE 3

Chemical Analyses of Groundwater Samples from Piezometers WP-3 and WP-11 at the Winderl Site and the Nearby Stevan's Farm Well. Piezometer Locations are Shown in Figure 7.

Well Number	WP-11	WP-3	Stevans Farm	Drinking Water Standards
Date	10-26-84	10-26-84	10-25-84	
Temperature	9.5	9.5	12	
Field pH	7.10	7.10	7.25	
Field Conductivity	6100	3500	750	
Lab pH @ 22°C	7.46	7.57	7.59	
Lab Conductivity	8521	1624	1018	
TDS mg/L	6113	1130	749	500*
Hardness mg/L	1440	303	411	
Alkalinity mg/L	398	189	263	
Ca mg/L	301	74	112	
Mg mg/L	167	28	32	
Na mg/L	1259	221	119	
K mg/L	60	16	23	
SO ₄ mg/L	467	38	51	250*
Cl mg/L	2659	401	95	250*
NO ₃ mg/L	0.5	6.6	35	
Fe µg/L	28	105		300*
Mn µg/L	2421	740		50*
Cr µg/L	1.1	2.2		50**
Pb µg/L	2.6	2.6		50**

* Recommended Permissible Concentration (RPC)

** Maximum Permissible Concentrations (MPC)

samples were collected from all three intervals to determine concentration variations with depth. These variations are illustrated with concentration profiles for each of the indicator parameters (Figures 18-21).

Variation with depth of TDS, Cl, Na, and Ca are similar, as illustrated by their similar concentration profiles. At two of the monitor-well locations (WP-7 and WP-20), the highest concentrations were detected in the sand and gravel unit with the maximum concentrations in WP-7 (TDS=14,203 mg/L, Cl=6007 mg/L, Na=2323 mg/L and Ca=1174 mg/L). Background TDS from WP-3 is 1130 mg/L, whereas for all other wells screened within this sand and gravel aquifer TDS exceeded 3000 mg/L. The total-dissolved-solids concentration in groundwater from shallow glaciofluvial aquifers in the area is typically less than 1700 mg/L (Pettyjohn and Hutchinson, 1977; and Randich and Kuzniar, 1984).

At the remaining six monitor-well locations, the highest concentrations were detected in wells screened in the upper interval of the till. These wells are screened directly in the till or in isolated sand lenses within the till. Piezometer WP-13 is screened in a sand lens approximately 10 feet (3.0 m) below the base of the sand and gravel unit and yielded the following concentrations of dissolved constituents: TDS=70,492 mg/L, Cl=42,105 mg/L, Na=20,013 mg/L and Ca=4415 mg/L. Well WP-22, which is screened in a sand lense approximately 15 feet (4.6 m) below the surface also yielded high concentrations: TDS=34,806 mg/L, Cl=19,412 mg/L, Na=6331 mg/L, and Ca=4028 mg/L. Both WP-13 and WP-22 are located southwest of the disposal pit along Spring Coulee Creek (Figure 7). High concentrations of contaminants are not limited to wells screened within the sand lenses. Well WP-16, which is located directly

Figure 18. Concentration profiles of total dissolved solids, chloride, sodium, calcium, chromium, and lead in the groundwater at piezometer locations WP-1 and WP-4 at the Winderl site (Fig. 7). See Figure 8 for explanation of lithology.

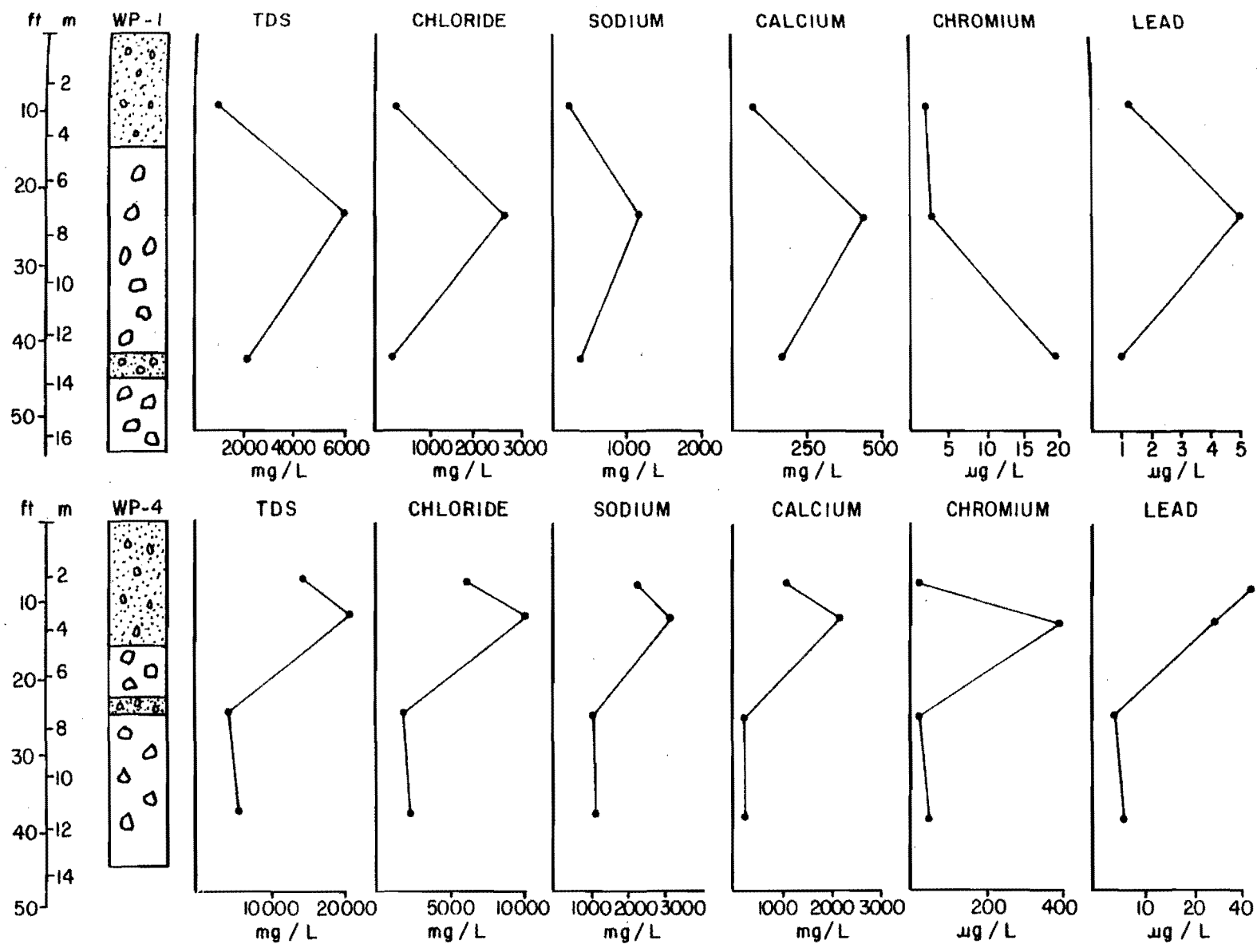


Figure 19. Concentration profiles of total dissolved solids, chloride, sodium, calcium, chromium, and lead in the groundwater at piezometer locations WP-8 and WP-14 at the Winderl site (Fig. 7).

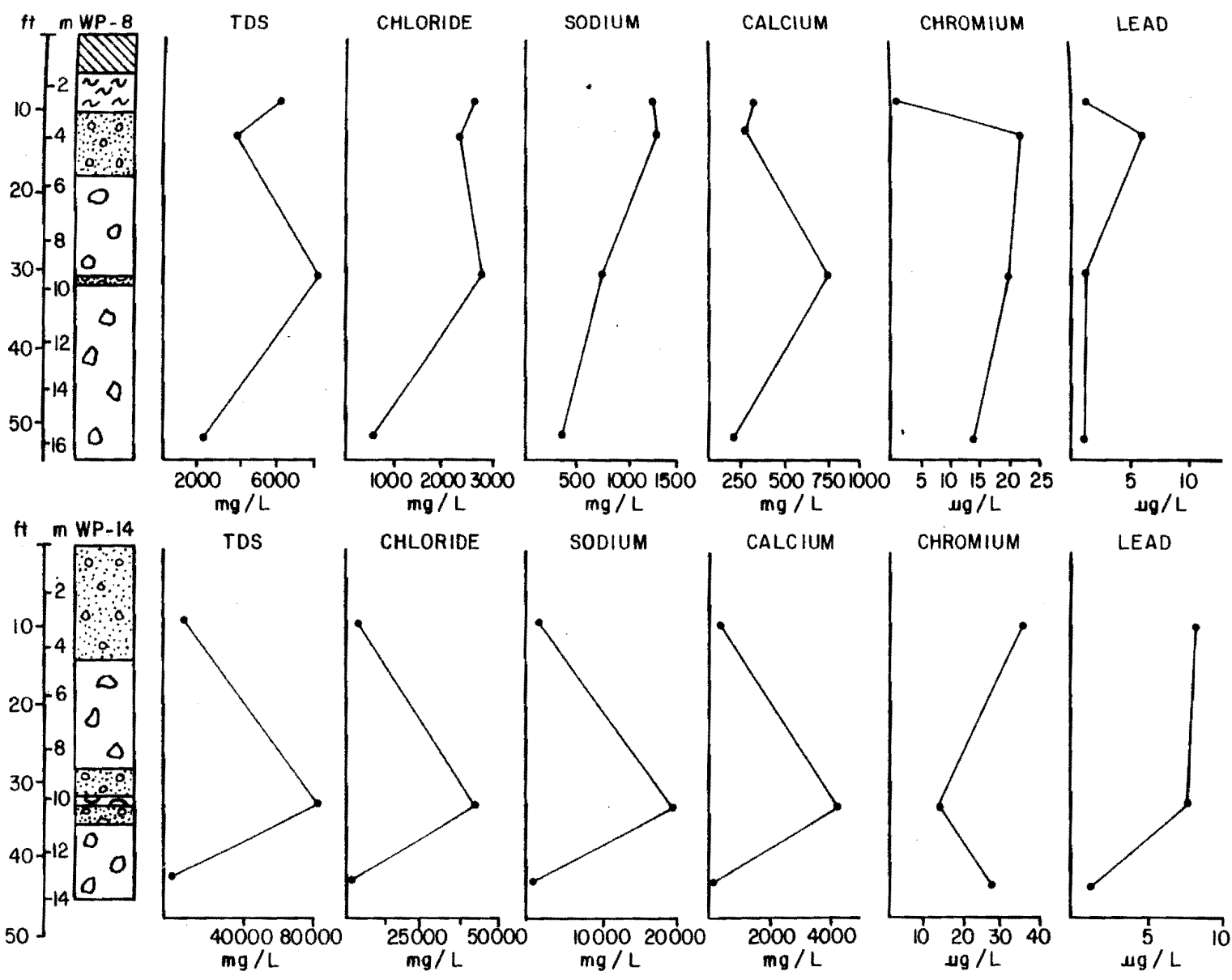


Figure 20. Concentration profiles of total dissolved solids, chloride, sodium, calcium, chromium, and lead in the groundwater at piezometer locations WP-15 and WP-18 at the Winderl site (Fig. 7).

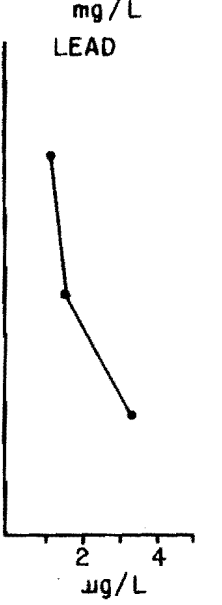
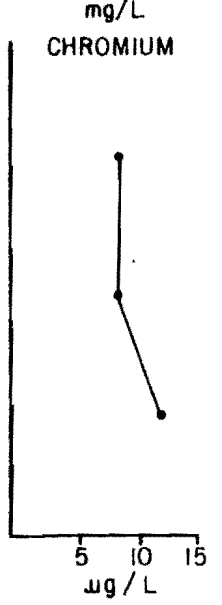
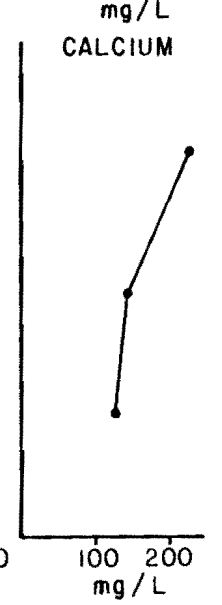
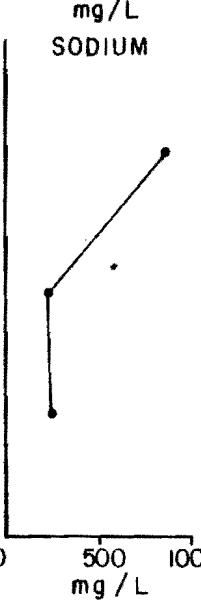
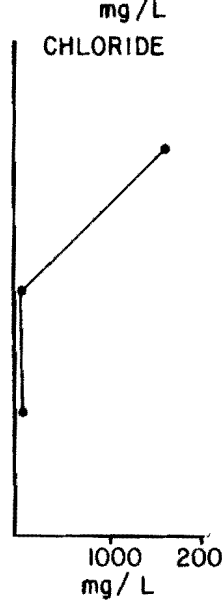
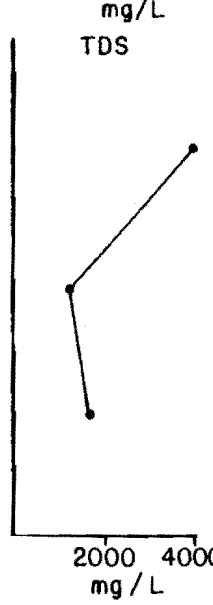
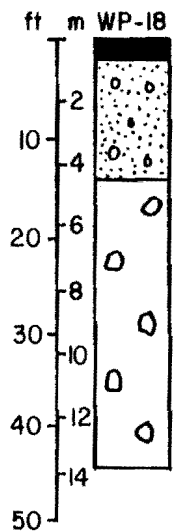
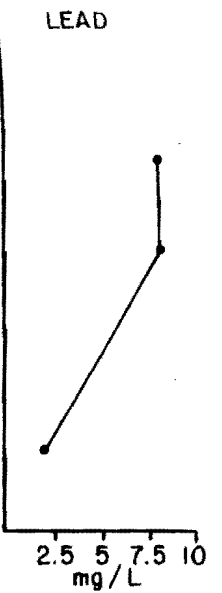
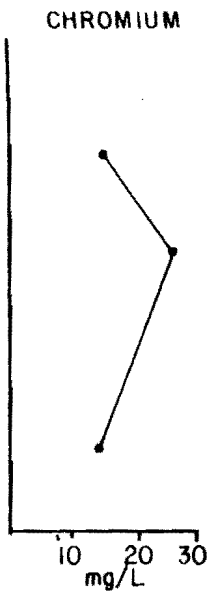
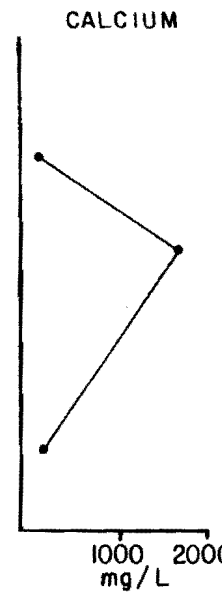
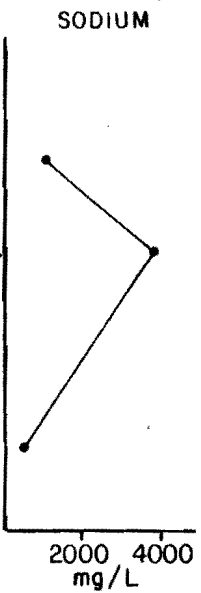
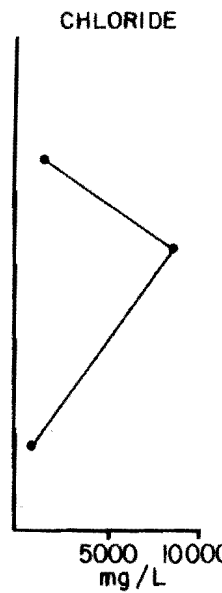
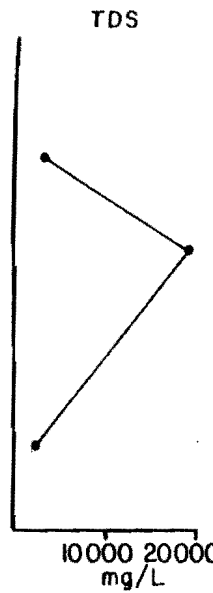
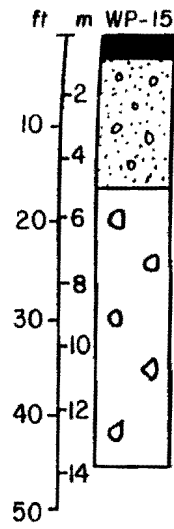
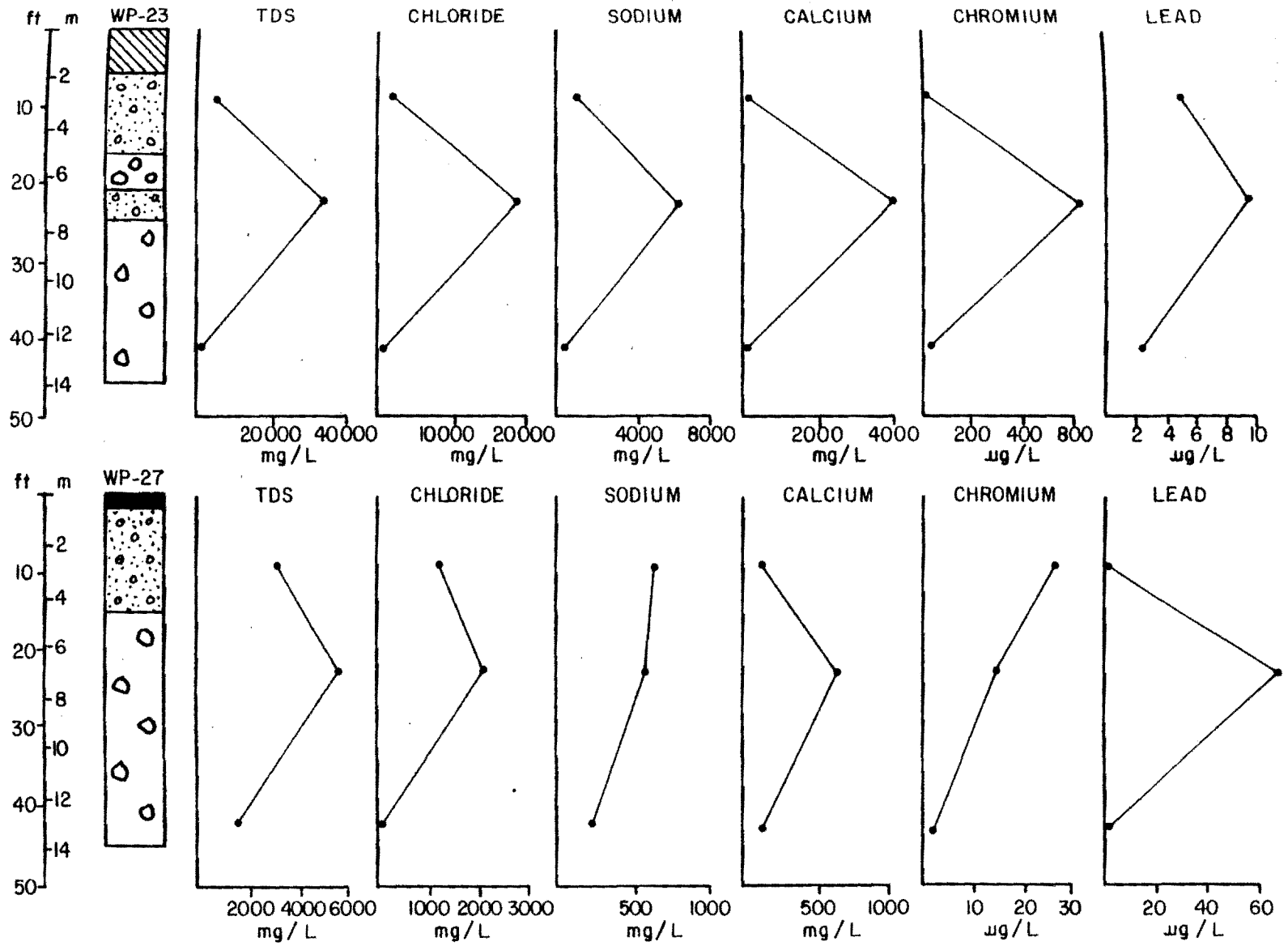


Figure 21. Concentration profiles of total dissolved solids, chloride, sodium, calcium, chromium, and lead in the groundwater at piezometer locations WP-23 and WP-27 at the Winderl site (Fig. 7).



south of the disposal pit, is screened in till and contains groundwater with total dissolved solids of 18,669 mg/L. To put these values in perspective, the average concentration of total dissolved solids in sea water is 34,479 mg/L (Blatt and others, 1980).

The concentration profiles of lead and chromium commonly differ from those of the other indicator parameters, as illustrated by Figures 18-21. The maximum permissible concentrations (MPC) in drinking water for both these parameters is 50 ug/L. The chromium concentrations detected above MPC are from wells in the sand and gravel unit at WP-6 (417 ug/L) and also in an isolated sand lens at WP-22 (635 ug/L). The lead concentrations above MPC were detected in the till at WP-28 (69.5 ug/L).

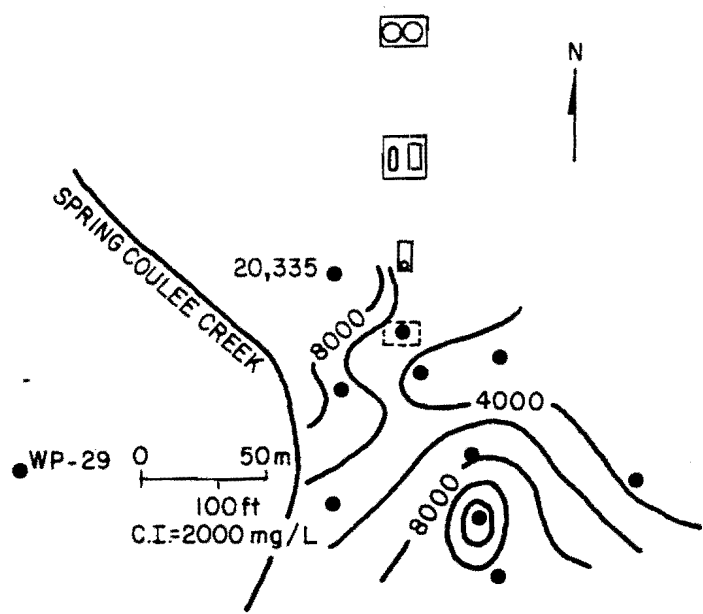
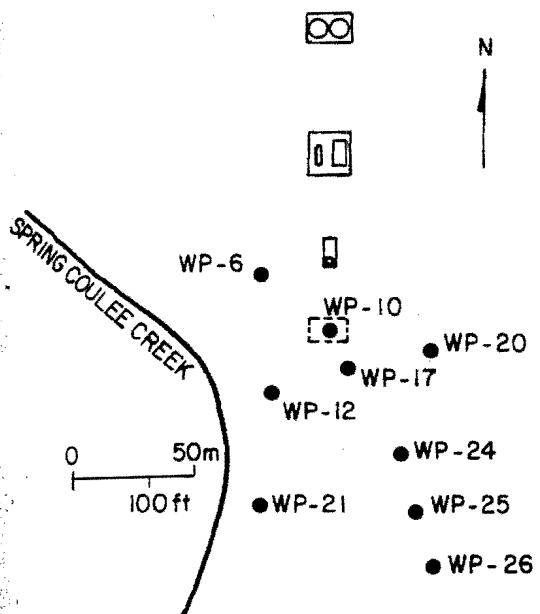
The areal distributions of total dissolved solids, chloride, sodium, calcium, magnesium, chromium, and lead are illustrated with isoconcentration maps of the sand and gravel interval (Figures 22 and 23). The distribution of contamination at the site is discussed in more detail in Section 4.2.1.

3.5.2 Fossum Federal #4

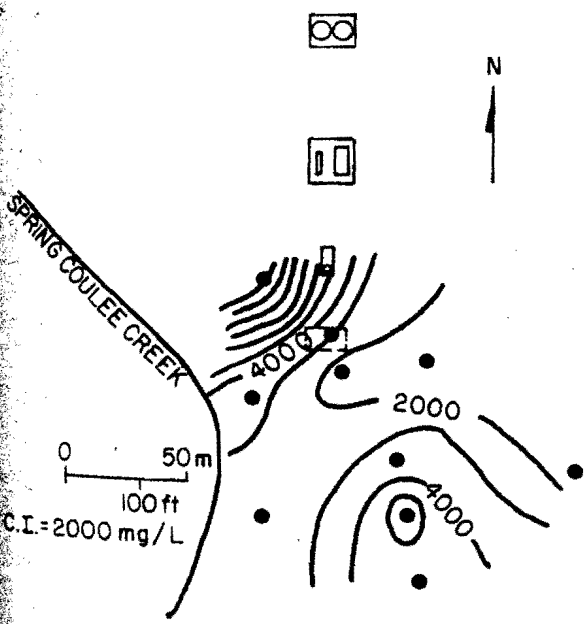
Water samples were collected from the twelve wells at the Fossum site. Eight of the eleven pressure-vacuum lysimeters yielded samples. Because the water table at the site is higher than was estimated during installation of the monitoring equipment, several of these lysimeter samples were collected from the saturated zone.

Similar to the approach taken for the Winderl site, the water chemistry of a background sample at the Fossum site is compared to the chemistry of a sample from beneath the disposal pit (Table 4). The background sample (FL-1) was collected from a lysimeter and the sample beneath the disposal pit (FL-9) was also from a lysimeter; both FL-1 and

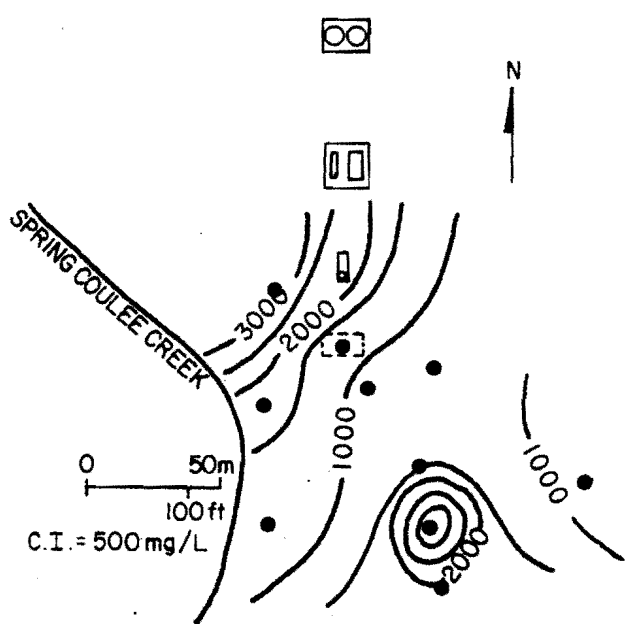
Figure 22. Piezometer location map and isoconcentration maps of total dissolved solids, chloride, and sodium in groundwater at the Winderl site.



TDS



CHLORIDE

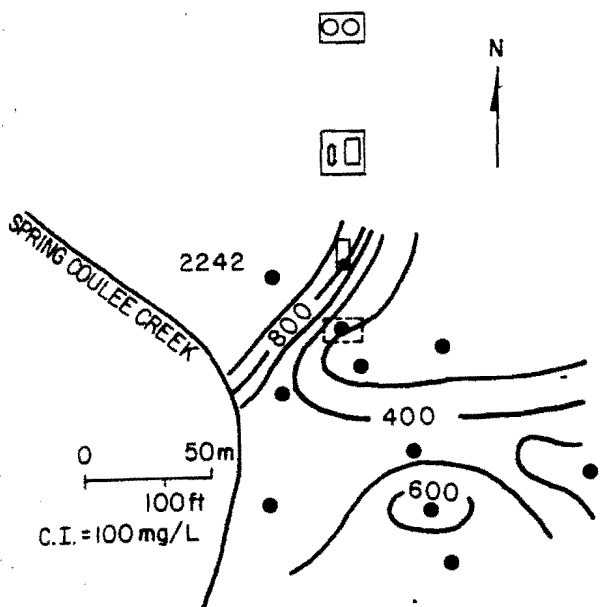


SODIUM

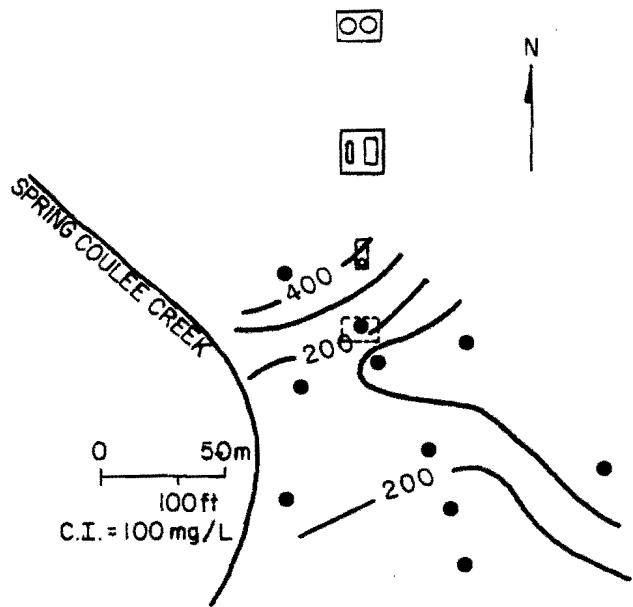
C.I.=2000 mg/L

C.I.=500 mg/L

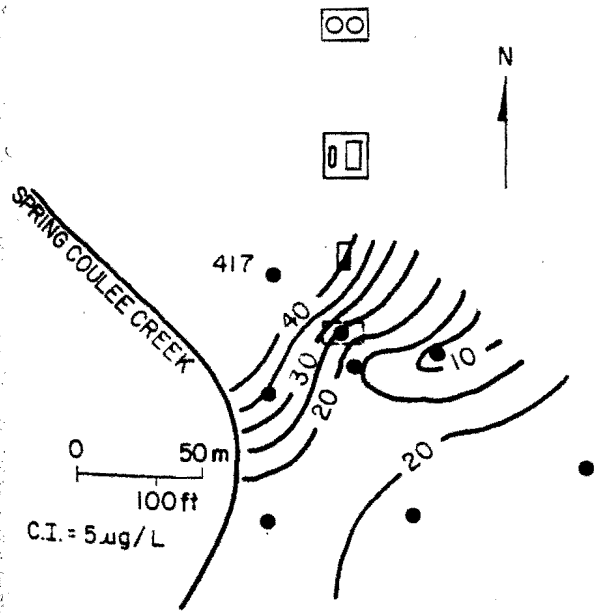
Figure 23. Isoconcentration maps of calcium, magnesium, chromium, and lead in groundwater at the Winderl site.



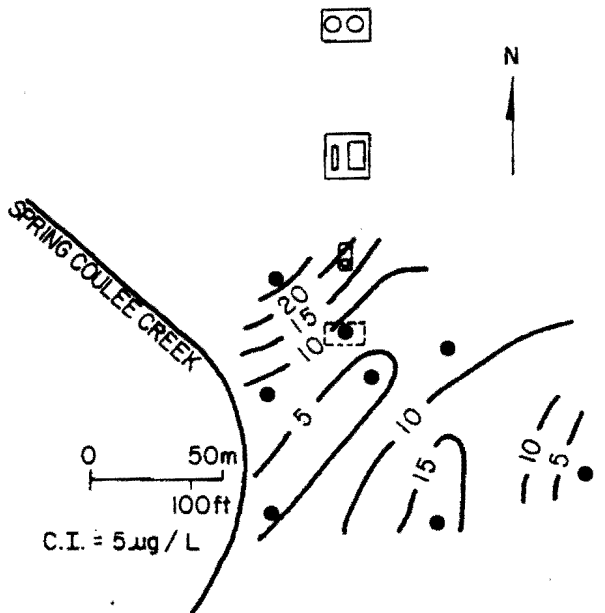
CALCIUM



MAGNESIUM



CHROMIUM



LEAD

TABLE 4

Chemical Analyses of Pore Water/Groundwater from
Lysimeters FL-1 and FL-9 at the Fossum Site
Locations of Lysimeters are Shown on Figure 10

Well Number	FL-1	FL-9
Date	10-23-84	10-23-84
Temperature °C	7.2	8
Field pH	6.87	6.56
Field Conductivity (μ mhos/cm)	1300	>20000
Lab pH @ 22°C	7.5	6.5
Lab Conductivity (μ mhos/cm)	3151	90624
TDS (mg/L)	3268	123684
Hardness (mg/L)	1986	19006
Alkalinity (mg/L)	271	272
Ca (mg/L)	419	3797
Mg (mg/L)	228	2313
Na (mg/L)	178	38348
K (mg/L)	25	1497
SO ₄ (mg/L)	1664	2231
Cl (mg/L)	165	73280
NO ₃ (mg/L)	0.2	---

FL-9 are below the water table at a depth of 14 feet (4.3 m) beneath the surface. In addition, Table 4 also lists the recommended permissible concentrations for sulfate, chloride, iron, and manganese and the maximum permissible concentrations for lead and chromium.

Table 4 indicates that the leachate generated from the buried disposal pit has increased total dissolved solids, hardness, calcium, magnesium, sodium, potassium, sulfate, and chloride. The six parameters selected to indicate contamination include total dissolved solids, chloride, sodium, calcium, chromium, and sulfate. At the Winderl site, lead was selected rather than sulfate; however, at Fossum the relatively high concentrations of sulfate in FL-9 (2231 mg/L) and low concentrations of lead in all the wells (<10 ug/L) suggest that sulfate will better define contamination from the disposal pit.

Concentration profiles illustrating variations in the concentrations of the indicator parameters with depth are presented in Figures 24-26. The highest concentrations of five of the indicator parameters were detected in FL-9, (TDS=123,684 mg/L, Cl=73,280 mg/L, Na=38,348 mg/L, Ca=3797 mg/L, and Mg=2231 mg/L) with values generally decreasing both with depth and distance from the disposal pit. One notable exception is the high sulfate concentrations detected from a lysimeter situated 4 feet (1.3 m) deep and approximately 50 feet (15.2 m) north of the disposal pit (FL-6 (20,236 mg/L)). For comparison, 3577 mg/L of sulfate was detected in pore water from a lysimeter (FL-7) situated at a depth of 4 ft (1.3 m) within the disposal area.

Similar to the Winderl site, the areal distribution of contaminants is illustrated with isoconcentration maps, which are presented in Figures 27 and 28. These maps were constructed from the water analyses of the

Figure 24. Concentration profiles of total dissolved solids, chloride, sodium, calcium, sulfate, and chromium in the groundwater at piezometer locations FP-1 and FP-3 at the Fossum site (Fig. 10). See Figure 11 legend for lithology.

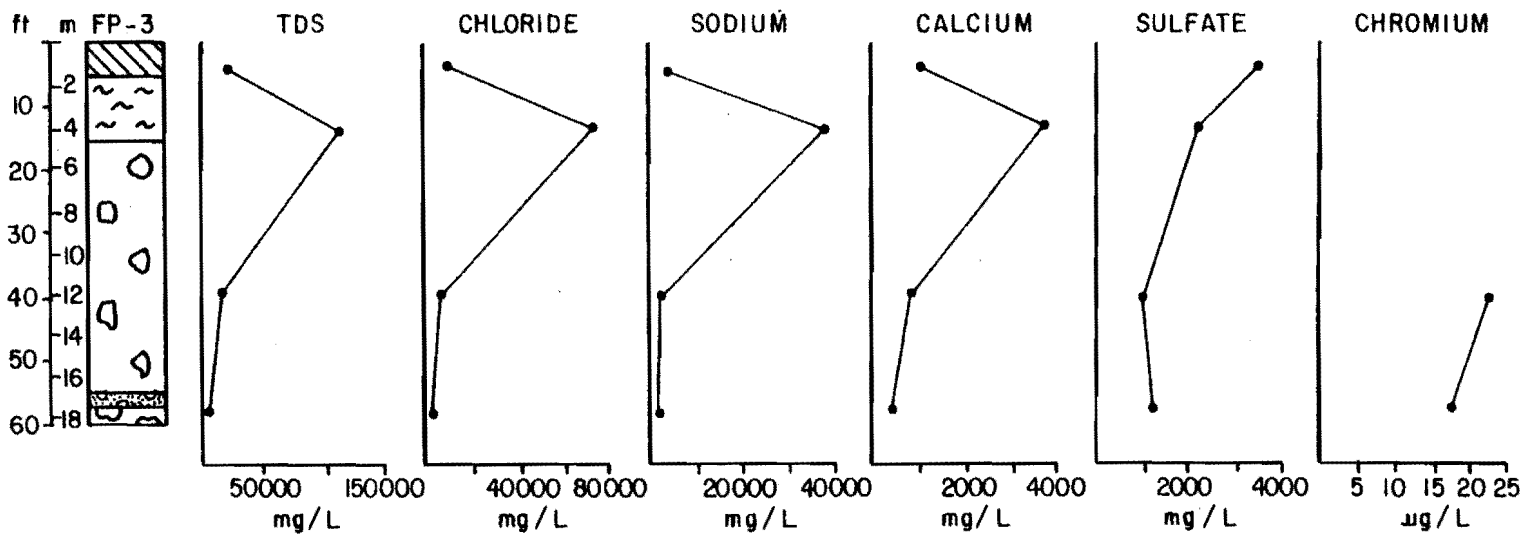
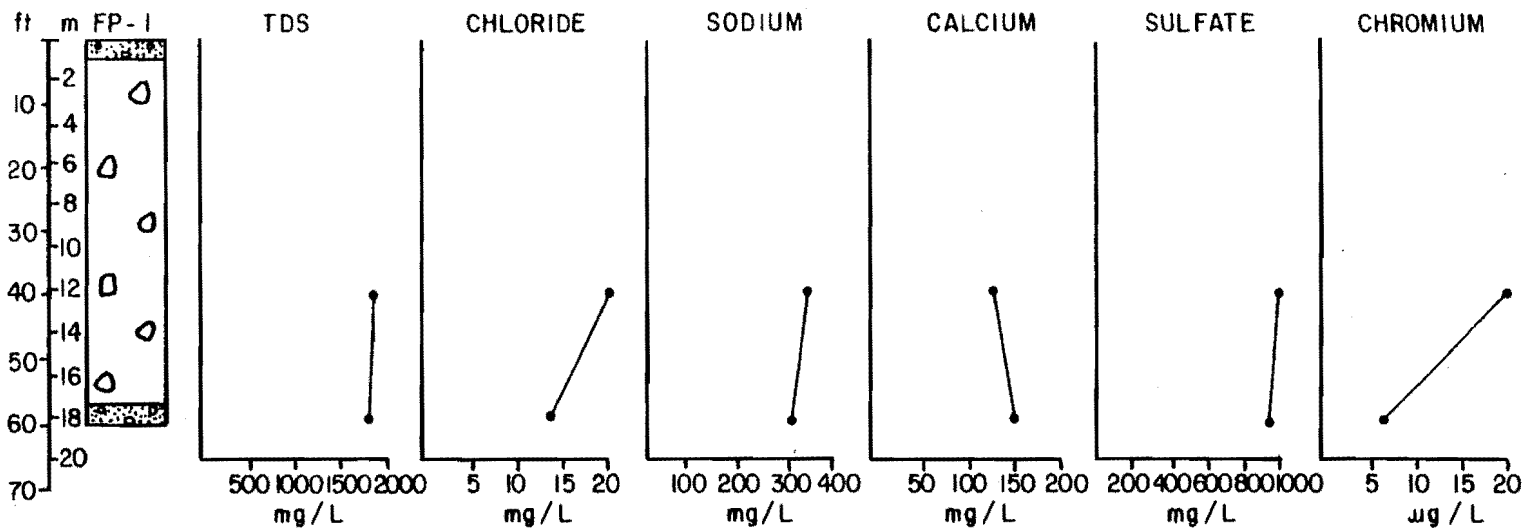


Figure 25. Concentration profiles of total dissolved solids, chloride, sodium, calcium, sulfate, and chromium in the groundwater at piezometer locations FP-5 and FP-7 at the Fossum site (Fig. 10).

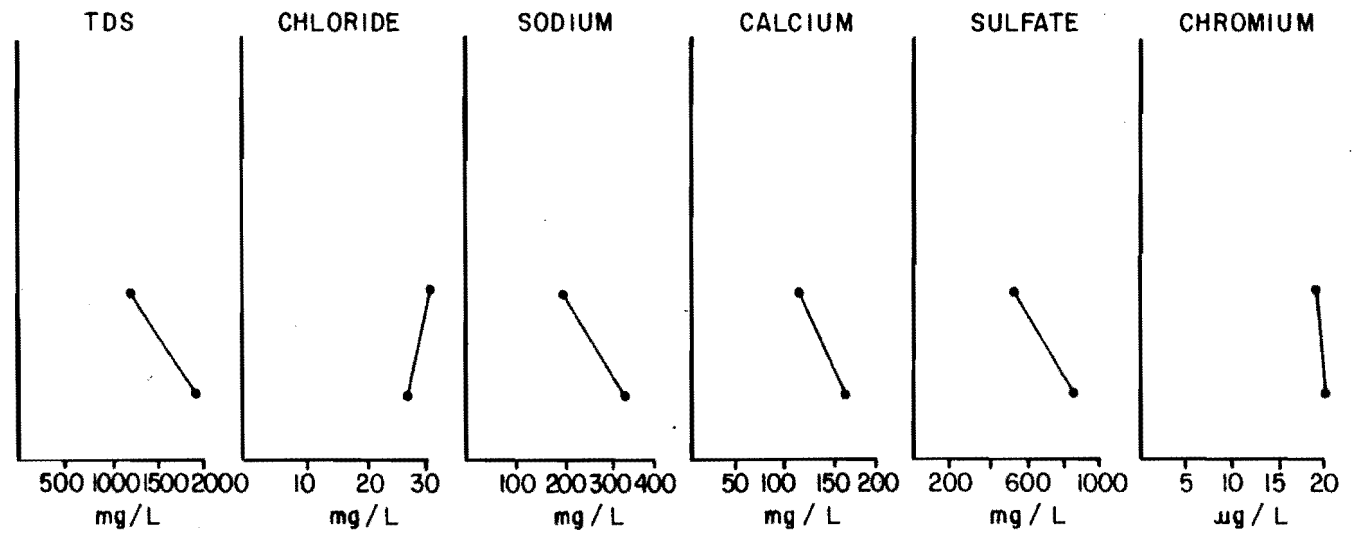
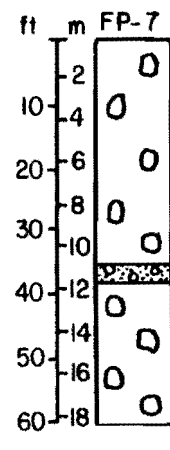
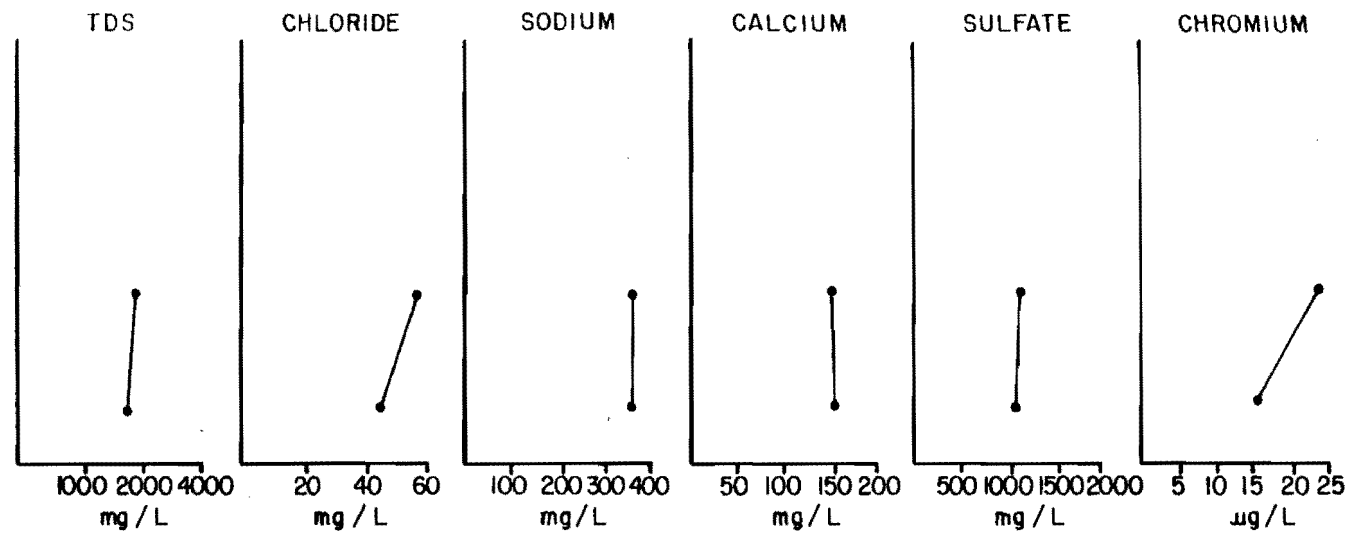
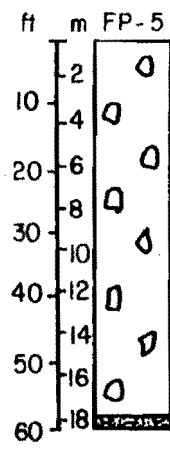


Figure 26. Concentration profiles of total dissolved solids, chloride, sodium, calcium, sulfate, and chromium in the groundwater at piezometer locations FP-9 and FP-12 at the Fossum site (Fig. 10).

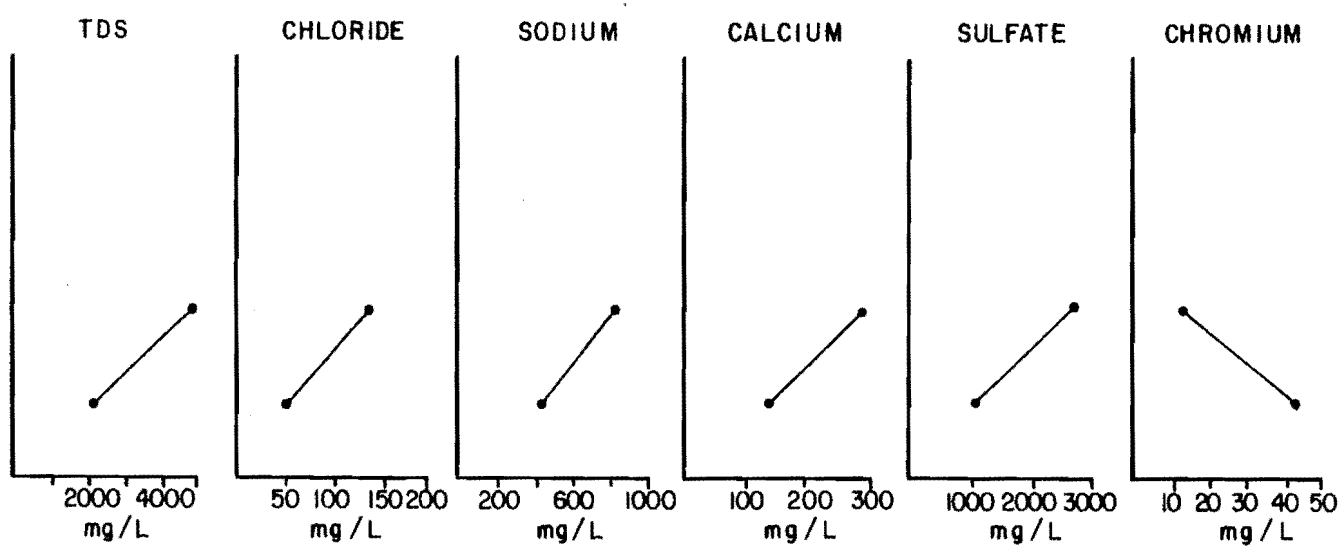
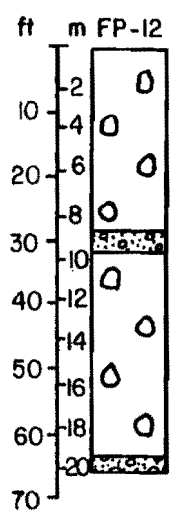
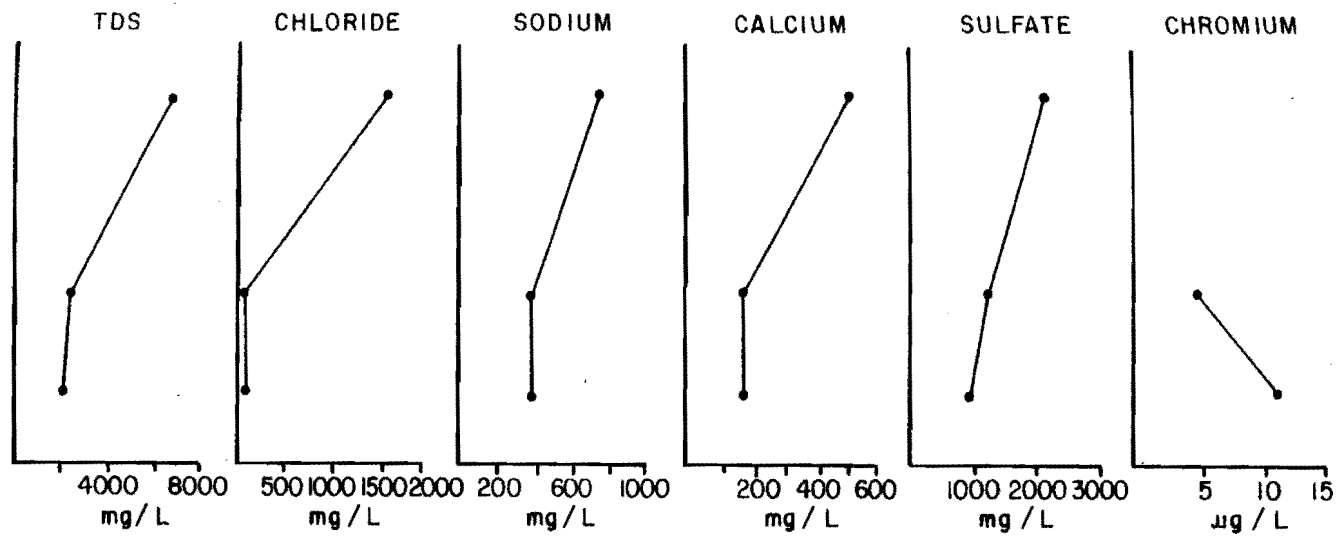
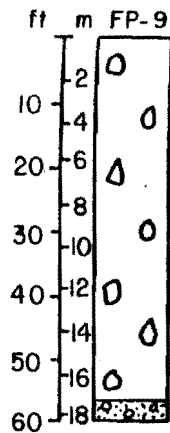
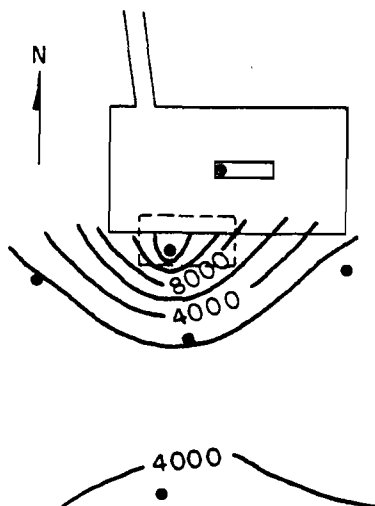
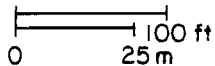
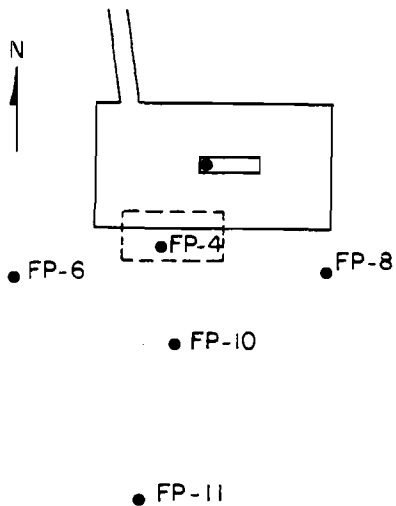
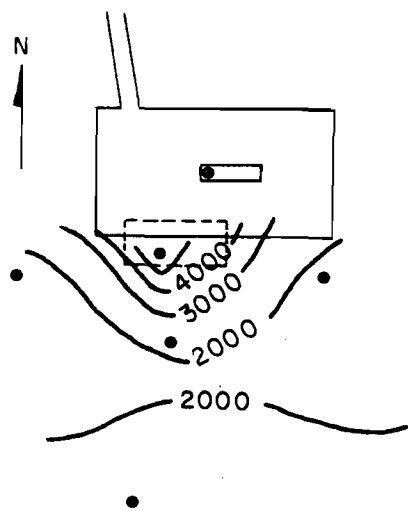


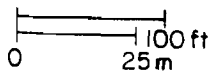
Figure 27. Piezometer location map and isoconcentration maps of total dissolved solids, chloride, and sodium in groundwater at the Fossum site.



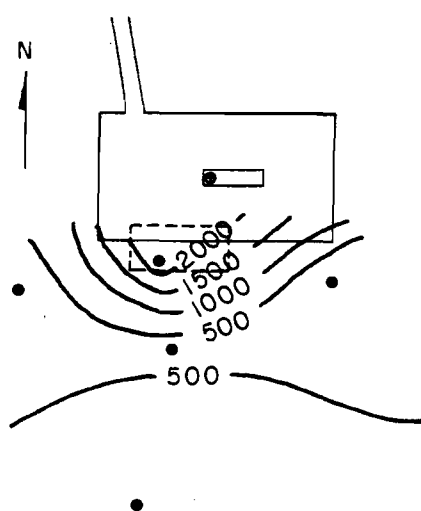
TDS



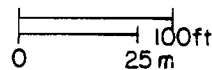
CHLORIDE



C.I. = 1000 mg/L

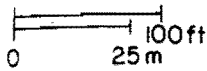
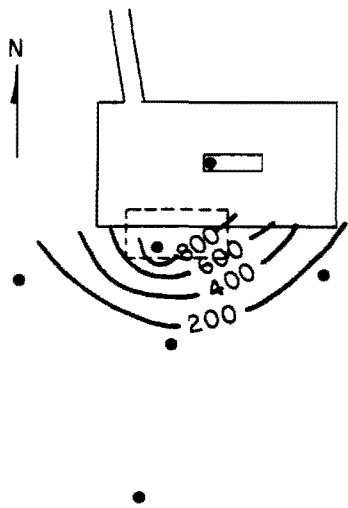


SODIUM



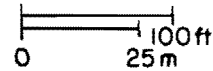
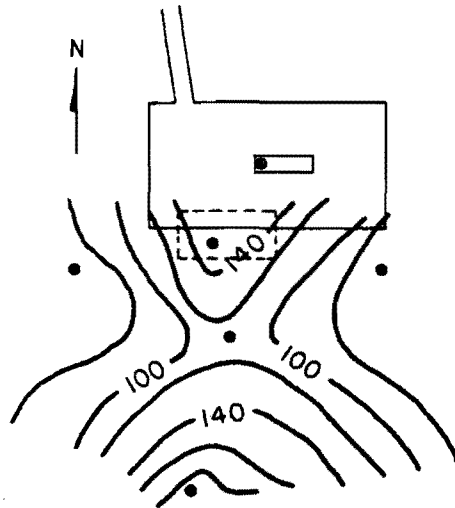
C.I. = 500 mg/L

Figure 28. Isoconcentration maps of calcium, magnesium, sulfate, and chromium in groundwater at the Fossum site.



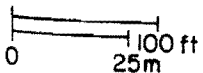
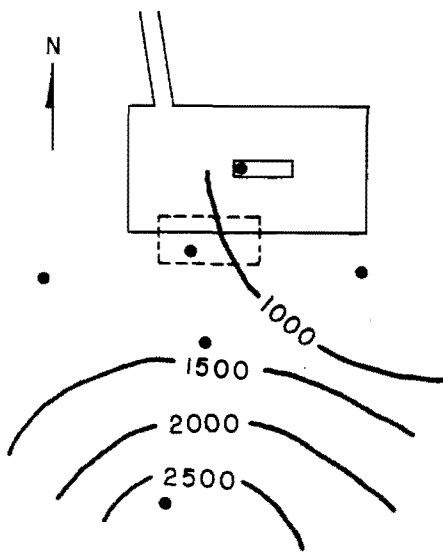
C.I. = 200 mg/L

CALCIUM



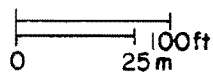
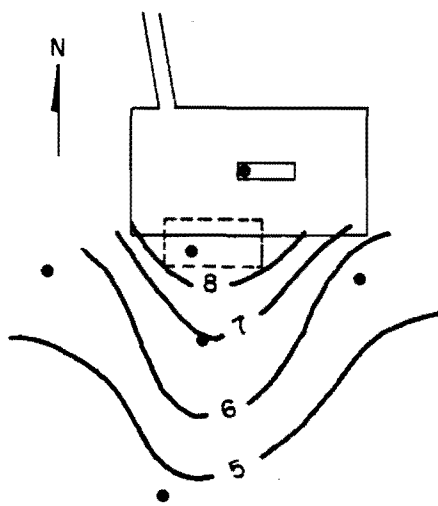
C.I. = 20 mg/L

MAGNESIUM



C.I. = 500 mg/L

SULFATE



C.I. = 1 µg/L

CHROMIUM

wells screened in the upper interval of the piezometer nests. Chloride is a good indicator of contamination at the Fossum site. The chloride concentrations detected beneath the disposal pit (FP-4) are 5025 mg/L compared to a background concentration of 20 mg/L from FP-2. Wells FP-2 and FP-4 are screened at approximately the same depth (45 to 35 feet (13.7 to 10.7 m) below the surface). Chloride concentrations of 2203 mg/L were detected from the deep well (FP-3) screened 60 to 55 feet (18.3 to 16.8 m) beneath the surface at the disposal pit. Approximately 200 feet (61.0 m) south of the disposal pit, 146 mg/L of chloride was detected at FP-11. The remainder of the wells yielded chloride concentrations of less than 60 mg/L. As discussed in previous sections, the wells are screened significantly below the water table. As a result, these isoconcentration maps might not be a good indicator of the horizontal distribution of contamination. The distribution and extent of contamination at the Fossum site is discussed further in Section 4.4.

3.6 Saturated-Paste Extract

Information on the soil-water chemistry of selected sediment samples was obtained by saturated-paste extract analyses. One sample (WP-9) was analyzed from the Winderl site--a split-tube sample collected at a depth of 18.5 feet (5.6 m) beneath the surface. A total of 20 Shelby-tube samples from the Fossum site was analyzed. These samples were collected at depths ranging from 5 ft (1.5 m) to 30 ft (9.1 m) below the surface. The results of these analyses are presented in Appendix N.

The saturated-paste extract analyses from the Fossum site are plotted on vertical distribution diagrams for six parameters: electrical conductivity, chloride, sodium, calcium, magnesium, and sulfate (Figures 29-31). In general, there is an abrupt decrease in contamination with

Figure 29. Concentration profiles of electrical conductivity, chloride, sodium, magnesium, and sulfate from saturated-paste extract analyses of Shelby-tube samples FS-2 and FS-3 at the Fossum site (Fig. 10). See Figure 11 legend for lithology.

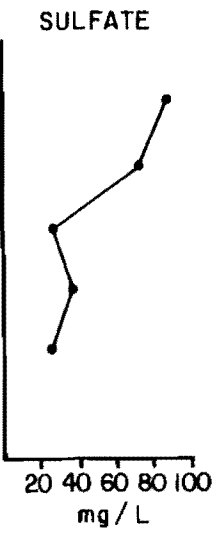
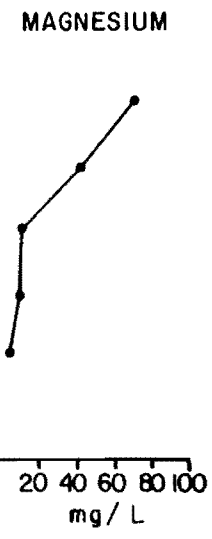
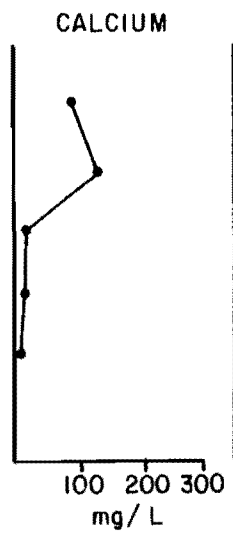
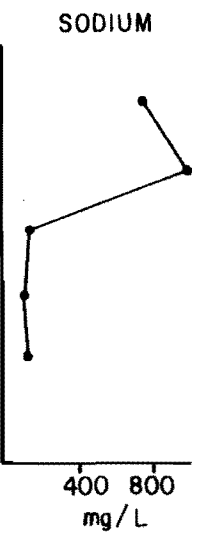
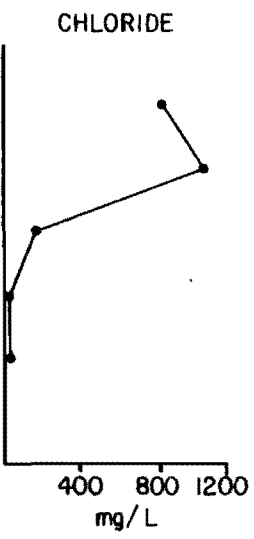
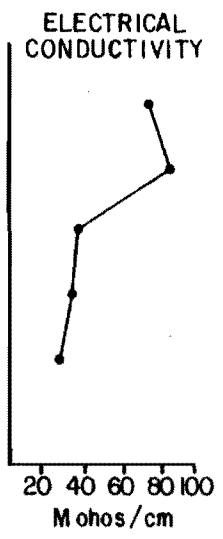
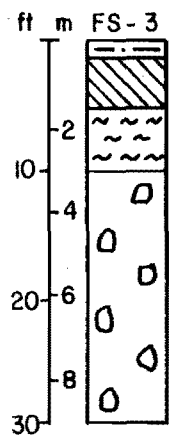
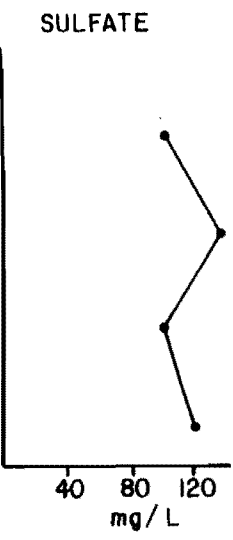
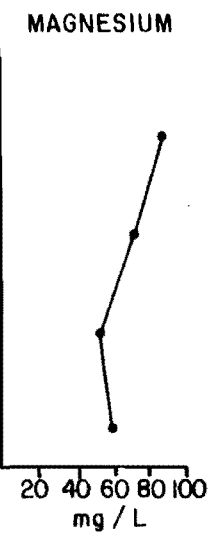
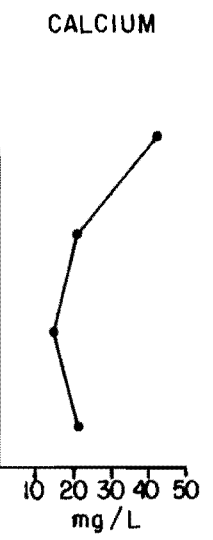
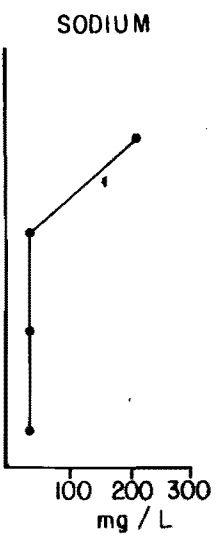
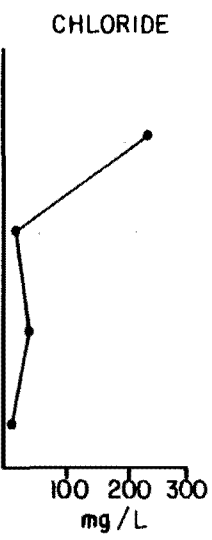
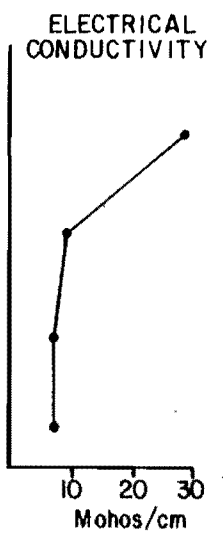
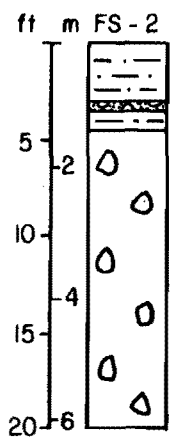


Figure 30. Concentration profiles of electrical conductivity, chloride, sodium, magnesium, and sulfate from saturated-paste extract analyses of Shelby-tube samples FS-5 and FS-6 at the Fossum site (Fig. 10).

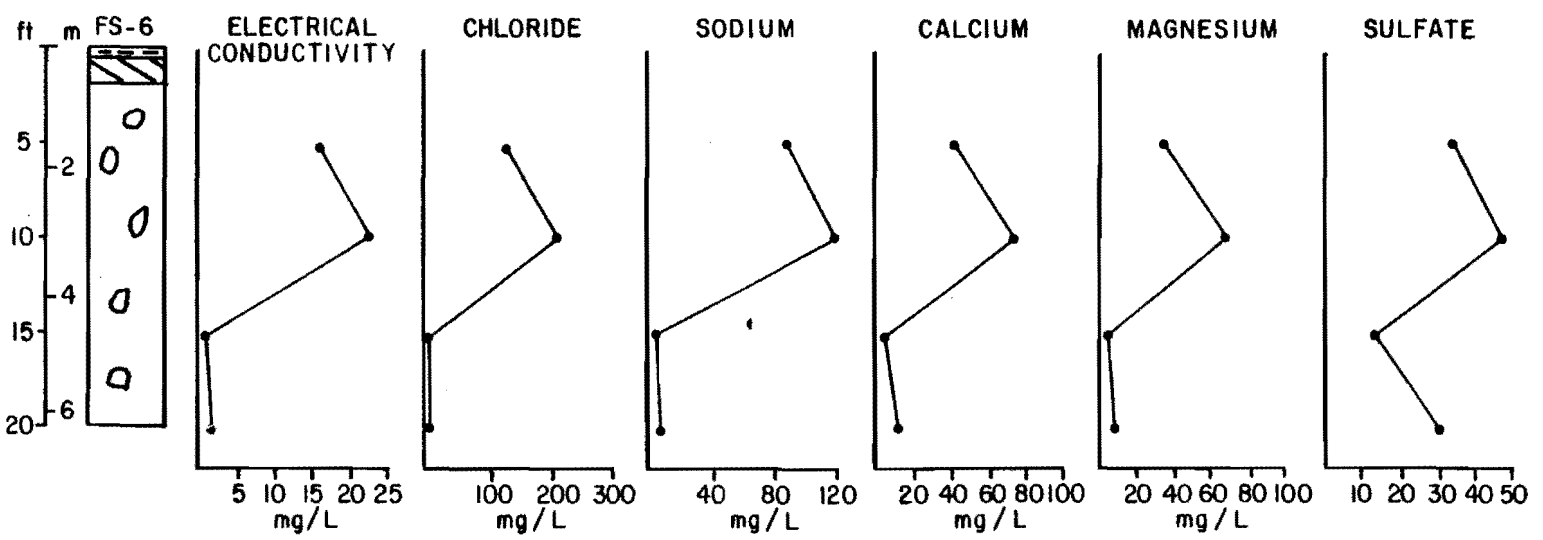
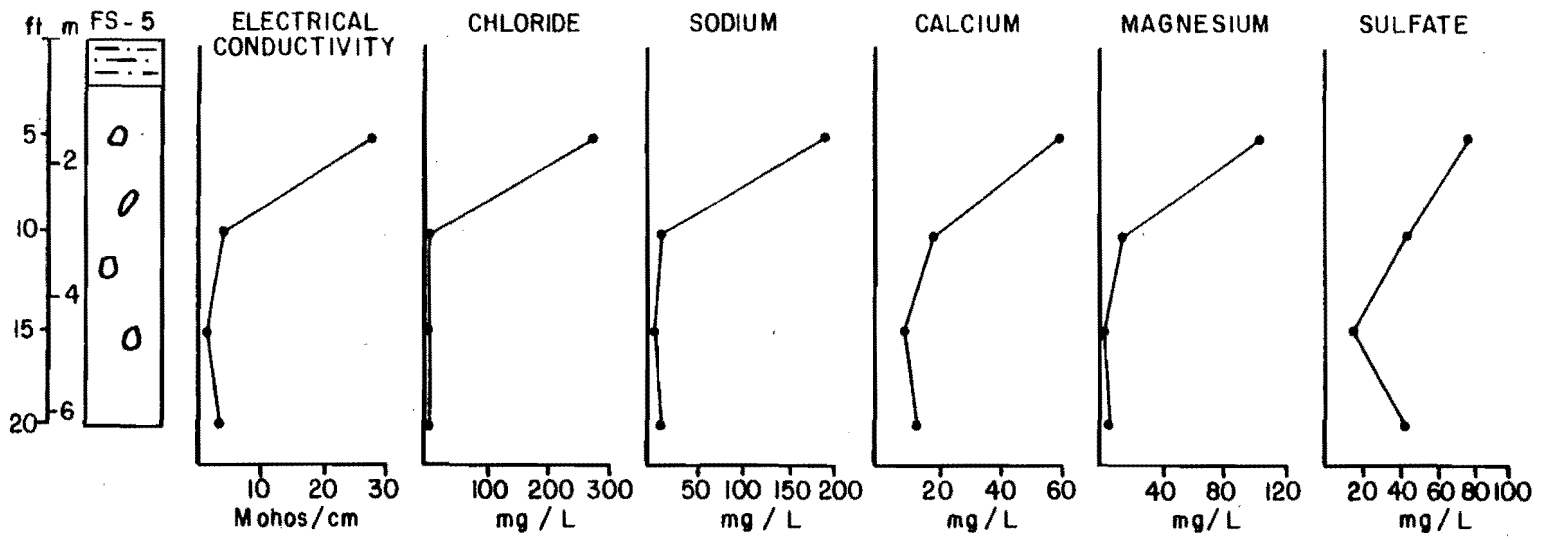
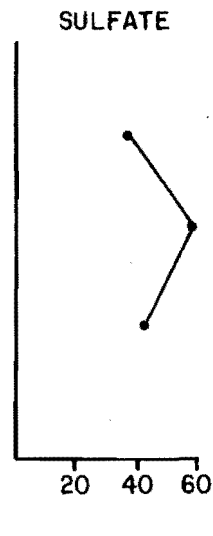
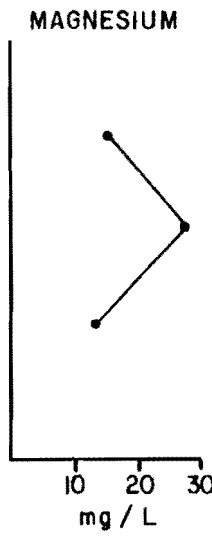
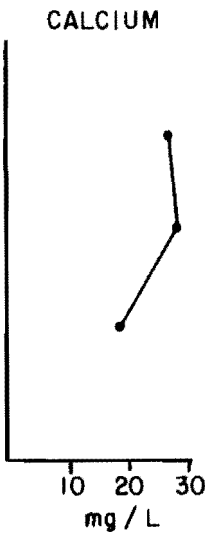
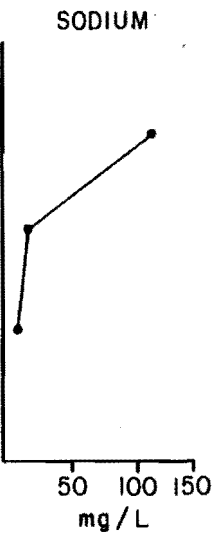
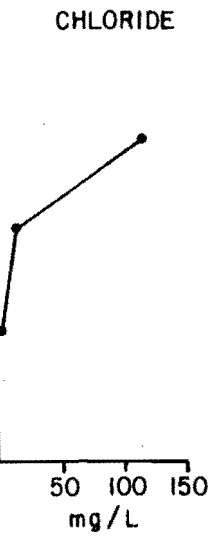
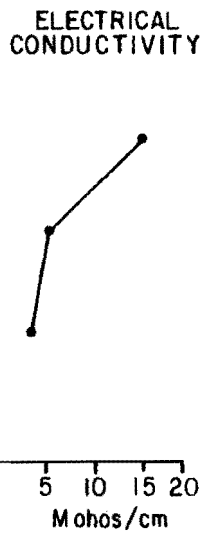
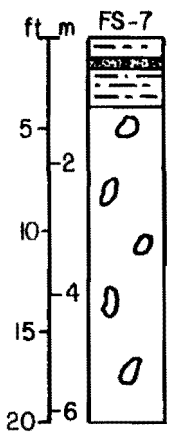


Figure 31. Concentration profiles of electrical conductivity, chloride, sodium, magnesium, and sulfate from saturated-paste extract analyses of Shelby-tube samples FS-7 at the Fossum site (Fig. 10).



depth. Boring FS-3 was drilled directly through the disposal pit and the chloride concentration decreases from a maximum of 1111 mg/L at a depth of 10 ft (3.0 m) to 2.54 mg/L at a depth of 20 feet (6.1 m). There is a similar vertical relationship for the other parameters.

Laterally, the concentrations of the contaminants decrease with distance from the buried disposal pit. The maximum chloride concentration detected beyond 60 ft (18.3 m) of the disposal pit was 122 mg/L at FS-7. Sulfate is an exception to this trend. The highest sulfate concentration detected in the saturated paste extract samples (130 mg/L) was approximately 40 ft (12.2 m) northwest of the disposal pit at FS-2.

3.7 XRF Experiment

Sediment samples, obtained from Shelby tubes, were prepared for XRF major ion and trace-metal analysis in the Natural Materials Analytical Laboratory at the University of North Dakota. The XRF results are presented in Appendix O. Unfortunately, NMAL is still in the process of developing reliable standards, and at the time this thesis was prepared the data were not reproducible. Although presented in the appendices, the XRF results are not discussed further in the text.

4.0 DISCUSSION

4.1 Characterization of Contaminant

Several attempts to obtain the drilling-mud chemistry from both disposal pits were unsuccessful. Chevron Inc., the owner of the Fossum and Winderl wells, was contacted; however, they were unable to provide any chemical data. Without the specific chemistry of the drilling muds, the chemical analyses of water and soil samples around the pit site can be utilized to obtain some indication of the chemistry of the drilling mud.

Results from the chemical analyses of both water and soil samples, which are presented in Section 3, indicate that the major chemical constituents of the contaminant are sodium and chloride with lesser amounts of calcium, magnesium, sulfate, and potassium. As discussed in Section 1.2, the muds in North Dakota are salt-based, which accounts for the high concentrations of sodium and chloride. The produced brines that are commonly added to the muds may contain many of the other major ions that constitute the contaminant. Table 5 summarizes the chemical analyses of the brines from drill-stem tests conducted near the two study sites.

Chromium and lead, which were both detected above maximum permissible concentrations, are common constituents of drilling muds. Chromium lignosulfate is a corrosion inhibitor, and lead compounds can be added to the muds as a weighting material (Murphy and Kehew, 1984). The concentration of these trace metals, as well as the other ions, is not only a function of the character of the contaminant, but also the

TABLE 5

Chemical Analyses of Brines from the Madison Formation in the Wylie Field, Bottineau County. Data Obtained from Drill-Stem Tests.

Temp	Res	pH	TDS (mg/L)	Ca (mg/L)	Mg (mg/L)	Na (mg/L)	Fe (mg/L)	Cl (mg/L)	CO ₃ (mg/L)	HCO ₃ (mg/L)	SO ₄ (mg/L)
68	55	7.0	203,519	3934	1020	72,914	0	122,000	0	195	2200
68	52	6.8	214,018	3934	1190	77,111	0	129,000	0	98	1725
68	61	6.4	193,017	3919	1187	69,526	0	115,420	0	162	2885
68	91	6.1	112,719	2897	671	39,774	0	65,670	0	148	3634
68	350	6.2	21,287	1348	302	6,141	0	10,250	0	425	3034
68	180	5.8	45,087	2565	696	13,576	0	25,104	0	380	2959
68	49	5.3	258,322	5510	1972	92,435	0	156,900	0	295	1360
68	110	5.4	78,507	3325	870	25,605	0	45,501	0	220	3098
68	52	5.3	216,405	2755	870	80,596	0	129,704	0	280	2369
68	53	5.3	231,463	4940	1566	83,103	0	140,160	0	362	1516
68	55	6.6	228,032	4763	1155	82,565	0	137,900	0	181	1560
68	96	7.0	124,901	5715	2310	39,156	0	75,045	0	82	1835
68	98	7.1	126,597	5334	2310	40,238	0	76,830	0	93	1839
68	650	6.5	253,093	4572	1848	91,580	0	153,660	0	121	1374
68	71	6.6	197,030	5334	1848	68,636	0	119,185	0	88	1984
68	50	7.1	268,036	5130	1903	96,823	0	163,000	0	159	1102
68	57	6.4	212,316	5148	1357	75,584	0	127,660	0	440	2350
68	55	5.8	224,405	5148	1298	80,460	0	135,240	0	425	2050
HIGH	68	650	268,036	5510	2310	96,823	0	163,000	0	440	3634
LOW	68	49	21,287	1348	302	6,141	0	10,250	0	82	1102
MEAN	68	93	182,414	4338	1298	64,535	0	109,686	0	227	2133

geochemical processes occurring in the groundwater flow regime. These processes are discussed in Section 4.3.

The chemistry of drilling muds can be complex, as indicated in Section 1.2. Consequently, not all of the possible chemical constituents of drilling muds were included in the water and soil analyses. In addition, the disposal pits are commonly receptacles for all types of other wastes generated during the well-drilling process. It is important to understand that the results of this study are limited by the uncertainty of the chemical character of the contaminant.

4.2 Solute Transport

Two different approaches are utilized to evaluate the solute transport at the two study sites. The different approaches are necessary due to the different hydrogeologic settings. At the Winderl site, contaminants are thought to migrate primarily in the glaciofluvial sand and gravel deposit, and so the advection-dispersion equation is utilized to analyze the transport of solutes. In contrast, the contaminants at the Fossum site are thought to migrate along the fractures in the till, and not follow the advection-dispersion equation. The groundwater velocity along the fractures is compared with the velocity in the till matrix, and the transport of contaminants is evaluated using information collected from previous studies on contaminant migration through fractured tills.

4.2.1 J.J. Winderl No. 1

The transport of non-reactive solutes in groundwater commonly is described by two processes: advection, or transport due to the bulk movement of the groundwater, and dispersion, which is the spreading out of the contaminant as it flows through the subsurface (Anderson, 1984). Advection will cause the contaminant to travel away from the source in

the direction of groundwater flow. Dispersion results in dilution of the contaminant downgradient as it spreads out over a larger area.

The one-dimensional advection-dispersion equation for non-reactive dissolved constituents in a saturated-homogeneous medium under steady-state conditions can be written as follows:

$$D \frac{\partial^2 C}{\partial l^2} - \bar{v} \frac{\partial C}{\partial l} = \frac{\partial C}{\partial t} ,$$

where t is time, l is the groundwater flow direction, C is the concentration of solute, \bar{v} is the average linear velocity, and D is the coefficient of hydrodynamic dispersion. The hydrodynamic dispersion coefficient has two components, dispersivity and diffusion. Except for very fine-grained sediments, diffusion is considered negligible.

This one-dimensional equation is utilized to evaluate solute transport in the Spring Coulee Creek Aquifer at the Winderl site. With a hydraulic conductivity (K) of 8.4×10^{-2} cm/s (the average value from the grain-size distribution curves in Appendix J), a porosity (n) of 0.25, and a gradient (i) of 0.001 (obtained from the October 1984 water table map), the average linear velocity (\bar{v}) is calculated from the following equation:

$$\bar{v} = \frac{K i}{n} ,$$

yielding a value of 0.29 m/day (0.95 ft/day).

The dispersivity parameter controls the degree of spreading and dilution of a solute plume. Dispersivity is related to the heterogeneity of a unit and also the scale of observation. Accordingly, to quantify dispersivity accurately, field tracer tests should be conducted, which are beyond the scope of this study. Gelhar and others (1985) present results of several investigations with field tracer tests to estimate

dispersivity in glaciofluvial sediments. These results were utilized to select three different dispersivity values (1m, 25m and 100m) that are thought to create a range that includes the dispersivity of the Spring Coulee Creek Aquifer at the scale of this investigation.

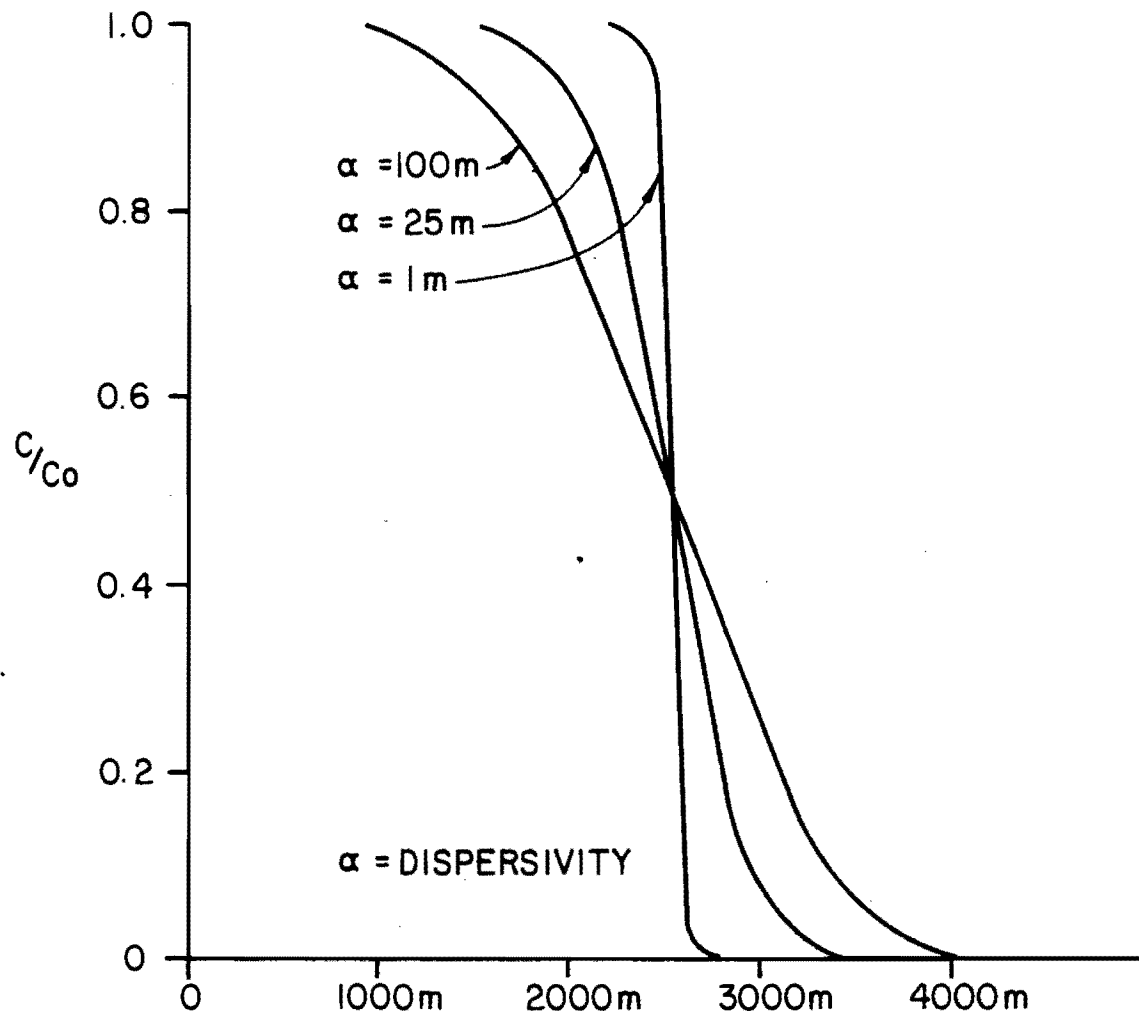
A computer program, ODAST (Javandel and others, 1984), was utilized to solve this one-dimensional equation. It was assumed that a point source had been active from 1960 to 1984. Breakthrough curves that depict the theoretical distribution of the contaminant with distance are presented in Figure 32. These curves illustrate the potential for widespread contamination within the Spring Coulee Creek Aquifer. The analytical solution predicts concentrations of non-reactive constituents that approach the concentration at the source at distances up to 3280 and 7218 feet (1000 to 2200 m) downgradient from the buried disposal pit, for dispersivities of 1 metre and 100 metres, respectively.

Several problems are inherent with the one-dimensional analytical solution approach. A homogeneous isotropic medium with steady-state flow is never duplicated in actual situations. Also, the disposal pit at the Winderl site probably does not act as a continuous point source, but rather has diminished in concentration with time. Concentrations in the vicinity of the disposal pit are less than other areas at the study site, which indicates the source of contamination has been diluted.

4.2.2 Fossum Federal No. 4

The lithologic and hydrologic data from the Fossum site indicate that fractures in the till cause permeabilities several orders of magnitude greater than is indicated by the grain size of the till matrix. As a result, the groundwater-flow velocity through these fractures is orders of magnitude greater than the velocity through the till matrix.

Figure 32. Hypothetical breakthrough curves at the Winderl site for the transport of non-reactive solutes at dispersivities of 1 m, 25 m, and 100 m. C/C_0 is the ratio of the concentration at any point in the flow system (C) to the original concentration at the source (C_0).



The average linear velocity is determined by dividing the specific discharge (the hydraulic conductivity times the gradient) by the porosity (the fracture porosity is much less than the intergranular porosity). Grisak (1975) suggests values for fracture porosity on the order of 2×10^{-4} . With an average hydraulic conductivity from the Fossum site of 1.8×10^{-5} cm/s, a gradient of 0.05 (obtained from the October 1984 potentiometric map), and a fracture porosity of 2×10^{-4} , the average linear velocity along the fractures of is 3.8 m/day (12.8 ft/day). The intergranular velocity calculated with the same gradient, a porosity of 0.30, and a hydraulic conductivity of 5.0×10^{-9} cm/s (suggested by Grisak and Cherry (1975)), is 7.2×10^{-7} m/day (2.4×10^{-6} ft/day). Although the groundwater velocity along the fractures is high, the quantity (or flux) of water is low due to the small volume of pore space these fractures constitute.

Several studies have been conducted on the migration of contaminants through fractured till. Experiments by Grisak and others (1980) demonstrated that diffusion in the till matrix is an important retardation mechanism. As the solute migrates along the fractures, solute concentration gradients between the groundwater in the fractures and the till matrix cause diffusion of these solutes into the matrix, and the low intergranular velocity in the matrix prevents any further significant migration. The retardation of contaminants migrating in the fractures, accompanied by the relatively low flux of water associated with fracture permeability, limits the potential for contaminant migration in the fractured tills.

4.3 Geochemical Processes

The movement of solutes in the subsurface is affected by geochemical processes that can cause chemical attenuation and reduce the concentration of the contaminants. Cherry and others (1984, p. 47) identify the major attenuation processes for inorganic contaminants as adsorption and ion exchange, oxidation-reduction, and precipitation. Chloride, the major constituent of the contaminant at both sites, is considered to be relatively unaffected by these processes. However, the other common constituents (i.e., Na, Ca, Mg, and SO_4^{2-}) as well as the trace metals do undergo chemical attenuation. The purpose of this section is to qualitatively relate some of these geochemical processes to the chemical character of the groundwater at the two disposal sites.

Adsorption and ion exchange are major processes that control groundwater chemistry. These reactions are known to occur on colloidal particles, commonly clays, and hydrous oxides on sand grains (Jenne, 1968). Among the constituents of the drilling muds, the concentrations of sodium, calcium, and magnesium are probably most affected by these exchange processes. Because the exact nature of the contaminant was not defined, neither could the extent to which these reactions occur. The elevated concentrations of calcium and magnesium could result from the initial concentrations in the drilling mud or possibly exchange reactions with sodium on colloidal particles. The x-ray diffraction analyses have characterized the clays as predominantly smectite, which have a high cation exchange capacity (Krauskopf, 1979). Additionally, these reactions are known to occur on iron and manganese coatings on sand grains (Jenne, 1968).

Trace metals are also affected by adsorption and ion-exchange reactions. Griffin and others (1976) present results of column leaching experiments that demonstrate the adsorption of trace metals on clay particles. Both lead and chromium participate in these exchange reactions, although their concentrations are largely dependent upon other geochemical processes.

Oxidation and reduction (or redox) reactions can also affect the solute concentrations of the contaminants. Characteristically, the mobility of trace metals is strongly dependent upon the redox conditions of the groundwater. Both lead and chromium are relatively immobile under typical groundwater redox environments.

The mobility of the contaminants will also be affected by solubility controls. As the contaminant travels within the groundwater, precipitation will occur when equilibrium is reached with a solid phase. The solubility is controlled by the concentrations of the species that constitute the solid phase and the thermodynamics of the reactions. Therefore, the concentrations of certain solutes are dependent upon equilibrium between those solutes and a solid phase.

4.4 Distribution and Extent of Contamination

A major objective of this study was to evaluate the areal and vertical extent of contamination that has resulted from leachate migration out of the buried disposal pit. The water chemistry, resistivity, and saturated extract data were utilized for this evaluation.

4.4.1 J.J. Winderl No. 1

As discussed in Section 3.5, the highest concentrations of contamination was detected in the wells screened in the till, rather than the more permeable sand and gravel deposit of the overlying glaciofluvial

channel. In Section 4.2 it was demonstrated that groundwater velocity through these tills can be high; however, the flux of water, thus the mass of contaminants, is low. Also, these contaminants are attenuated by matrix diffusion as they migrate along fractures. There is little potential for downward migration through the sand and gravel because the flow through this unit is predominantly horizontal. It is therefore unlikely that the highest concentrations of contaminants are in the till. A better explanation for the high concentrations in the till groundwater samples is density stratification of the contaminant in the sand and gravel unit, and cross contamination between the two units due to poor well construction.

The high concentration of total dissolved solids in the contaminated groundwater (up to 70,000 mg/L) causes the contaminant plume to be more dense than fresh water. The plume will tend to migrate along the sand and gravel/till contact. Mixing with fresh water and dilution occurs along the front of this plume, but the mixing is not complete, and the result is density stratification of the contaminant.

Density stratification is indicated by the water samples from wells WP-6 and WP-7. These wells are screened at two different intervals in the sand and gravel unit. Well WP-6 is screened from 14.5 ft (4.4 m) to 9.5 ft (2.9 m) below the surface and WP-7 is screened from 4.5 ft (1.4 m) to 9.5 ft (2.9 m) below the surface. The concentration of total dissolved solids in the WP-6 sample is 20,335 mg/L, compared to 14,203 mg/L in the sample from the shallower WP-7. Similarly, among the wells in the marshy area screened in the sand and gravel unit (WP-25, WP-26, and WP-27), the highest concentration of total dissolved solids was detected in the well screened at the greatest depth, rather than the well

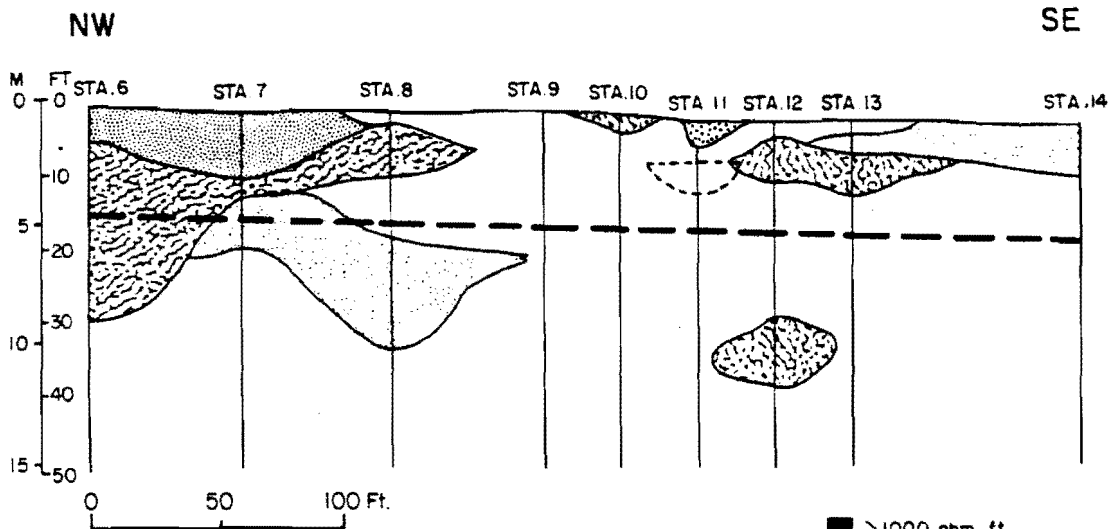
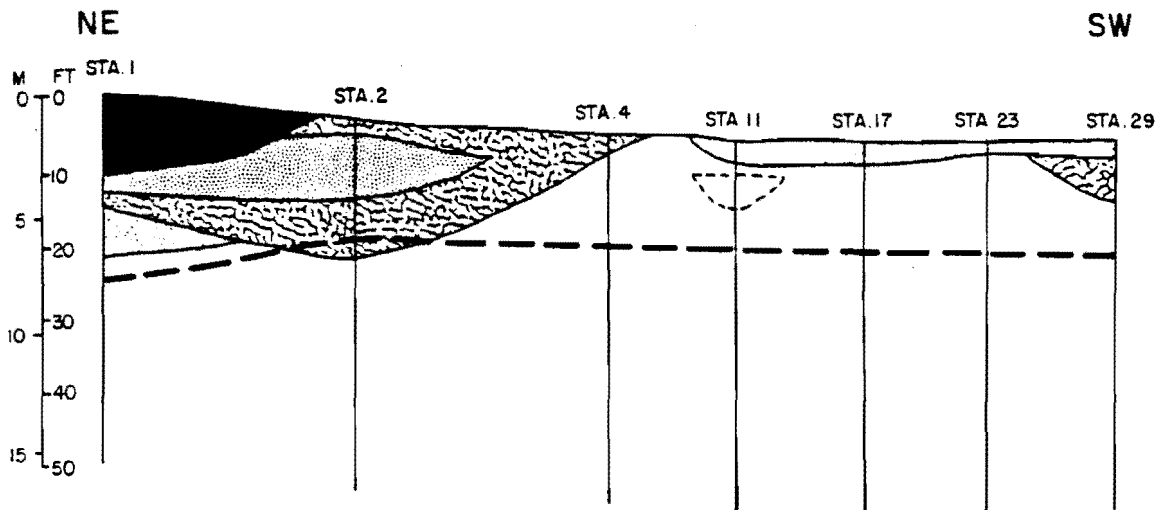
nearest to the contaminant source. In contrast, the shallower well indicated the greater contamination between WP-10 and WP-11. These wells, however, are screened in the disposal area where much of the sand and gravel deposit has been excavated.

The annular space above the well screens, for the wells screened in till, was filled with approximately 2 ft (0.61 m) of cement and then backfilled to the surface with cuttings. The backfill material consisted primarily of sand and gravel. The dense contaminants were probably able to migrate down the annulus and accumulate above the cement layer. A seal from the cement layer is unlikely due to the low volume of cement in the hole, and the fact that the cement was poured from the surface through an annulus filled with saltwater. Purging of the wells before sampling could have allowed for downward migration of contaminants through the cement layer and to the well screen.

The highest concentrations were detected in wells screened in till because samples from the wells screened in the overlying sand and gravel unit are diluted by the "less-contaminated water" collected from above the sand and gravel till contact. Groundwater in the cross-contaminated till wells, on the other hand, is from the annular space above the cement plug where the dense contaminants had accumulated.

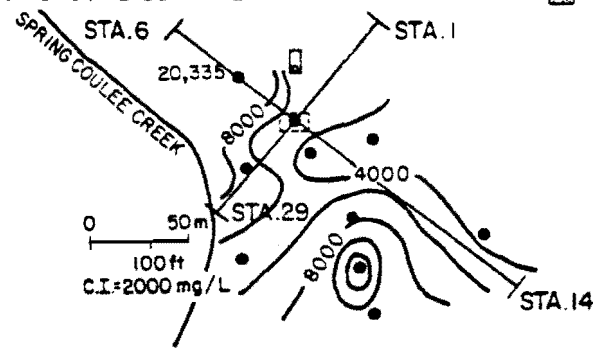
The interpreted resistivity values are utilized to evaluate the distribution of the contaminant at the Winderl site. Two cross sections illustrating Dar-Zarrouk interpreted values of resistivity with depth are presented in Figure 33. For comparison, the isoconcentration map of total dissolved solids is also shown. A layer of high resistivity is indicated in the northeastern part of the study area near station 1 (Figure 33). These high resistivity values are probably a reflection of

Figure 33. Northeast-southwest and northwest-southeast cross-sections of Dar-Zarrouk interpreted resistivity and isoconcentration map of total dissolved solids in groundwater at the Winderl site. See Figure 14 for location of resistivity stations.



- - - - ESTIMATED SAND AND GRAVEL / TILL CONTACT
 - - - - ESTIMATED LOCATION OF DISPOSAL PIT
 NOTES: SEE FIGURE FOR LOCATIONS OF STATIONS
 RELIEF OF GROUND SURFACE IS APPROXIMATE

	> 1000 ohm-ft
	100 - 1000
	50 - 100
	25 - 50
	< 25



the thickening of the sand and gravel unit to the north, and also the higher surface elevation (i.e., thicker unsaturated zone). These lithologic variations tend to mask any variations in resistivity due to groundwater contamination. Figure 33 indicates relatively high resistivity values (100 to 1000 ohm-ft (30.5 to 304.8 ohm-m)) in the northeastern part of the study area near stations 6 and 7. There are no wells or borings in this area so it is not evident whether these resistivity values are a reflection of lithology or groundwater conductivity.

South of the buried disposal pit, the thickness of the sand and gravel unit is relatively uniform and resistivity is thought to be a good contaminant indicator. The cross sections in Figure 33 illustrate that the southern area is interpreted to be underlain primarily by a low-resistivity layer (<50 ohm-ft; 15.2 ohm-m). An isolated area of higher resistivity (50 to 100 ohm-ft; 15.2 to 30.5 ohm-m) is interpreted approximately 5 ft (1.5 m) below the surface, southeast of the disposal pit, near stations 12 and 13. The TDS plume map (Figure 33) also shows a decrease in the concentration of contaminants within this area. It is not clear, however, whether the lower TDS values are the cause of the higher resistivity. Regardless, the interpreted resistivity values to the south of the disposal pit are significantly below the 1000 to 10,000 ohm-ft (304.8 to 3048 ohm-m) typical of sand and gravel units (Soiltest, 1968). Both the interpreted resistivity cross-sections and the TDS plume map support the conclusion that contaminants have migrated beyond the limits of the study area (Figure 33) to the south and west to Spring Coulee Creek. A reduction in the contamination occurs to the southeast, but TDS values in this area are still above the recommended drinking water standard of 500 mg/L, and also above the TDS value reported as 1700

mg/L, typical for glaciofluvial aquifers in the region (Randich and Kuzniar, 1984).

The extent of contamination to the north is not well defined due to the lithologic variations and associated problems with interpreting the resistivity survey, and also the lack of chemical data from the area. The highest concentration of contaminants detected within the sand and gravel unit was north of the disposal pit at WP-6 (TDS=20,335 mg/L). This well is located near the area where a second pit was constructed during workover operations; the high concentrations could reflect contamination from this second pit. The situation is further complicated to the north by a disposal pit from another oil well located approximately 1320 ft (402 m) north of the three background wells (WP-1, WP-2, and WP-3). The chloride concentrations detected in these wells exceed 6000 mg/L, which is significantly greater than the typical concentrations for these glaciofluvial sediments. It is not clear whether these wells were contaminated from the disposal pit at the Winderl site, or the disposal pit to the north.

As discussed above, the high concentrations of contaminants detected in wells screened in till are thought to reflect cross contamination from the upper sand and gravel unit. Therefore, any interpretation of the vertical extent of contamination from the water chemistry data is subject to error. Also, density stratification of the contaminant has hampered any accurate qualitative interpretation of the horizontal distribution of contamination. The isoconcentration maps not only reflect the concentration of contaminants that have migrated horizontally, but also the depths and screen lengths of the wells.

The near surface low-resistivity layers complicate any interpretation of the vertical variations in resistivity that could indicate contamination with depth. The high conductivity of these layers causes the electric current, induced during the resistivity surveys, to travel horizontally rather than penetrate deeper as the a-spacing is increased. Therefore, the assumption that the electrode spacing is equal to the depth of current penetration is not valid.

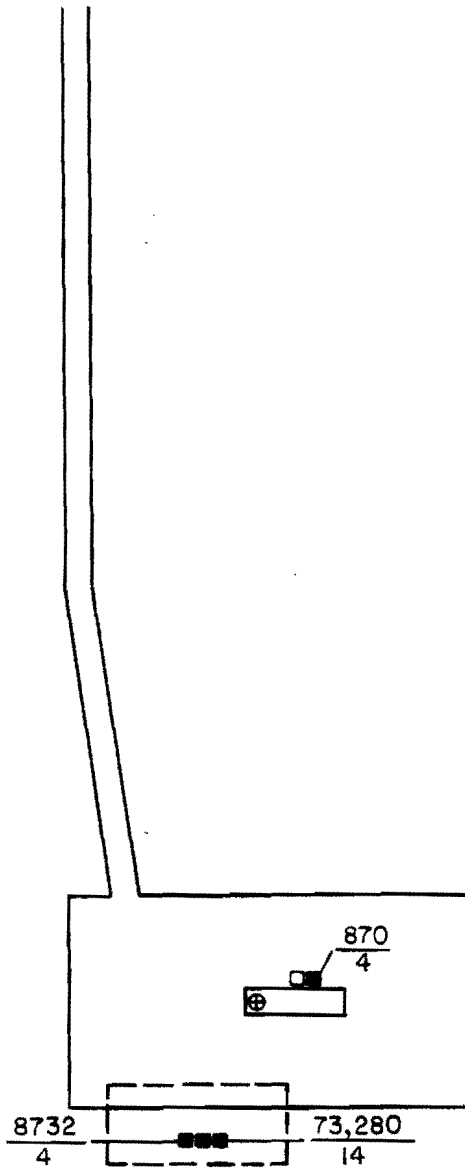
Although the vertical extent of contamination could not be evaluated, boring data indicate that the sand and gravel unit (Spring Coulee Creek Aquifer) is the only aquifer identified within 50 feet (15.2 m) of the surface in the vicinity of the Winderl site. The major environmental concern is the extensive horizontal migration that has occurred within this unit.

4.4.2 Fossum Federal No. 4

Results from the chemical analyses of the lysimeter samples at the Fossum site indicate that contaminants are migrating radially away from the disposal area at a depth close to the water table. These results further indicate a significant decrease in the concentration of the contaminants with distance from the source. To illustrate the distribution of contaminants in the groundwater, the results of the lysimeter analyses for chloride concentrations are presented in Figure 34. The primary component of contaminant migration is thought to be to the south because chloride concentrations of 1678 mg/L were detected approximately 60 ft (18.3 m) to the south of the disposal pit at (FL-11); a significantly lower concentration of 870 mg/L was detected in the sample from FL-6, which is located about 60 ft (18.3 m) north of the disposal pit. The potentiometric data indicate the east-west components

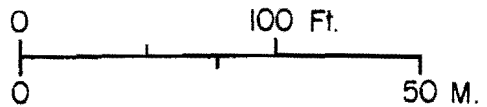
Figure 34. Chloride concentrations in porewater and shallow groundwater at the Fossum site. Refer to Figure 10 for lysimeter numbers.

$\frac{165}{14}$ ■■■



□■ $\frac{1678}{14}$

■ CHLORIDE CONCENTRATIONS IN mg/L
DEPTH OF LYSIMETER



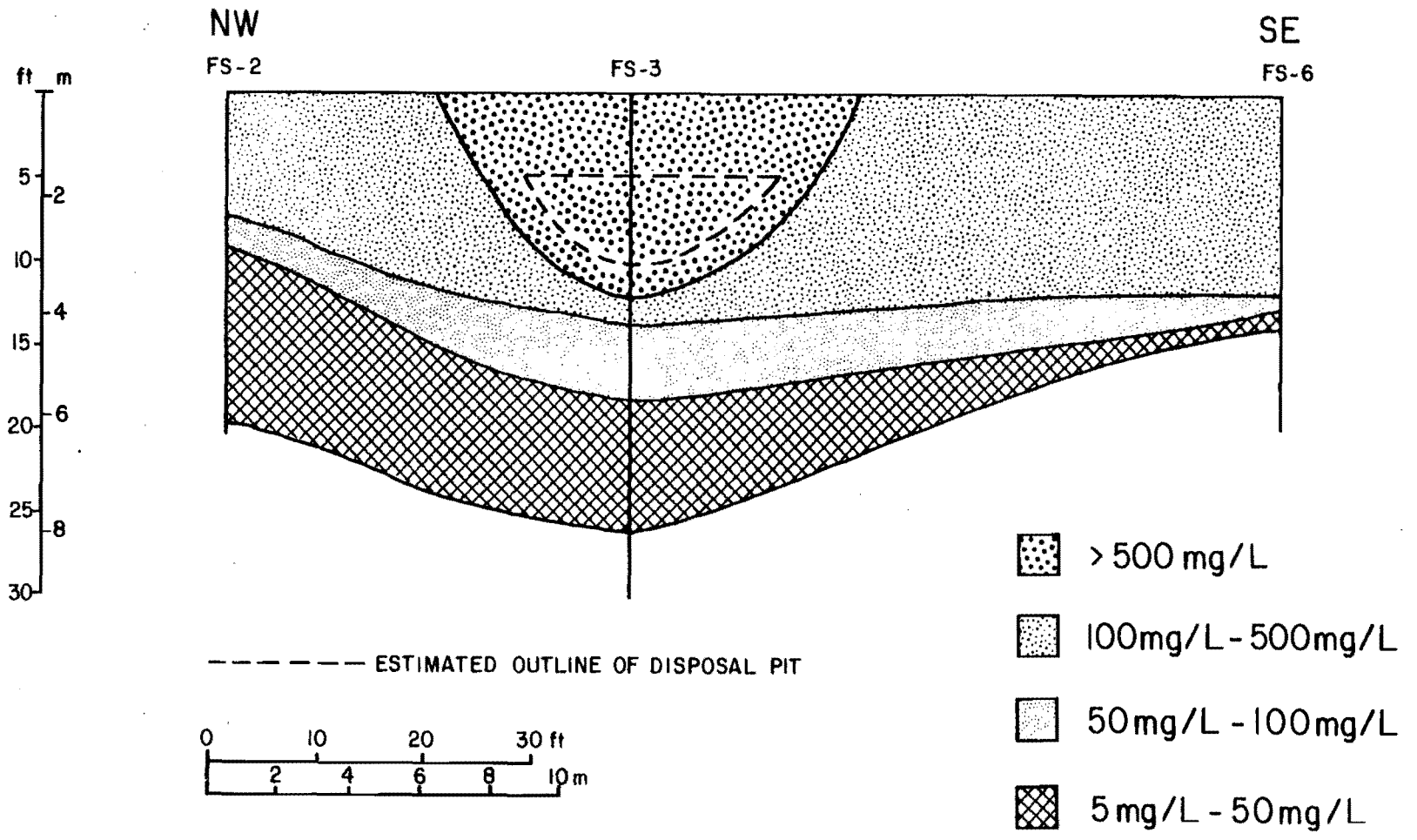
of flow are small, and there is little potential migration in these directions.

An anomalously high sulfate concentration of 20,236 mg/L, approximately 10 times the level of sulfate in the other lysimeters, was detected in the FL-6 sample. Lysimeter FL-6 is in an area covered by fill material that was laid down for construction of the drilling pad. The high sulfate concentration could result from contaminants in the fill, or possibly spills that have occurred in the area.

The resistivity survey was of limited value at the Fossum site. Several of the resistivity soundings in the vicinity of the disposal pit could be conducted only for the smaller electrode spacings due to the extremely low resistivity values detected near the surface. The problems with the resistivity survey at the Fossum site are thought to result from physical obstructions in the area. Electrical lines and pipelines are known to exist throughout the subsurface. These obstructions will interfere with the electrical current and cause anomalous resistivity readings. The apparent resistivity values could not be interpreted by the Dar Zarrouk analysis for the resistivity stations near the disposal area. Consequently, interpreted resistivity cross sections were not constructed. However, the iso-resistivity maps presented in Section 3.4 support the interpretation of the water chemistry data. The low resistivity area, indicating contamination, is centered around the disposal pit and slightly skewed to the south. Resistivity increases with distance from the disposal area in all directions. The high resistivity values to the north probably reflect the near surface sand layer in that area.

As discussed in Section 3.1, the saturated extract data indicate the contaminants are confined primarily to the upper 20 ft (6.1 m) of the

Figure 35. Cross-section showing chloride concentrations from saturated-paste extracts of sediment at the Fossum site.



subsurface. A cross section of chloride concentration with depth was constructed from the soluble extract data (Figure 35) to illustrate the vertical distribution of contamination in the sediment. The location of this cross section is depicted in Figure 10. Figure 35 further indicates that the contaminants have migrated horizontally in the sediment beyond the limits of the saturated paste extract data. Nevertheless, the saturated paste extract results illustrate a significant reduction in contaminants laterally from the disposal pit.

Contamination was detected at depths as great as 60 ft (18.3 m) in the groundwater. As discussed in previous sections, the wells were installed at depths ranging from approximately 20 to 50 ft (6.1 to 15.2 m) below the water table. The isoconcentration maps, which are presented in Section 3.5, illustrate that the contaminants detected in these wells generally are confined to the impoundment area. Slightly elevated concentrations of the indicator parameters were detected in the wells to the south, but these are significantly below those detected in the lysimeter samples, further indicating that horizontal movement of the contaminants occurs directly below the water table.

The contaminants will migrate in these tills due to high groundwater velocities associated with the fractures. The maximum horizontal extent of contamination was not determined. However, the data indicate that the contaminants are attenuated within a relatively short distance of the disposal pit. The till is not a source of water for either stock or domestic purposes, and no aquifers are threatened in the area. Therefore, migration of the contaminants from the disposal pit should not present any environmental problems at the Fossum site.

4.5 Evaluation of Disposal Practices

Disposal of drilling fluids in glaciofluvial sediments in north-central North Dakota is not recommended. At the Winderl site, disposal in a glaciofluvial meltwater channel has resulted in widespread contamination and degradation of the Spring Coulee Creek Aquifer. Even if these pits are lined, fluid is pushed into unlined trenches during reclamation, which allows for infiltration through these permeable sediments.

Murphy and Kehew (1984) suggest a reclamation procedure in which a synthetic liner is utilized to contain the drilling fluid, and compacted fill is mounded over the disposal pits to prevent leachate generation. In north-central North Dakota, however, the water table is close to the surface, and portions of the disposal pits are commonly in the saturated zone. Leachate would be generated by either vertical infiltration or horizontal flow through the buried disposal pits. Containment of this leachate would be dependent solely upon the integrity of the synthetic liner and careful disposal techniques that prevent movement of groundwater through the disposal pits. Because of the difficulties of ensuring proper disposal and the potential for contaminant migration in these glaciofluvial sediments, this disposal method is also not recommended.

The environmental impact from disposal of drilling muds in till is dependent upon the geologic setting. Results from the Fossum site investigation indicate that contaminant migration will occur in these tills through fractures. However, the contaminants are attenuated within a relatively short distance from the disposal pits. Nevertheless, numerous sand lenses were encountered within the till. These permeable lenses could provide avenues for migration of contaminants to nearby aquifers. A subsurface investigation should be conducted at each

disposal site to identify all permeable strata in the area and locate any nearby aquifers.

Since 1984, some local operators have been transporting the drilling muds off site to a central disposal site located in southeastern Williams County (Prairie Disposal). This site is under the jurisdiction of the North Dakota State Department of Health's Division of Hazardous Waste Management. The chemical analyses of the drilling mud must be provided to this agency for approval prior to disposal at this site. In addition to the Prairie Disposal site, there are currently three other proposed central disposal sites in central and western North Dakota (Tillotson, 1986).

The advantage of consolidation of this waste is that the number of disposal areas is decreased, which allows for more efficient regulation. However, a major aspect that reduces the potential for more environmental problems resulting from drilling-fluid disposal is the relatively low volume of waste associated with the drilling-fluid reserve pits. The consolidation of these wastes will increase the potential for adverse environmental impact problems if improper disposal techniques are utilized. The state of North Dakota should carefully regulate these centralized disposal areas and require groundwater monitoring to ensure that leachate migration does not occur.

5.0 CONCLUSIONS

The following conclusions have been derived from the results of this study:

1. The contaminant is characterized as predominantly chloride and sodium with lesser amounts of calcium, magnesium, sulfate, and potassium. In addition, chromium and lead were detected above the maximum permissible concentration (MPC) in drinking water at the Winderl site, and chromium was detected above MPC at the Fossum site. The exact chemical composition of the contaminant could not be determined because the chemical analyses were conducted for a limited number of parameters.
2. A one-dimensional analytical solute transport analysis indicates high concentrations of contamination at the Winderl Site over 3300 ft (1000 m) downgradient from the disposal pit. The analytical solution is a simplified approach, although the analysis does suggest the potential for widespread solute migration within these glaciofluvial sediments. Fractures within the till at the Fossum site result in permeability values much greater than the grain size of these tills indicates. The groundwater velocity through these fractures is estimated at 12.8 ft/day (3.9 m/day). Molecular diffusion within the tills, however, is an important retardation mechanism that reduces the concentration of the contaminants along the fractures with increased distance from the source.
3. The movement of the contaminants is probably affected by several attenuation mechanisms including adsorption and ion exchange,

oxidation and reduction, and chemical precipitation. The extent of these reactions is dependent upon the exact composition of the contaminant and geochemistry of the sediments.

4. At the Winderl site, contamination has extended horizontally beyond the boundary of the study area and resulted in extensive degradation of the Spring Coulee Creek Aquifer. The vertical extent of contamination could not be determined due to cross contamination between units during well construction. At the Fossum site, the horizontal extent of contamination is also not well defined; however, attenuation is evident, reducing the potential for widespread contamination. Although contaminants were detected in the groundwater at depths as great as 60 ft (18.3 m) at the Fossum site, contaminant migration primarily is occurring in the upper portion of the till unit directly below the water table.
5. Disposal of drilling fluids in glaciofluvial sediments is not recommended. The Winderl site exemplifies the adverse effects that seepage from drilling fluid disposal pits can have on glaciofluvial aquifers. The environmental impact of drilling fluid disposal in till is dependent upon the geologic setting. Migration of the drilling fluid constituents will occur along fractures in the till, and widespread contamination can occur if these contaminants intersect permeable lenses that provide avenues for migration. Therefore, a subsurface investigation is necessary at the till disposal sites to identify these permeable lenses and locate any nearby aquifers.

APPENDICES

APPENDIX A

Elevations of Piezometers, Depths to Screened
Intervals, and Depths of Lysimeters

Piezometer Number	Depth of Screened Interval from Surface (feet)	Piezometer Elevation (feet)	Drilling Remarks
WP-1	40.2 - 45.2	1552.52	Used Mud
WP-2	20.8 - 25.8	1553.61	Used Mud
WP-3	4.1 - 14.1	1553.52	Used Mud
WP-4	34.9 - 39.9	1550.08	Used Mud
WP-5	22.0 - 27.0	1549.84	Used Mud
WP-6	9.5 - 14.5	1550.09	Used Mud
WP-7	4.5 - 9.5	1550.18	Used Mud
WP-8	49.5 - 54.5	1550.17	Used Mud
WP-9	27.7 - 32.7	1550.09	Used Mud
WP-10	10.2 - 15.2	1550.11	Used Mud
WP-11	6.5 - 11.5	1550.11	Used Mud
WP-12	4.5 - 14.5	1549.48	Used Mud
WP-13	30.2 - 35.2	1549.14	Used Mud
WP-14	40.0 - 45.0	1548.98	Used Mud
WP-15	41.3 - 46.3	1548.53	Used Mud
WP-16	20.0 - 25.0	1548.67	Used Mud
WP-17	5.7 - 15.7	1548.92	Used Mud
WP-18	36.1 - 41.1	1549.10	Used Mud
WP-19	23.7 - 28.7	1549.16	Used Mud
WP-20	6.4 - 16.4	1550.23	Used Mud
WP-21	4.5 - 14.5	1549.12	Used Mud
WP-22	20.0 - 25.0	1548.96	Used Mud
WP-23	39.4 - 44.4	1549.69	Used Mud
WP-24	6.1 - 8.6	*	Hand Auger

Piezometer Number	Depth of Screened Interval from Surface (feet)	Piezometer Elevation (feet)	Drilling Remarks
WP-25	10.5 - 13.0	*	Hand Auger
WP-26	5.8 - 8.3	*	Hand Auger
WP-27	40.5 - 45.5	1551.89	Used Mud
WP-28	20.8 - 25.8	1551.76	Used Mud
WP-29	4.9 - 14.9	1551.89	Used Mud
FP-1	56.3 - 61.3	1506.31	Used Soap
FP-2	39.2 - 49.2	1506.27	Air Drilled
FP-3	56.0 - 61.0	1506.64	Air Drilled
FP-4	35.4 - 45.4	1506.61	Air Drilled
FP-5	55.8 - 60.8	1505.38	Air Drilled
FP-6	35.5 - 45.5	1505.35	Air Drilled
FP-7	54.2 - 59.2	1506.82	Air Drilled
FP-8	36.0 - 46.0	1506.86	Air Drilled
FP-9	55.4 - 60.4	1505.91	Air Drilled
FP-10	36.2 - 46.2	1505.86	Air Drilled
FP-11	36.2 - 46.2	1506.67	Air Drilled
FP-12	54.0 - 59.0	1506.70	Air Drilled

* Note: Wells WP-24, WP-25 and WP-26 were installed after the survey for well elevations had been completed.

Lysimeter Number	Depth (feet)
FL-1	14
FL-2	9
FL-3	4
FL-4	19
FL-5	9
FL-6	4
FL-7	4
FL-8	9
FL-9	14
FL-10	9
FL-11	14
WL-1	4
WL-2	9

APPENDIX B

Slug Test Procedure

Either a 5- or 10-foot (1.5 to 3 m) slug was dropped down each piezometer. The 5-foot (1.5 m) slug raised the water level in the piezometers approximately 0.5 m; the 10-foot (3 m) slug raised the level approximately 1.0 m. It was observed that the water-level rise due to the attached rope significantly affects the results of the test; therefore, this water-level rise was also accounted for in the hydraulic conductivity calculations. After the slug was dropped down the piezometer, an electric tape was used to measure the water levels at specific time intervals. Linear regression analysis was conducted for each piezometer--regressing the unrecovered head difference against time. The hydraulic conductivity values were calculated from the following method outlined by Hvorsley (1952):

$$K = \frac{r^2 \ln(L/R)}{2LT_0},$$

where L is the length of the screen; R is the radius of the piezometer intake; r is the radius of the piezometer; T_0 is the basic time lag for 37% recovery, which was calculated from the linear regression analysis.

APPENDIX C

Textural Analysis Procedure

The sample was air dried and disaggregated to particles less than 15 mm. Approximately 45 grams of the sample were weighed and soaked in 125 ml of 4% Calgon solution overnight. A test solution of 125 ml of 4% Calgon with deionized water was prepared in a 1000 ml graduated cylinder and also allowed to stand overnight. After soaking, the sample was stirred and agitated until all the clumps had been broken up. The sample and solution then were placed in a 1000 ml graduated cylinder with deionized water and shaken until all the sediment was in suspension. After the sample settled for 2 hours and 30 minutes, a hydrometer reading was taken and the hydrometer reading of the test solution subtracted from it to determine the clay weight. The sample was wet-sieved to remove the silt and clay, and the remaining sand and gravel was oven-dried overnight. The sand and gravel fractions were separated with a Ro-Tap mechanical shaker and No. 10 (2 mm), No. 18 (1 mm), and No. 230 (0.063 mm) sieves. The sand and gravel percentages were calculated, and all the sediment not accounted for by clay, sand, or gravel was considered silt.

APPENDIX D

Sample Preparation Technique for X-Ray Fluorescence

Each sample was oven-dried overnight at 25°C. The samples taken from the disposal pit and those that smelled of hydrocarbons were oven-dried an additional five days at 75°C to "burn off" any hydrocarbons that could volatilize in the XRF sample chamber. Ten grams of the sample were ground up with a porcelain mortar and pestal until six grams would pass through a number 200 (.074 mm) sieve. Three drops of deionized water were thoroughly mixed with the sample to act as a binder. The pressed pellets were made by placing the sample in a 1.25 in (3.2 cm) diameter aluminum cap and applying five tons/square inches of weight for three minutes.

APPENDIX E

Saturated-Paste Extract Analysis Procedure

Deionized water was added to 200 to 1000 gms of air-dried sample with known weight and water content until the saturation point was reached. At the saturation point, the soil paste glistens as it reflects light, and the soil flows slightly as the container is tipped. The saturated percentage was calculated from the weight of the air-dried sample, and the sum of the weights of the water originally present in the sample plus the water that was added to reach the saturation point.

After the sample was allowed to stand at least four hours, the pH was determined. The paste then was transferred to a funnel equipped with filter paper, and the extract was removed with a vacuum. To prevent precipitation of CaCO_3 , 1 ml of $(\text{NaPO}_3)_6$ was added per 25 ml of extract. The electrical conductivity (EC) and sodium adsorption ratio (SAR) of the extract were determined in addition to concentrations of potassium, sodium, bicarbonate, sulfate, and chloride.

APPENDIX F
Driller's Lithologic Logs

WINDERL SITE

Depth (feet)	WP-1	Depth (feet)	WP-23
0-15	Sand and gravel	0-6	Fill
15-42	Till	6-16.5	Sand and gravel
42-45	Sand and gravel	16.5-21	Till
45-80	Till	21-25	Sand and gravel
		25-45	Till
	WP-4		WP-25
0-16	Sand and gravel	0-2.5	Organic material
16-23	Till	2.5-8.75	Sand and gravel
23-25	Sand and gravel		
25-45	Till		WP-27
	WP-8	0-2	Organic material
0-5	Fill	2-15	Sand and gravel
5-10	Drilling mud	15-45	Till
10-18	Sand and gravel		
18-31	Till		
31-32	Sand and gravel		
32-45	Till		
	WP-14		
0-14	Sand and gravel		
14-28	Till		
28-32	Sand and gravel		
32-33	Till		
33-35	Sand and gravel		
35-45	Till		
	WP-15		
0-2	Organic material		
2-16	Sand and gravel		
16-45	Till		
	WP-18		
0-2	Organic material		
2-14.5	Sand and gravel		
14.5-45	Till		

FOSSUM SITE

Depth (feet)	FP-1
0-2	Soil
2-3	Sand and gravel
3-57	Till
57-60.5	Sand and gravel
	FP-3
0-5	Fill
5-15	Drilling mud
15-55	Till
55-57	Sand and gravel
57-60	Till
	FP-5
0-59	Till
59-60	Sand and gravel
	FP-7
0-35	Till
35-37.5	Sand and gravel
37.5-60	Till
	FP-9
0-57	Till
57-60	Sand and gravel
	FP-12
0-28	Till
28-31	Sand and gravel
31-63	Till
63-65	Sand and gravel

APPENDIX G

Lithologic Description of Shelby-Tube Samples

WS-1 Depth (feet)

- 0-1 Silt; sandy, sand is very coarse grained, poorly sorted; very dark grayish brown, 10YR 3/2.
- 1-5 Sand and gravel; brown, 10YR 5/3.
- 5-8 Sand and gravel; light yellowish brown, 10YR 6/4.

WS-2 Depth (feet)

- 0-5.5 Sand and gravel mixed with soil.
- 5.5-6.5 Fill.
- 6.5-7.2 Drilling mud.

FS-1 Depth (feet)

- 0-1 Silt; sandy, sand is very fine grained, brown; 7.5YR 3/2; soil.
- 1-2 Silt; sandy, sand is medium grained; calcareous; light gray, 2.5YR 3/2.
- 2-3 Sand; medium-grained; well sorted; subrounded; calcareous; very pale brown, 10YR 7/4.
- 3-25 Loam; pebbly, pebbles are predominantly carbonates, some dark gray shale, lignite and igneous rock fragments; calcareous; iron staining; very pale brown, 10R 7/4; horizontal and vertical fractures below 5 feet;
- 3-8 iron staining; specs of microcrystalline calcite; yellowish brown, 10YR 5/6;
- 8-10 iron staining concentrated along fracture surfaces; dark yellowish brown, 10YR 4/6;
- 10-14 iron and spotted manganese staining concentrated along fracture surfaces; dark yellowish brown; 12.5 ft to 14 ft--mottled with very dark gray, 5Y 3/1;
- 14-17.5 manganese staining covers up to 50% of fracture surfaces; iron staining also along fractures; dark yellowish brown mottled with very dark gray;
- 17.5-21 iron staining concentrated exclusively along fracture surfaces; no manganese staining; very dark gray;
- 21-25 no staining; very dark gray.

FS-2 Depth (feet)

- 0-1 Silt; black, 7.5Y 7/2; soil.
- 2-3 Clay; silty; calcareous; light gray, 2.5Y 7/2.
- 3-3.5 Sand; very fine-grained; subrounded; silty; calcareous; iron-stained; light olive brown, 2.5Y 5/4.
- 3.5-4.5 Clay; silty; calcareous; light olive gray, 5Y 6/2.
- 4.5 Sand; medium-grained; subrounded; iron-stained, approximately 5-10 mm thick.
- 4.5-19.5 Loam; pebbly, pebbles predominately carbonates, and igneous and metamorphic rock fragments, some dark gray shale and lignite; horizontal and vertical fractures;
- 4.5-5 iron staining; olive yellow; 2.5YR 6/6;
- 5-12.5 iron staining concentrated along fractures; 1-3 mm thick lenses of microcrystalline calcite; nodules of gypsum; brown, 2.5Y 5/6; thin horizontal sand lenses at 6 ft and 7 ft; sand is fine-grained, subrounded to subangular, well sorted;
- 12.5-15 iron and manganese concentrated on fracture surfaces; manganese increases with depth and covers up to 50% of fracture surfaces; grayish brown, 2.5Y 3/2.
- 15-16 iron staining concentrated exclusively on fracture surfaces; no manganese staining; very dary gray, 5Y 3/1.
- 16-19.5 no staining; very dark gray, 5Y 3/1; 18.5 ft to 19 ft--well-sorted silt, light brownish gray, 10YR 6/2, mottled with very dark gray.

FS-3 Depth (feet)

- 0-1 Silt, calcareous; very dark gray, 2.5Y 3/1; soil.
- 1-5 Fill.
- 5-10 Drilling mud.
- 10-12.5 Mixture of drilling mud and sediment.
- 12.5-28 Loam; pebbly, pebbles are predominately carbonates and igneous and metamorphic rock fragments, some dark gray shale; calcareous; horizontal and vertical fractures;
- 12.5-15 iron and manganese staining; predominantly along fractures; olive brown, 2.5Y 4/4;
- 15-16 iron staining exclusively on fracture surfaces, no manganese staining; very dark gray, 5Y 3/1;
- 16-39.5 no staining; sandy, dark gray to olive gray, 5Y 5/2; sand inclusions and sand lenses throughout;
- 39.5-47.5 very dark gray; pebbles include clinker; thin lenses of very coarse-grained, subrounded sand.

FS-4 Depth (feet)

- 0-1 Silt; very dark brown, 10YR 2/2; soil.
- 1-2 Sand; fine-grained; subrounded; silty; slightly calcareous; dark grayish brown, 2.5Y 4/2.
- 2-2.5 Clay; sandy, sand is fine-grained, subrounded; iron staining; slightly calcareous; dark grayish brown, 2.5Y 4/2.
- 2.5-3 Clay; sandy, sand is fine-grained, subrounded; pebbly, pebbles are predominately carbonates and igneous and metamorphic rock fragments, some dark gray shale and lignite; 40% micro-crystalline calcite in a fenestral pattern; olive brown, 2.5Y 4/4, mottled with white.
- 3-4 Clay, silty; iron-stained; specks of calcite throughout; pale olive, 5Y 6/4.
- 4-20 Loam, pebbly, pebbles are similar to the 2.5-3 ft interval; calcareous; horizontal and vertical fractures;
- 4-12.5 iron staining and spotted manganese staining; dark grayish brown, 2.5Y 3/2;
- 12.5-14 iron and manganese staining concentrated along fractures; manganese covers up to 30% of fracture surfaces; increased concentration of lignite fragments; dark grayish brown;
- 14-15 iron staining concentrated exclusively on fracture surfaces, no manganese staining; very dark gray, 5Y 3/1;
- 15-20 no staining; very dark gray, 5Y 3/1; nodules of light gray well-sorted silt up to 60 mm in diameter

FS-5 Depth (feet)

- 0-1.2 Silt; specks of microcrystalline calcite throughout; black, 10R 2/1; soil.
- 1.2-2.4 Silt; calcareous; localized iron staining; light gray, 5Y 7/2.
- 2.4-3.5 Loam; pebbly, pebbles are predominately carbonates and igneous and metamorphic rock fragments, some dark gray shale and lignite fragments; 5-10% microcrystalline calcite; olive, 5Y 5/4.
- 3.5-30 Loam; pebbly; pebbles are the same as the 2.4 ft to 3.5 ft interval; horizontal and vertical fractures; calcareous;
- 3.5-5.75 iron staining; nodules of gypsum crystals; olive, 5Y 5/4;
- 5.75-6 20-30% microcrystalline calcite in a fenestral pattern; iron and manganese staining; nodules of gypsum crystals; olive;
- 6-9 iron and manganese staining; light olive brown, 7.5Y 5/6;
- 9-16.5 iron and manganese staining concentrated along fractures; manganese covers up to 30% of fracture surfaces; olive brown, 2.5Y 4/4.
- 16.5-17.5 iron staining concentrated exclusively along fractures, no manganese staining; very dark gray, 5Y 3/1;
- 17.5-30 no staining; very dark gray, 5Y 3/1; lenses of fine-grained, well-sorted, subangular sand 5-10 mm thick; 28.5-29 ft, sand--similar to the lenses.

FS-6 Depth (feet)

- 0-0.4 Silt; slightly calcareous; black, 10YR 2/1; soil.
- 0.4-1.4 Fill.
- 1.4-1.8 Silt; clayey; calcareous; laminated; light gray, 5Y 7/2.
- 1.8-3 Loam; very pebbly, pebbles are predominately carbonates and igneous and metamorphic rock fragments with some dark gray shale; calcareous; localized iron staining; light olive gray, 5Y 6/2; not sure of the length of the interval because there was only partial recovery.
- 3-5 Loam; silty; pebbly, pebbles are the same composition as the preceding interval; iron staining; 5-10% calcite in a fenestral pattern; olive brown, 2.5Y 4/4.
- 5-10 Loam; pebbly, pebble composition similar to the preceding interval; horizontal and vertical fractures from 7 ft to 10 ft.
- 10-15 No sample.
- 15-20 Loam; pebbly, pebbles are predominately carbonates and igneous and metamorphic rock fragments with some dark gray shale; calcareous; horizontal and vertical fractures;
- 15-16.5 iron and manganese staining concentrated on fracture surfaces; dark grayish brown, 2.5Y 3/2;
- 16.5-17.5 iron staining concentrated exclusively on fracture surfaces, no manganese staining; very dark gray 5Y 3/1;
- 17.5-20 no staining; very dark gray; at 19.5 is a thin lens of medium-grained, subrounded, poorly-sorted sand; 19.5 ft to 20 ft--nodules of fine-grained, subrounded, poorly-sorted sand.

FS-7 Depth (feet)

- 0-1.2 Silt, very dark grayish brown, 10YR 2/2; soil.
- 1.2-1.6 Sand; medium-grained; subrounded; well-sorted; slightly calcareous; light olive brown, 2.5Y 5/6.
- 1.6-3.0 Clay; silty; calcareous; slight iron staining; pale olive, 5Y 6/4.
- 3.0 Sand; fine-grained; subrounded; well-sorted; calcareous; iron stained; 5-10 mm thick; brownish yellow, 10YR 6/8.
- 3.0-3.5 Clay; silty; iron staining; light yellowish brown, 2.5Y 6/6, mottled with light gray, 2.5YR 3/2.
- 3.5-17.5 Loam; pebbly, pebbles are predominately carbonates, and igneous and metamorphic rock fragments, some dark gray shale and lignite fragments; calcareous; horizontal and vertical fractures;
- 3.5-8.5 sandy, sand is fine grained; iron staining; light olive brown, 2.5Y 5/4;
- 8.5-12 iron staining and spotted manganese staining concentrated along fractures; light olive brown;
- 12-14.5 iron staining and manganese staining concentrated on fractures--manganese covers up to 20% of fracture surfaces; olive brown, 2.5Y 4/5.
- 14.5-16 iron and manganese staining exclusively on fracture surfaces; very dark gray, 5Y 3/1;
- 16-16.8 iron staining concentrated exclusively on fracture surfaces, no manganese staining, very dark gray;
- 16.8-17.5 no staining; very dark gray.

APPENDIX H
Results of Textural Analyses

Hole	Depth (feet)	Sand (%)	Silt (%)	Clay (%)
WS-1	3-5	87.6	10.0	2.4
WS-1	5-8	94.5	5.5	0.0
WP-2	15	33.8	36.5	29.7
WP-9	18.5	33.2	37.0	29.8
WP-25	3-6	87.4	9.2	3.4
FS-1	5	60.5	25.9	13.6
FS-1	10	35.9	35.4	28.7
FS-1	15	35.6	36.2	28.2
FS-1	25	32.4	29.3	28.2
FS-2	18.5	0.7	88.3	11.0
FS-3	15	35.2	37.7	27.1
FS-3	20	36.1	38.0	25.9
FS-3	28	67.2	28.4	4.4
FS-3	40	49.2	30.8	20.0
FS-3	45	38.4	36.0	25.6
FS-5	1.5	19.2	55.7	25.1
FS-7	0.5	53.5	29.0	17.5
FS-7	1.5	70.2	18.8	11.0
FS-7	5	37.2	37.0	25.8
FS-7	10	35.4	38.1	26.5
FS-7	15	35.3	36.9	27.8

APPENDIX I

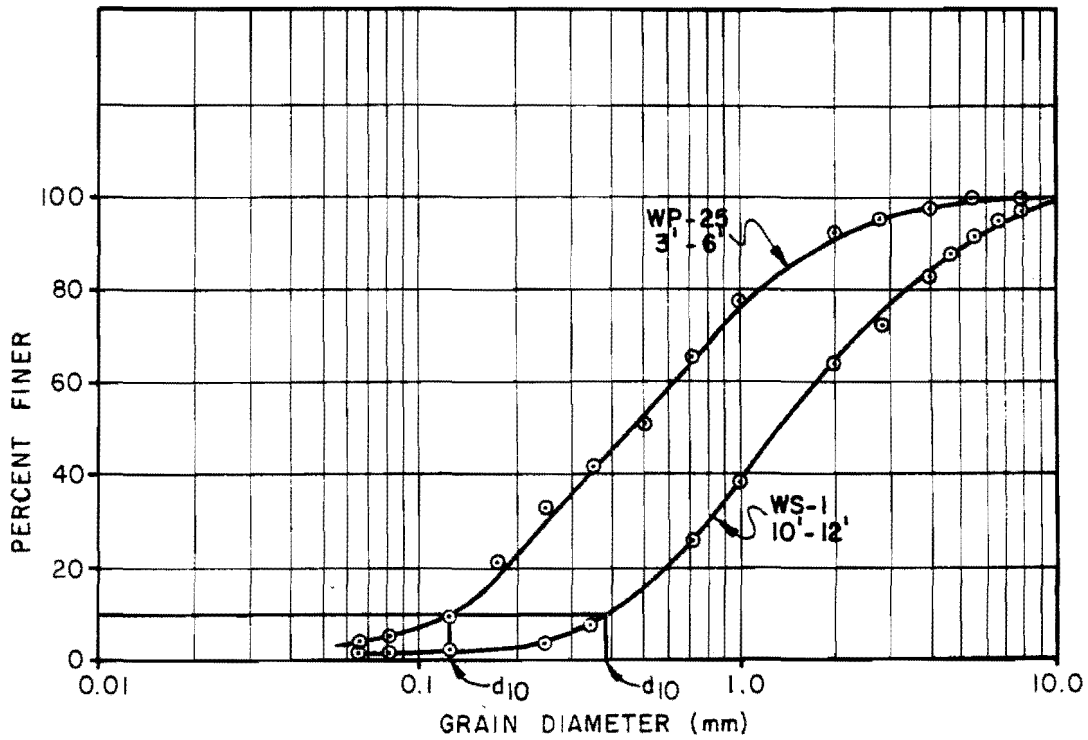
Hydraulic Conductivity Values From Slug Test Data

Piezometer	Depth (feet)	Hydraulic Conductivity (cm/s)
WP-2	22.8	5.6×10^{-3}
WP-6	26.0	8.3×10^{-5}
WP-7	38.8	5.5×10^{-5}
WP-8	53.5	1.8×10^{-5}
WP-9	31.7	1.8×10^{-4}
WP-13	34.2	1.3×10^{-4}
WP-14	44.0	1.2×10^{-4}
WP-16	45.2	3.7×10^{-4}
WP-22	24.0	1.4×10^{-4}
WP-23	42.3	2.4×10^{-6}
WP-27	43.4	5.0×10^{-6}
WP-28	23.8	2.2×10^{-5}
FP-1	60.3	4.0×10^{-5}
FP-2	48.2	5.2×10^{-6}
FP-3	60.0	5.7×10^{-6}
FP-4	44.4	1.6×10^{-5}
FP-5	59.8	2.7×10^{-5}
FP-6	44.5	2.1×10^{-5}
FP-7	58.2	1.7×10^{-5}
FP-8	45.0	4.5×10^{-6}
FP-9	59.4	5.7×10^{-5}
FP-10	45.2	8.1×10^{-6}
FP-11	45.2	6.0×10^{-6}
FP-12	58.0	1.5×10^{-5}

APPENDIX J

Grain Size Distribution Curves

Figure 36. Grain size distribution curves for sediments samples from the Winderl site.



WP-25
3'-6'

$d_{10} = 0.13 \text{ mm}$

$K = d_{10}^2 A$

$K = 1.7 \times 10^{-2} \text{ cm/s}$

WS-1
10'-12'

$d_{10} = 0.39 \text{ mm}$

$K = d_{10}^2 A$

$K = 1.5 \times 10^{-1} \text{ cm/s}$

APPENDIX K

Apparent and Interpreted Resistivity Profiles at the
Winderl and Fossum Study Sites

Figure 37. Apparent and interpreted resistivity profiles for stations 1-4 at the Winderl study site.

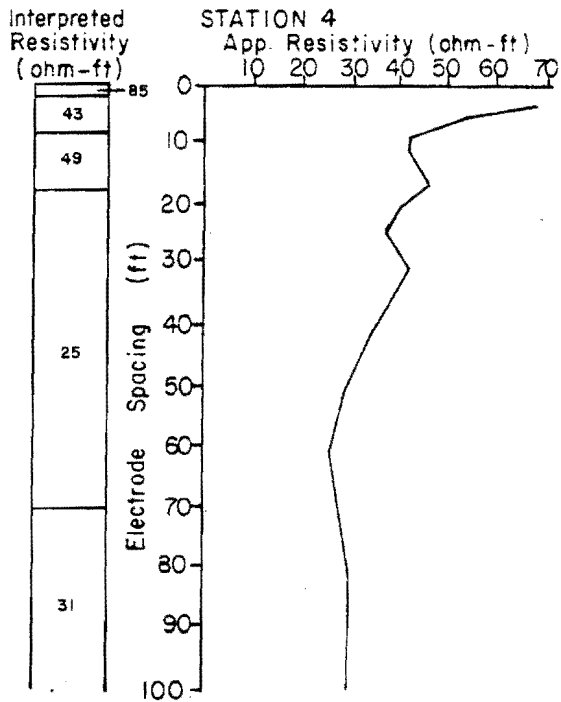
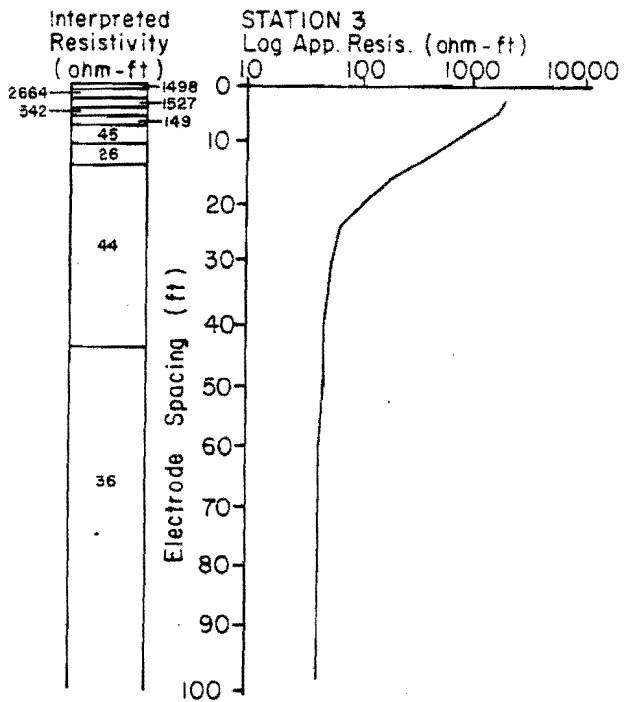
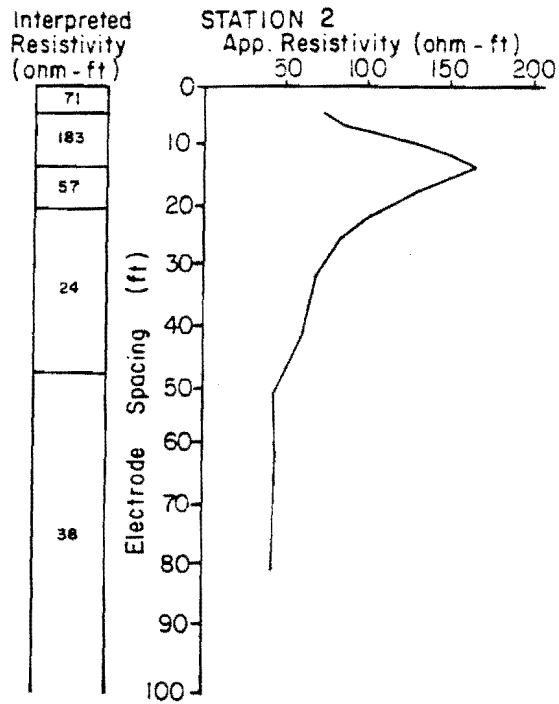
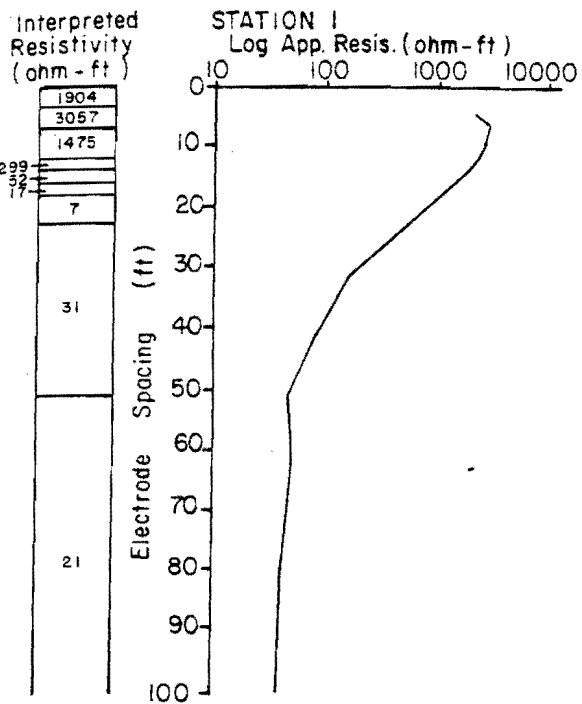


Figure 38. Apparent and interpreted resistivity profiles for stations 5-8 at the Winderl study site.

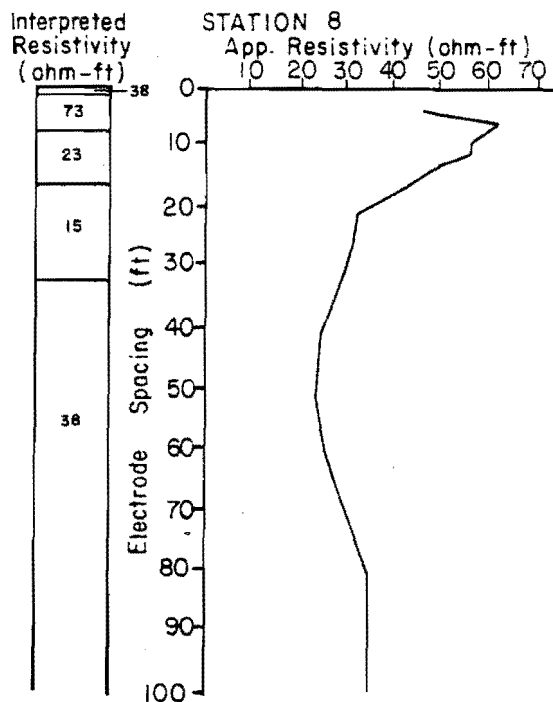
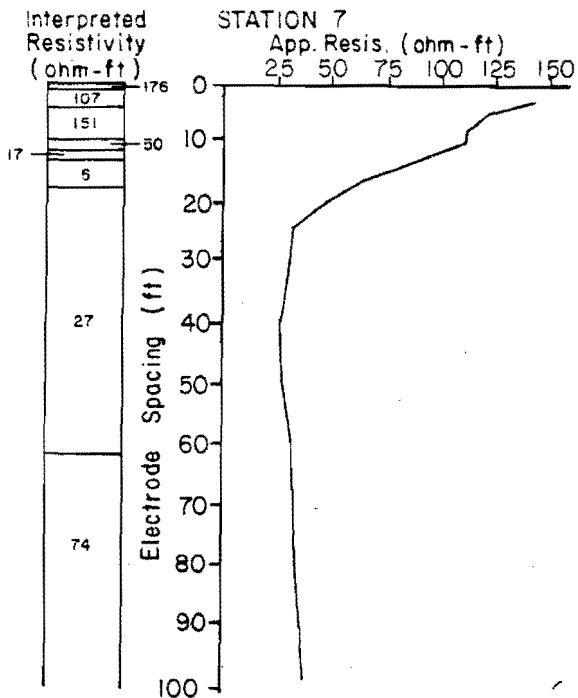
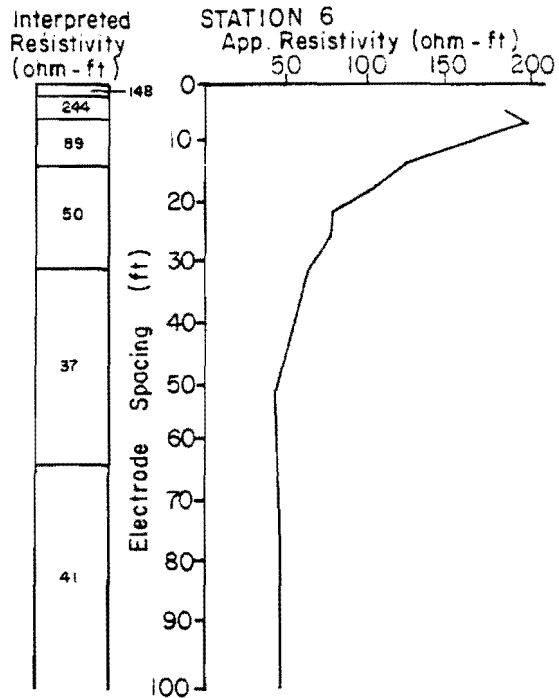
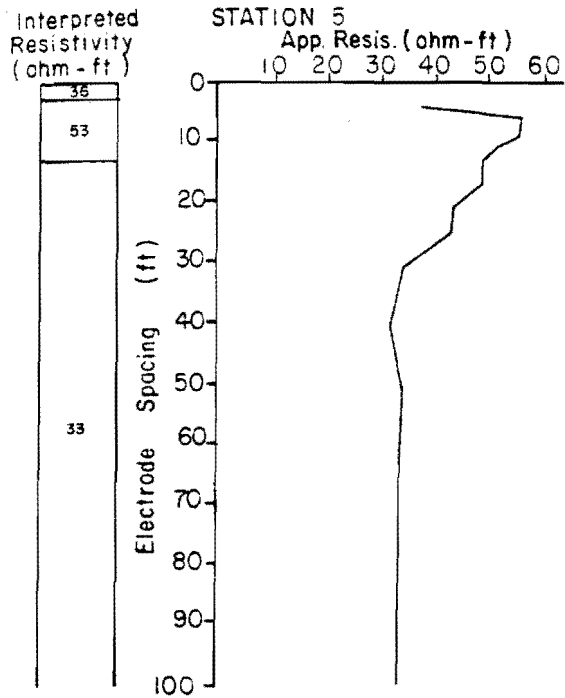


Figure 39. Apparent and interpreted resistivity profiles for stations 9-12 at the Winderl study site.

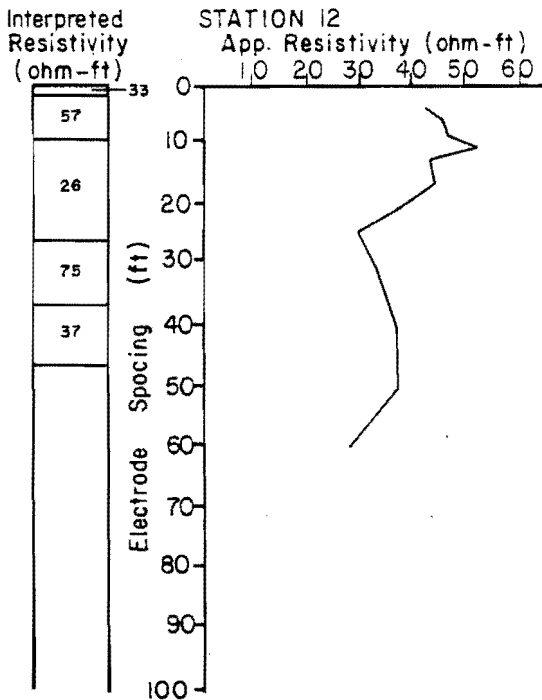
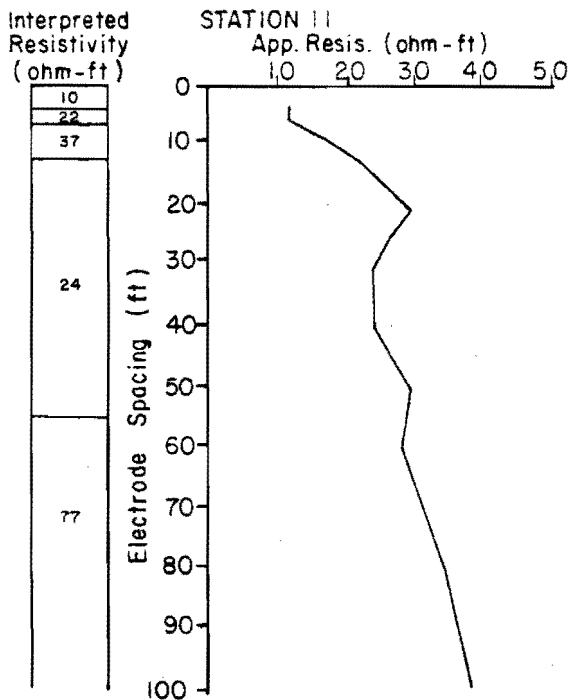
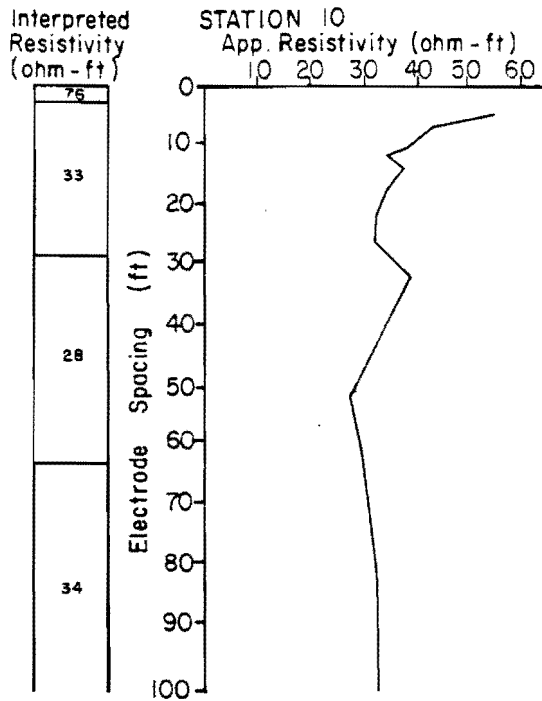
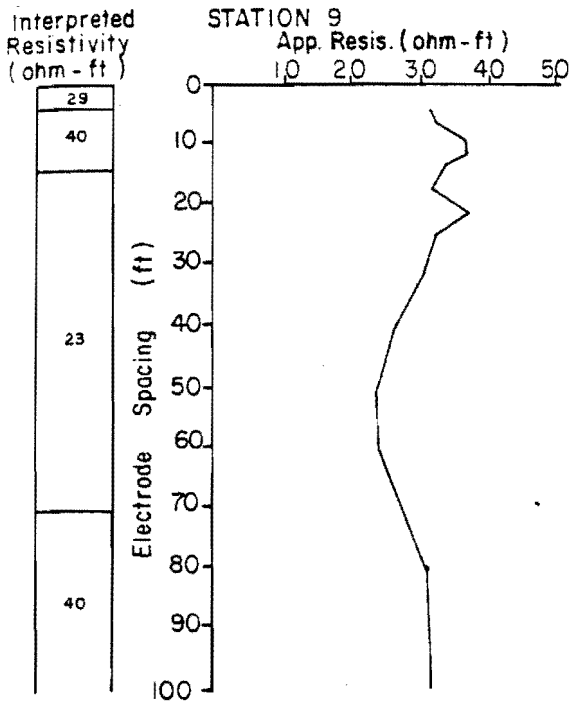


Figure 40. Apparent and interpreted resistivity profiles for stations 13-16 at the Winderl study site.

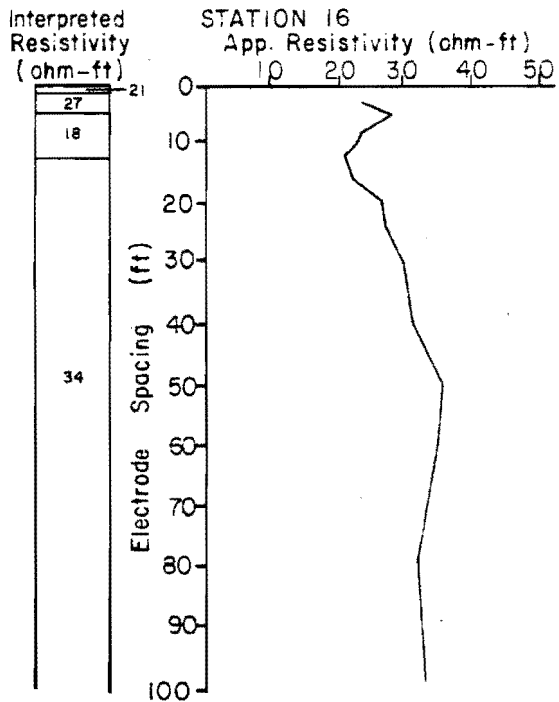
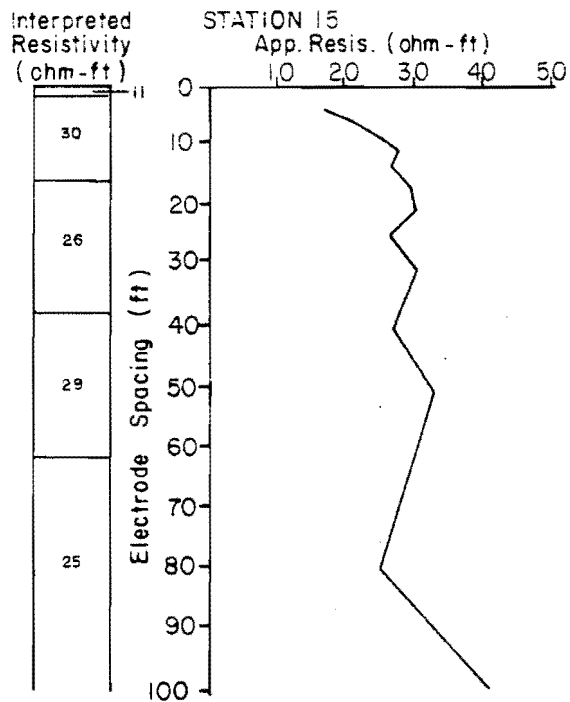
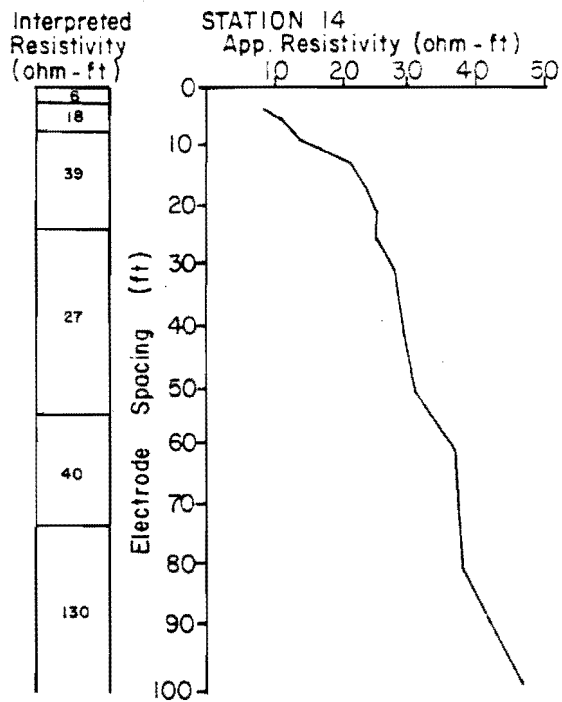
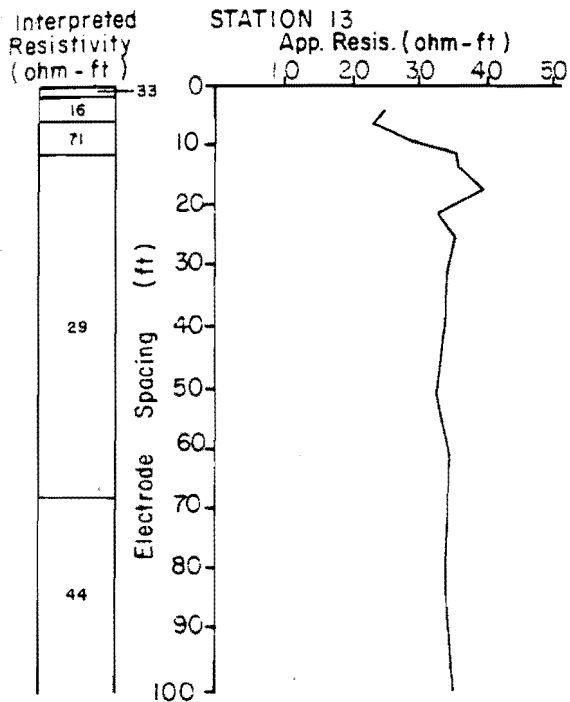


Figure 41. Apparent and interpreted resistivity profiles for stations 17-20 at the Winderl study site.

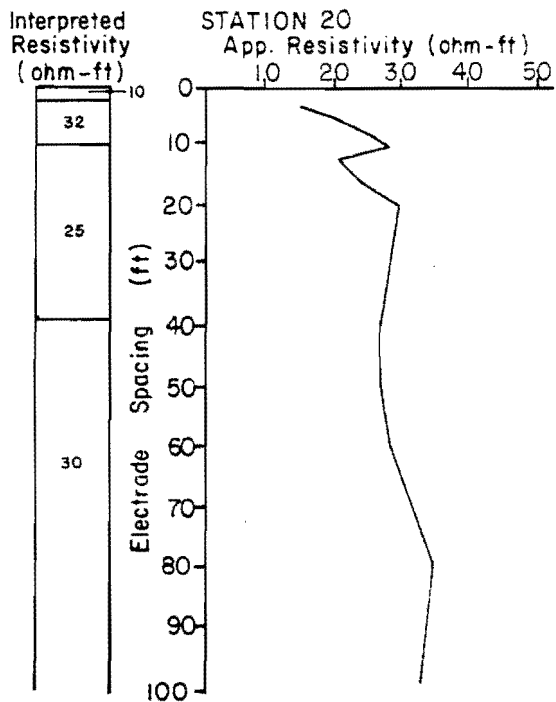
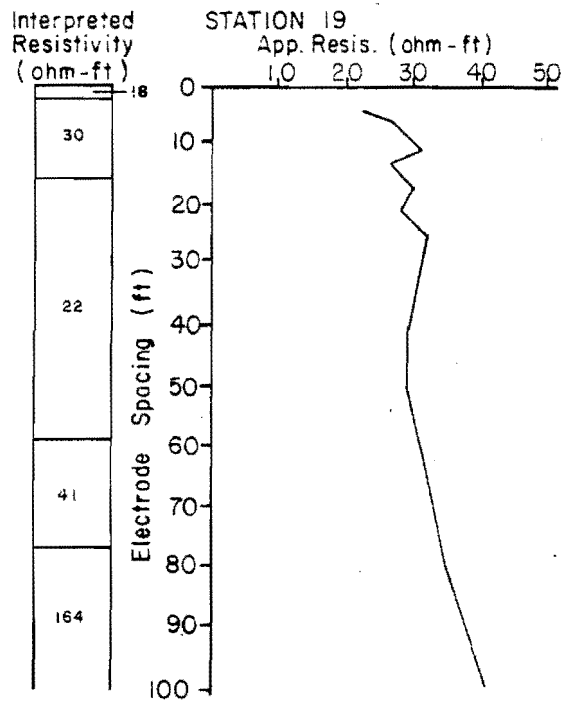
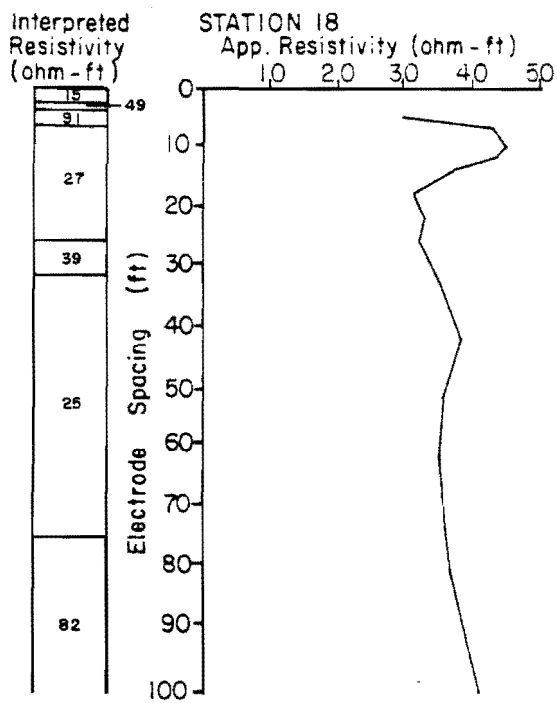
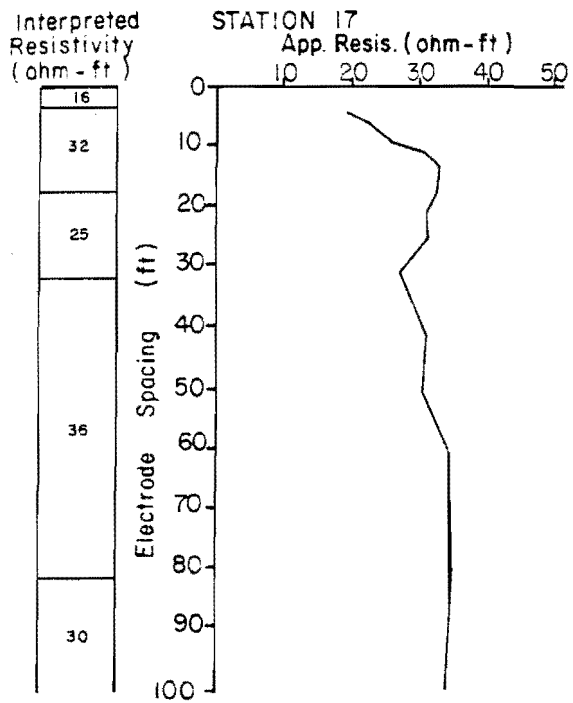


Figure 42. Apparent and interpreted resistivity profiles for stations 21-24 at the Winderl study site.

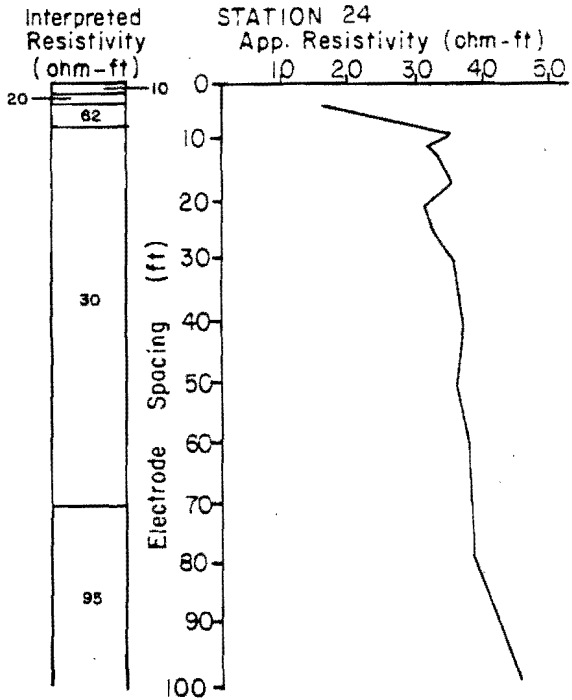
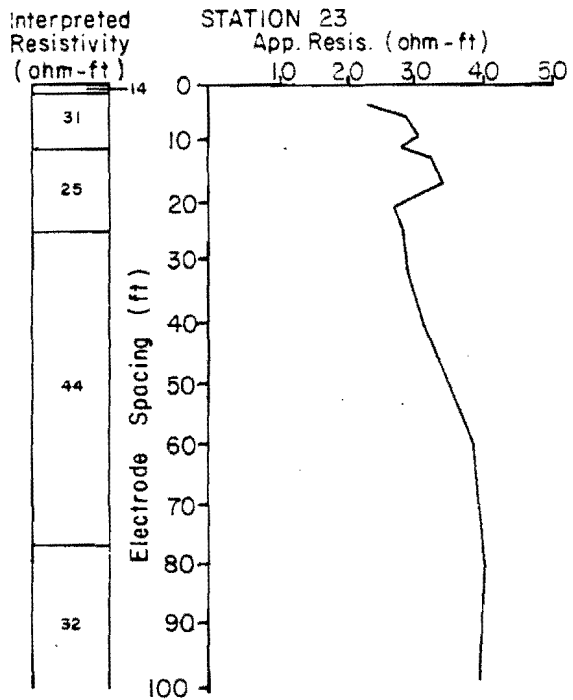
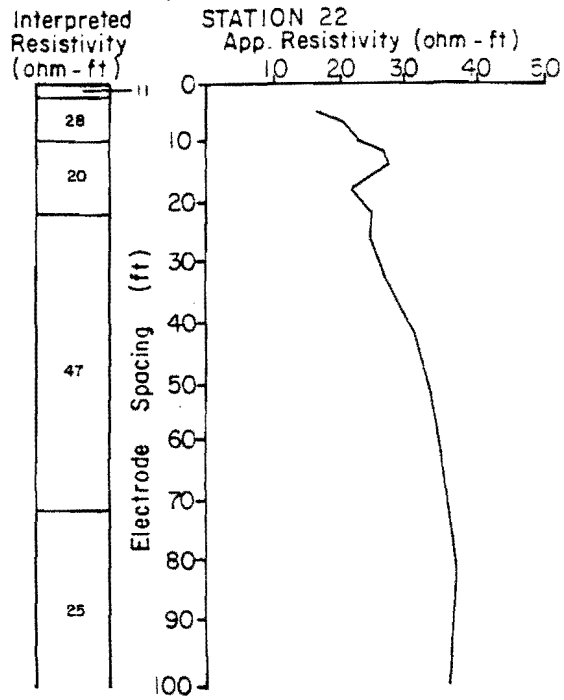
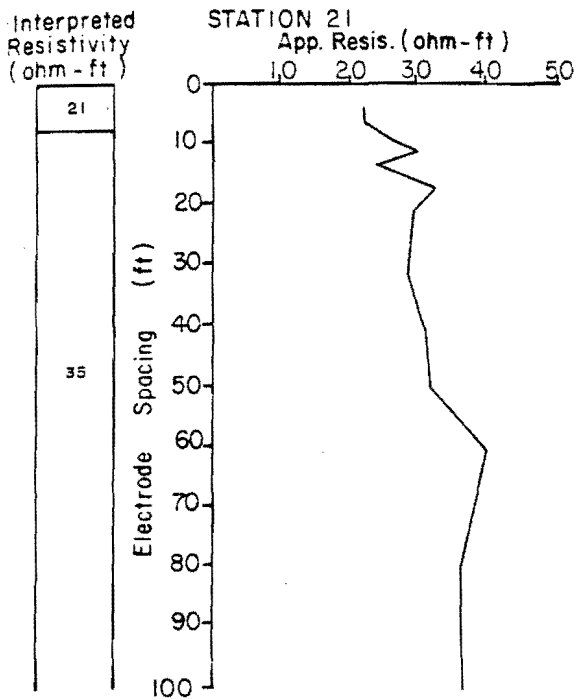


Figure 43. Apparent and interpreted resistivity profiles for stations 25-28 at the Winderl study site.

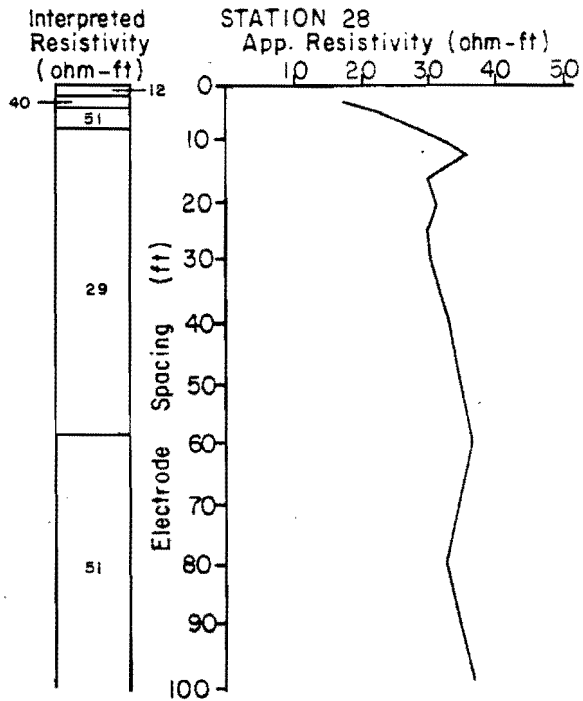
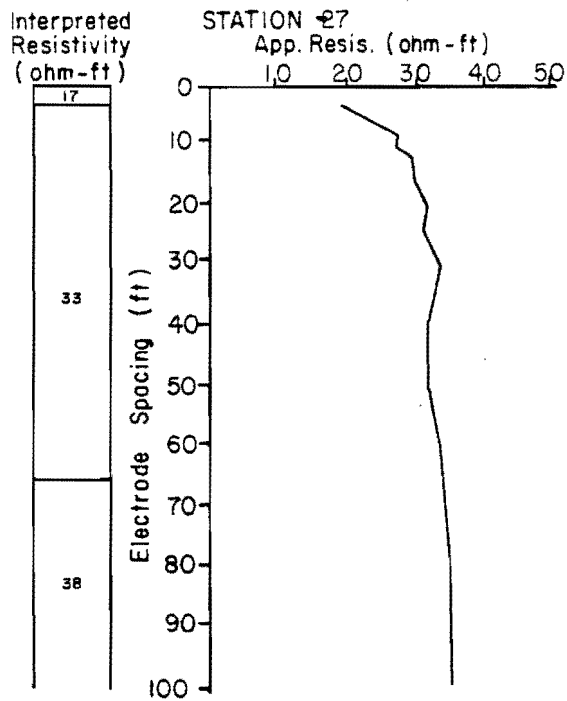
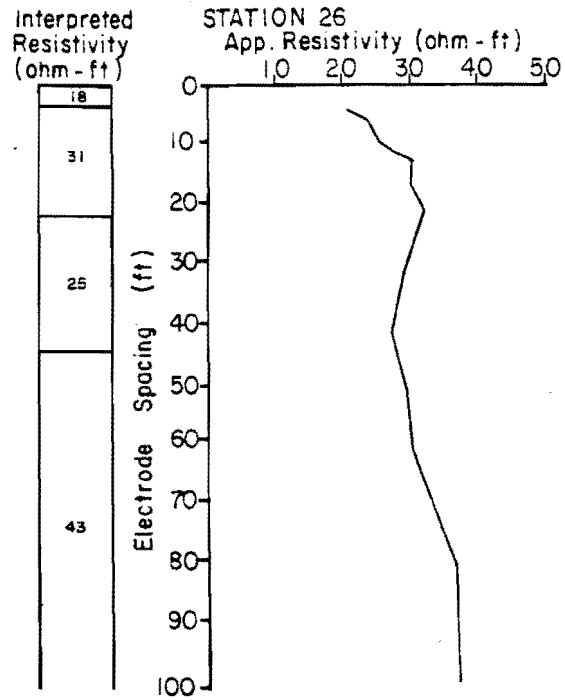
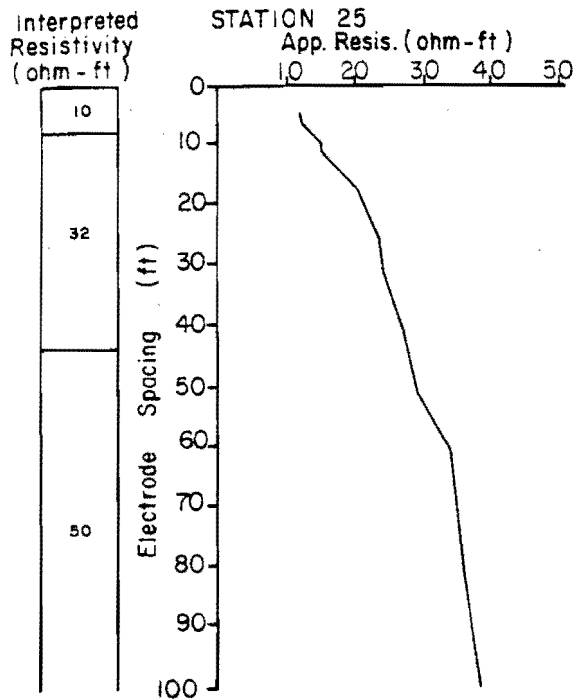


Figure 44. Apparent and interpreted resistivity profiles for stations 29 and 30 at the Winderl study site.

Interpreted Resistivity (ohm-ft)

STATION 29

App. Resist. (ohm-ft)

Interpreted Resistivity (ohm-ft)

STATION 30

App. Resistivity (ohm-ft)

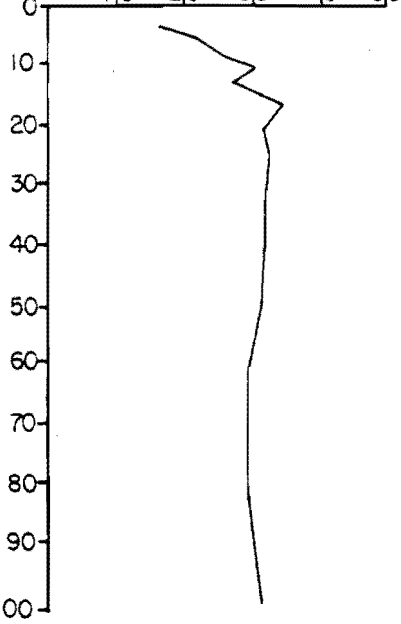
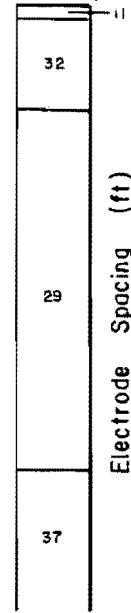
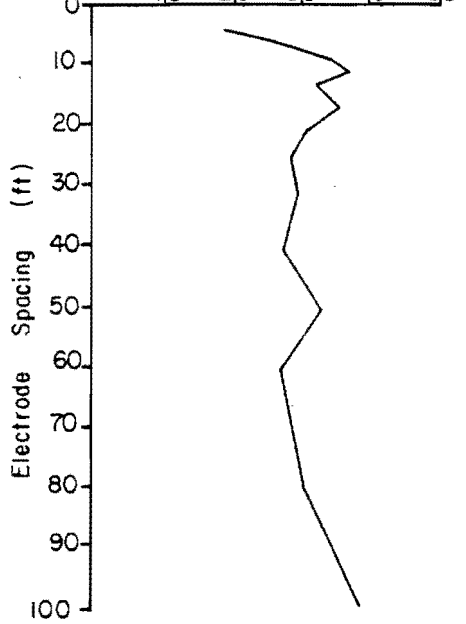


Figure 45. Apparent and interpreted resistivity profiles for stations 1-4 at the Fossum study site.

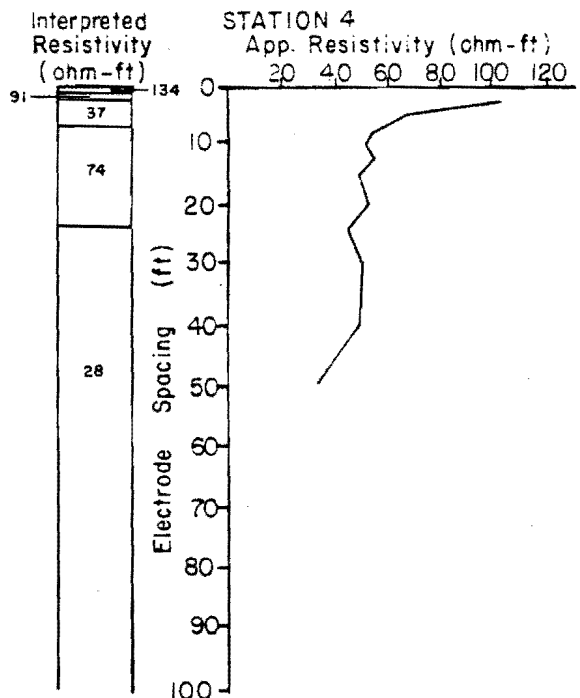
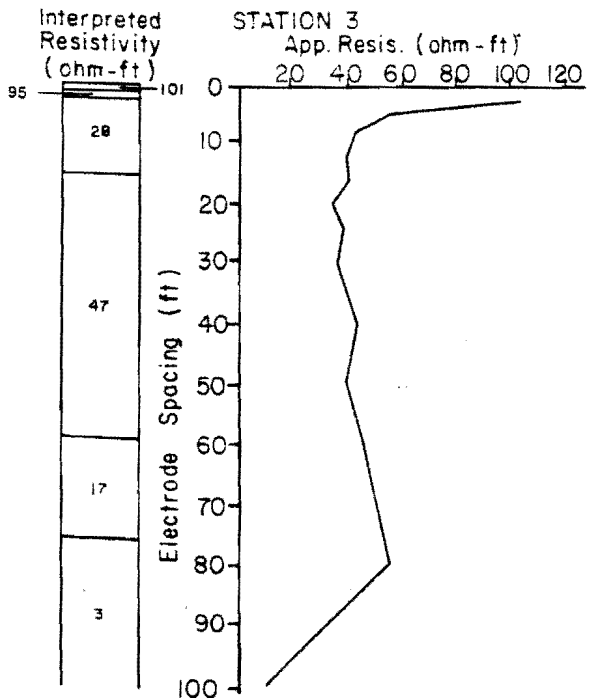
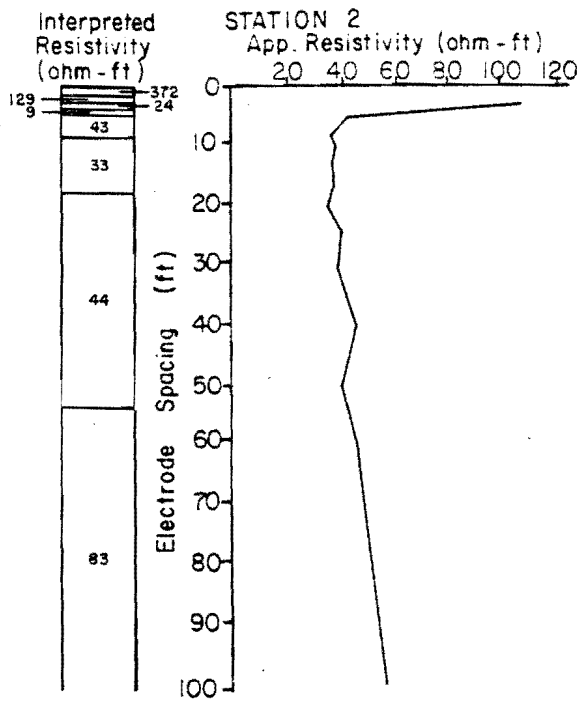
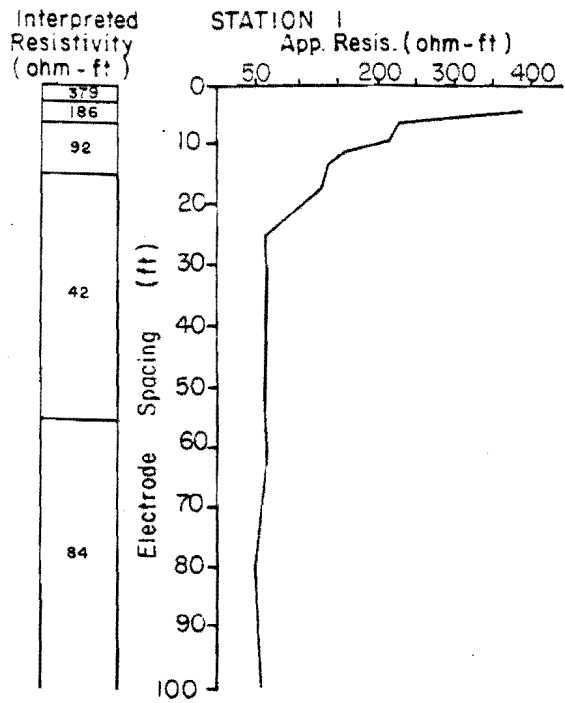


Figure 46. Apparent and interpreted resistivity profiles for stations 5-8 at the Fossum study site.

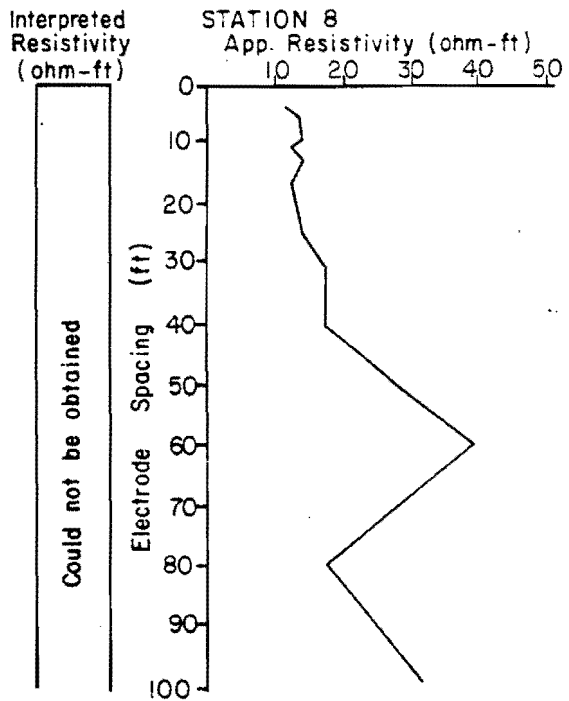
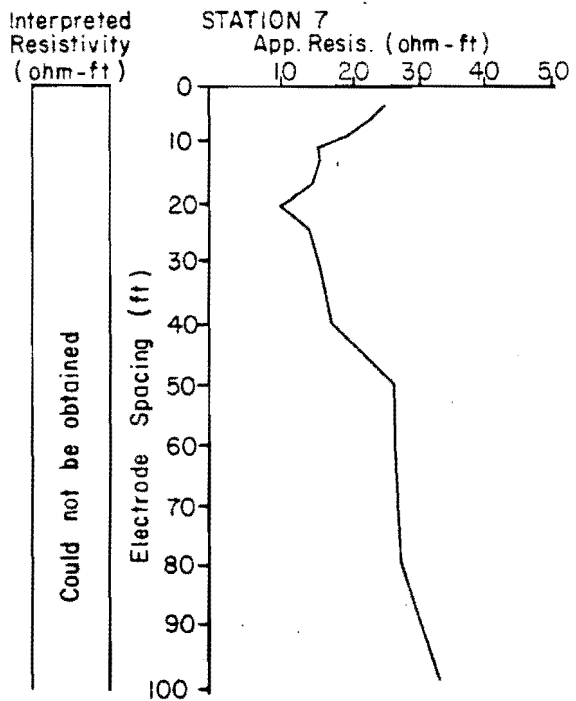
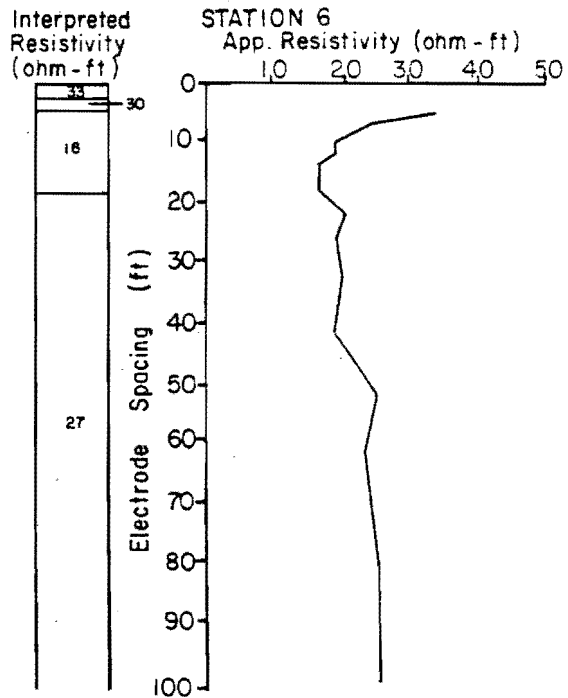
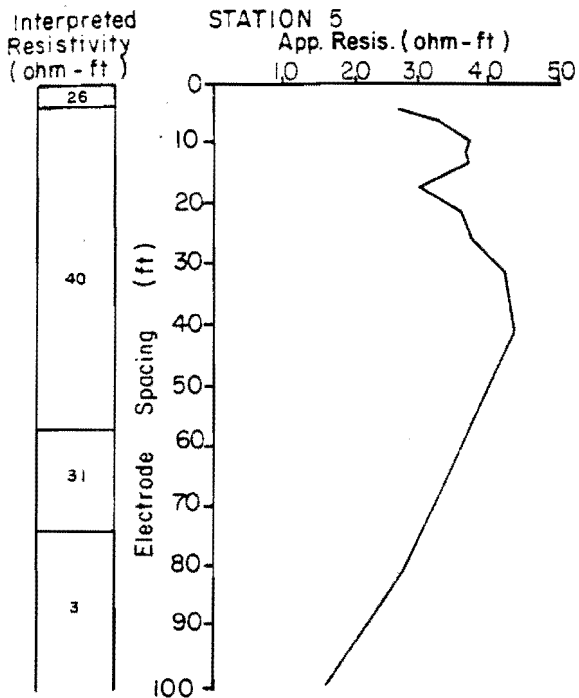
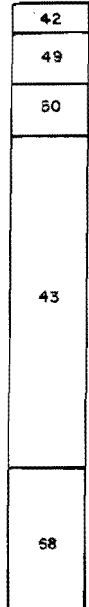


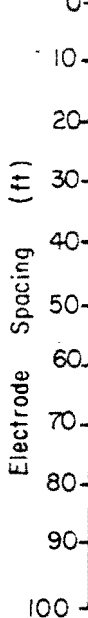
Figure 47. Apparent and interpreted resistivity profiles for stations 9-12 at the Fossum study site.

Interpreted Resistivity (ohm-ft)

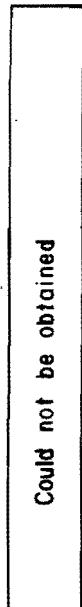


STATION 9

App. Resis. (ohm-ft)
10 20 30 40 50 60

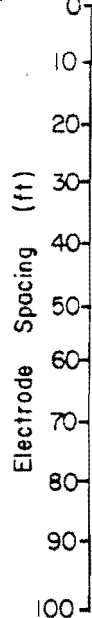


Interpreted Resistivity (ohm-ft)

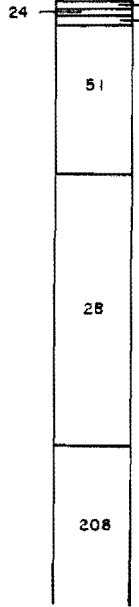


STATION 10

App. Resistivity (ohm-ft)
10 20 30 40 50 60

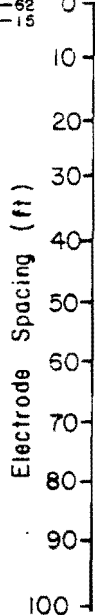


Interpreted Resistivity (ohm-ft)



STATION 11

App. Resis. (ohm-ft)
10 20 30 40 50 60



Interpreted Resistivity (ohm-ft)



STATION 12

App. Resistivity (ohm-ft)
10 20 30 40 50

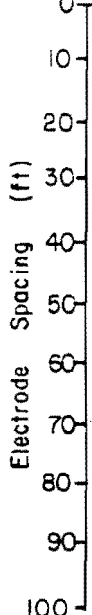


Figure 48. Apparent and interpreted resistivity profiles for stations 13-16 at the Fossum study site.

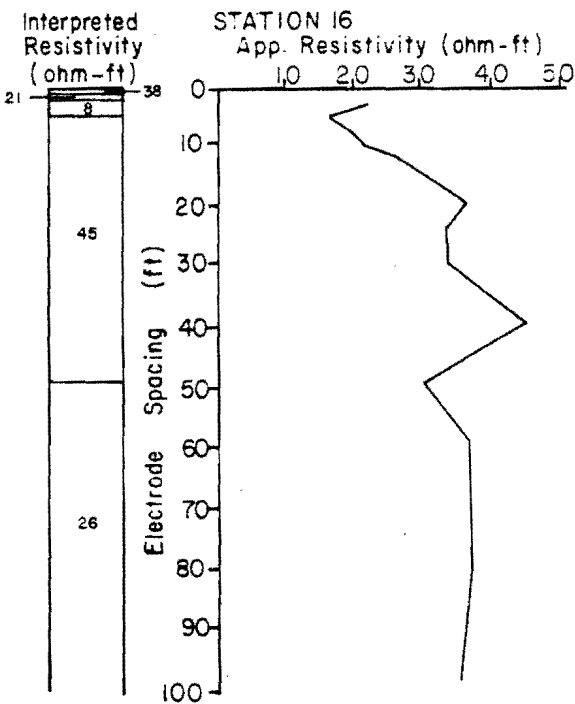
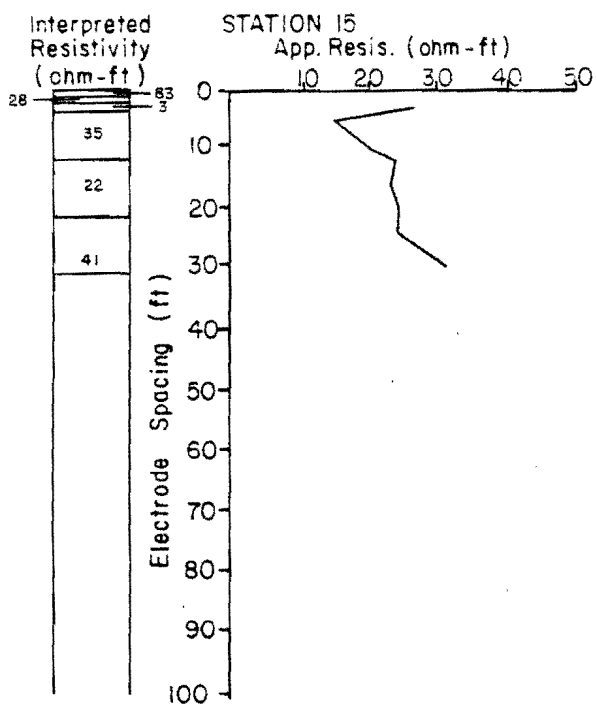
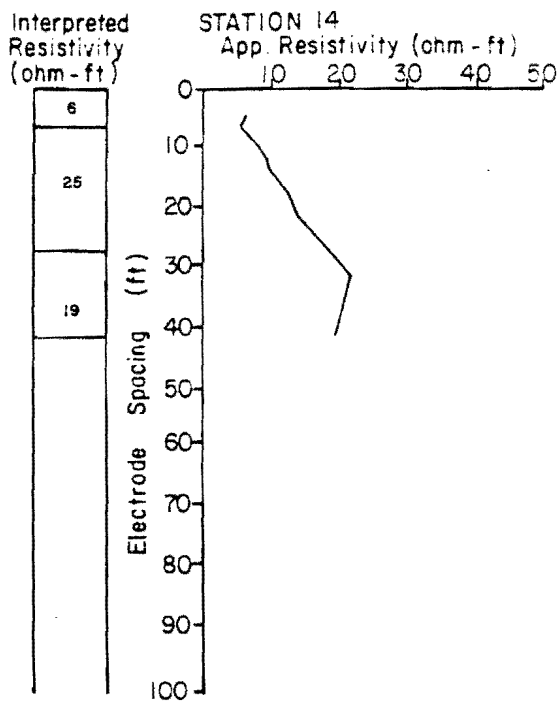
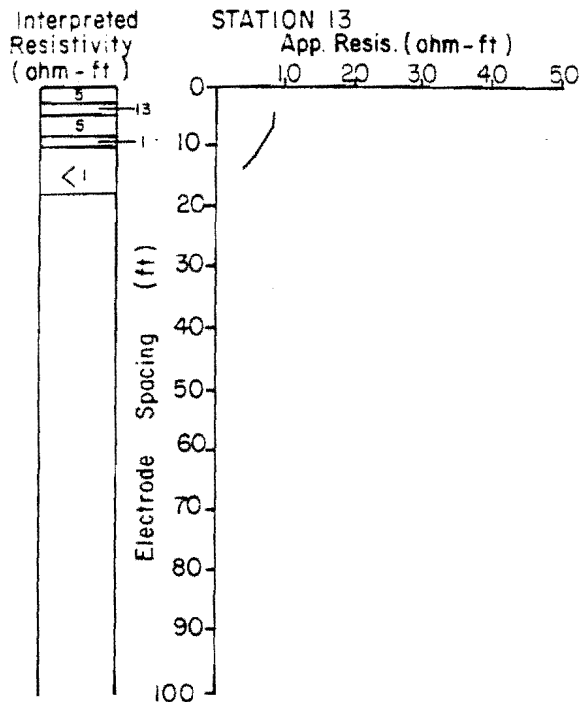


Figure 49. Apparent and interpreted resistivity profiles for stations 17-20 at the Fossum study site.

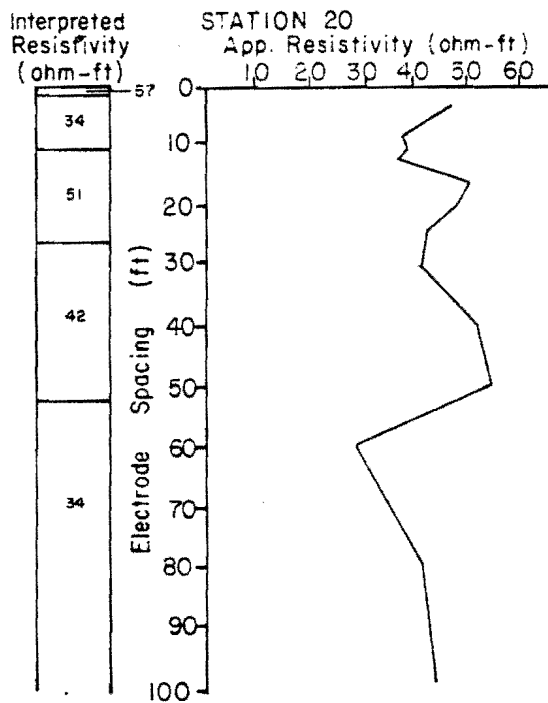
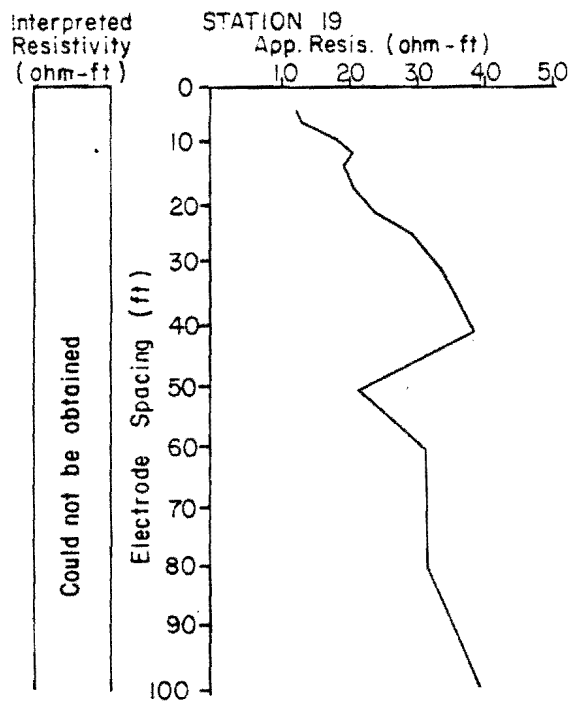
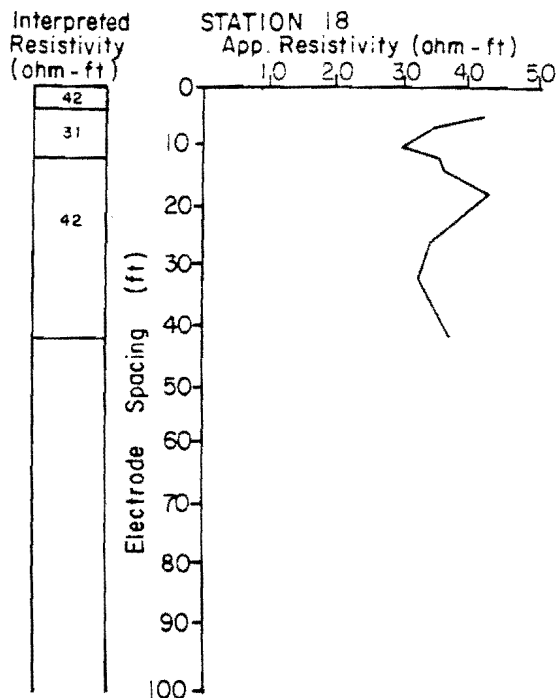
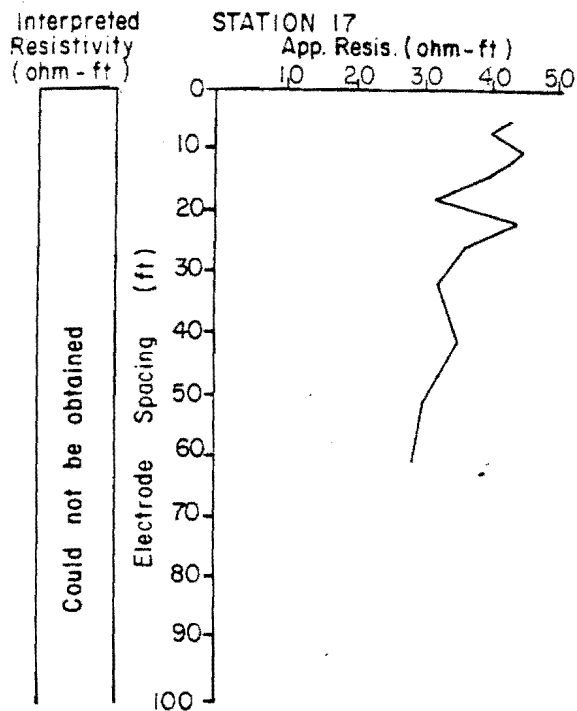
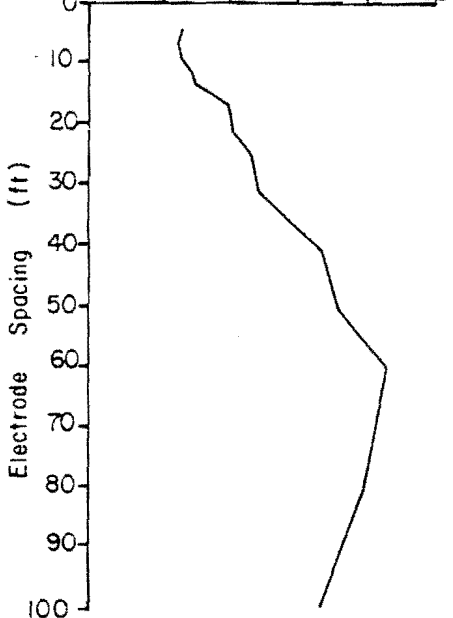


Figure 50. Apparent and interpreted resistivity profiles for stations 21-24 at the Fossum study site.

Interpreted Resistivity (ohm-ft)

16
11
29
90
47
22

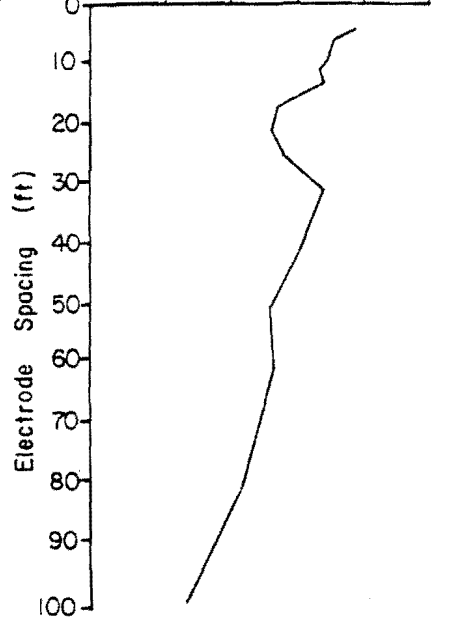
STATION 21
App. Resis. (ohm-ft)



Interpreted Resistivity (ohm-ft)

82
57
85
38
6

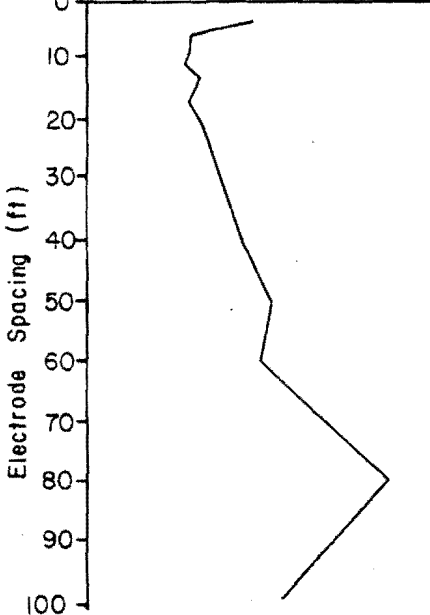
STATION 22
App. Resistivity (ohm-ft)



Interpreted Resistivity (ohm-ft)

Could not be obtained

STATION 23
App. Resis. (ohm-ft)



Interpreted Resistivity (ohm-ft)

50
42
41
19

STATION 24
App. Resistivity (ohm-ft)

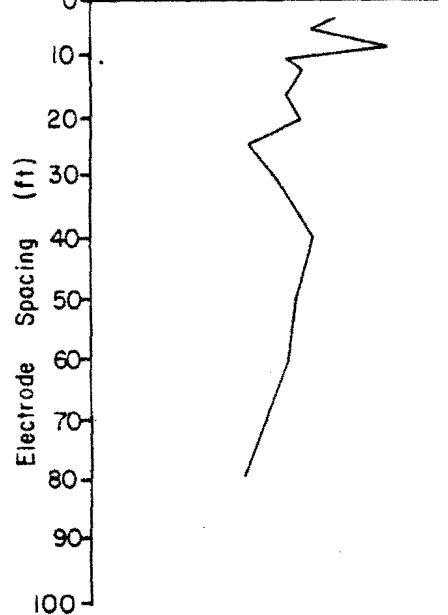
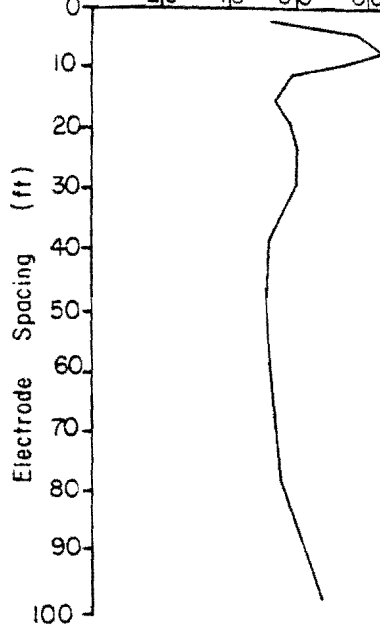


Figure 51. Apparent and interpreted resistivity profiles for station 25 at the Fossum study site.

Interpreted
Resistivity
(ohm-ft)

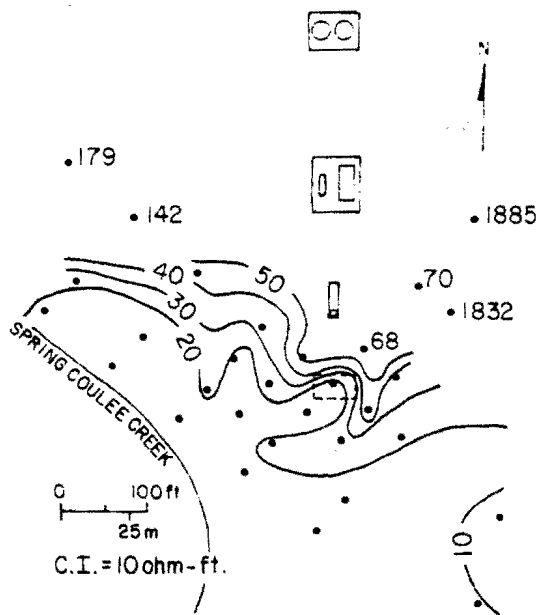
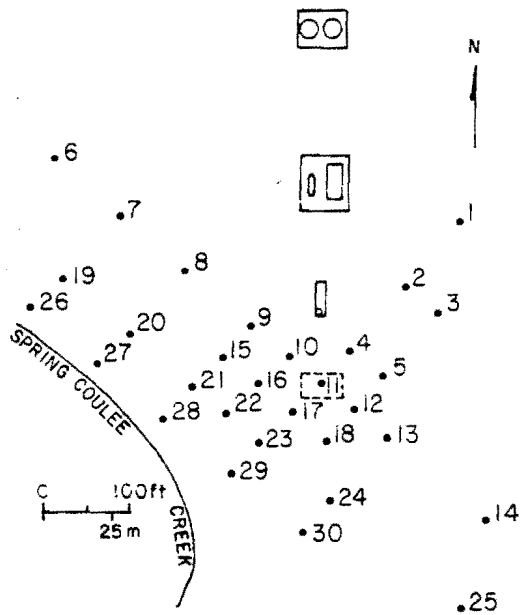
37
117
44
22
38
345

STATION 25
App. Resis. (ohm-ft)
20 40 60 80 100

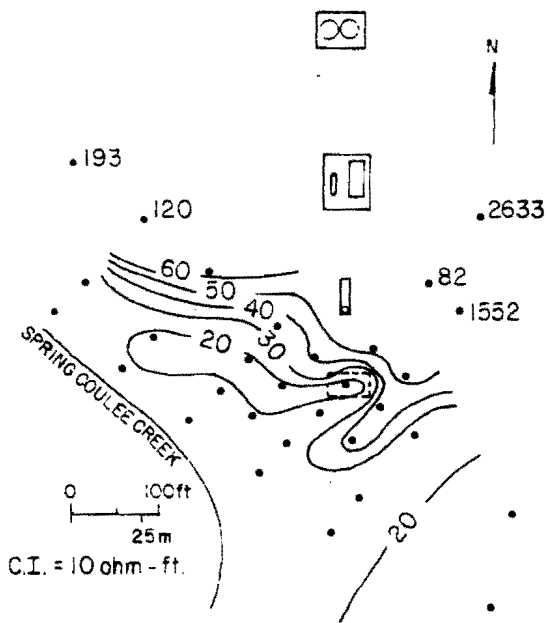


APPENDIX L
Isoresistivity Maps

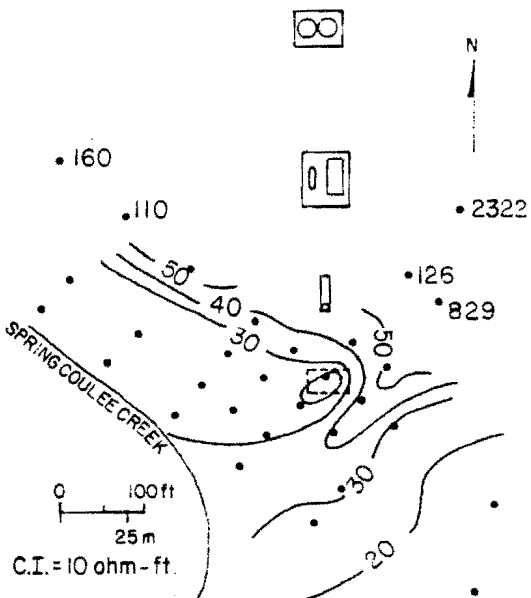
Figure 52. Location map for resistivity stations and iso-resistivity maps for electrode spacings of 3, 5, and 8 feet (0.9, 1.5, and 2.4 m) at the Winderl site.



3 FOOT ELECTRODE SPACING



5 FOOT ELECTRODE SPACING



8 FOOT ELECTRODE SPACING

Figure 53. Apparent iso-resistivity maps for electrode spacings of 10, 12, 16, and 20 feet (3.05, 3.7, 4.9, and 6.1 m) at the Winderl site.

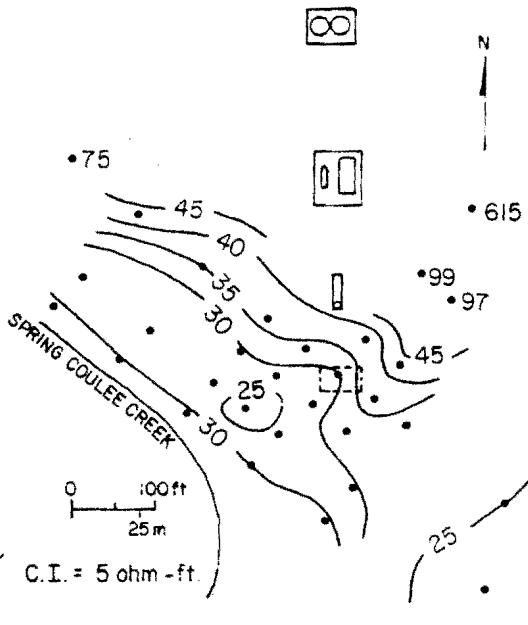
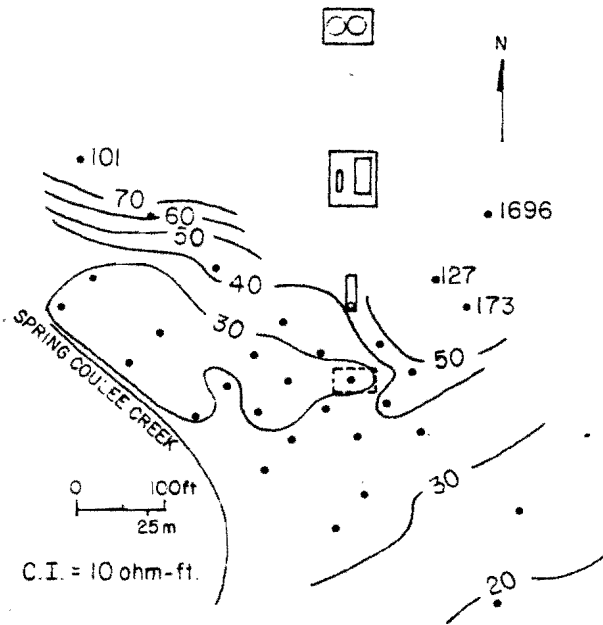
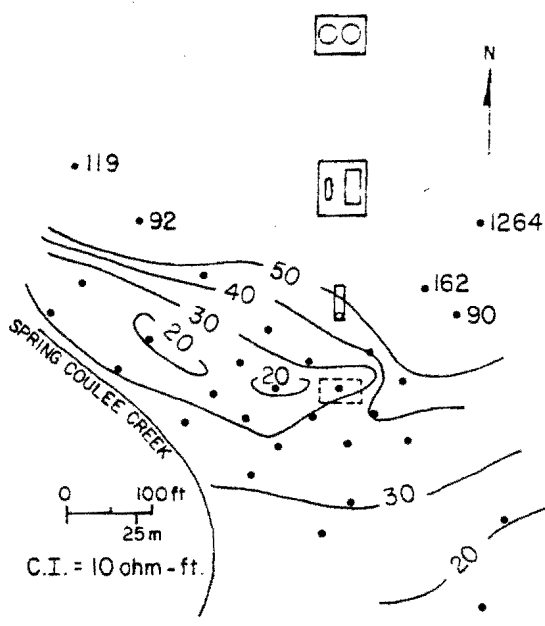
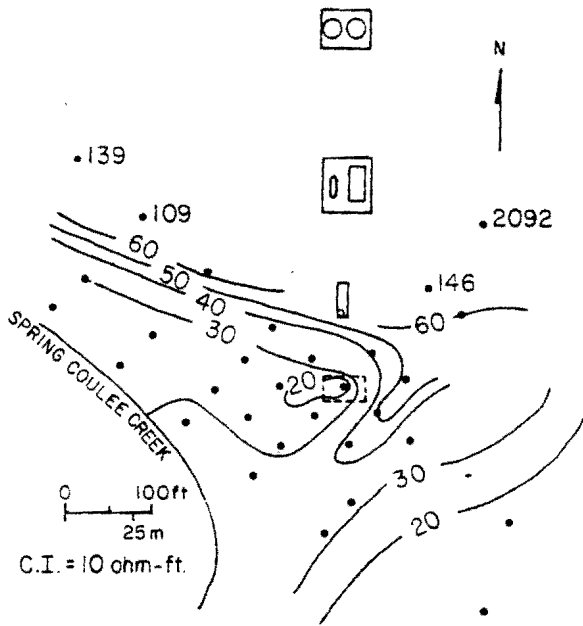
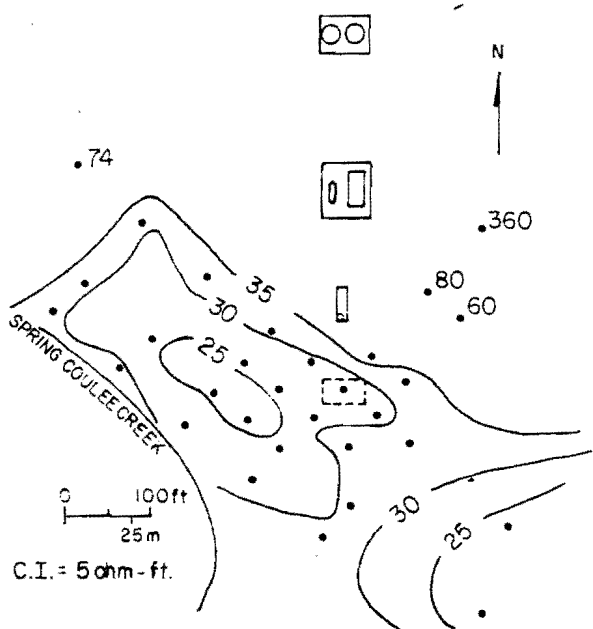
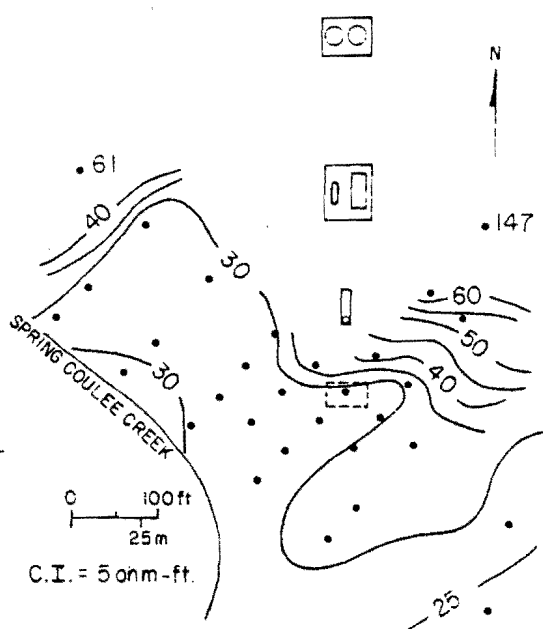


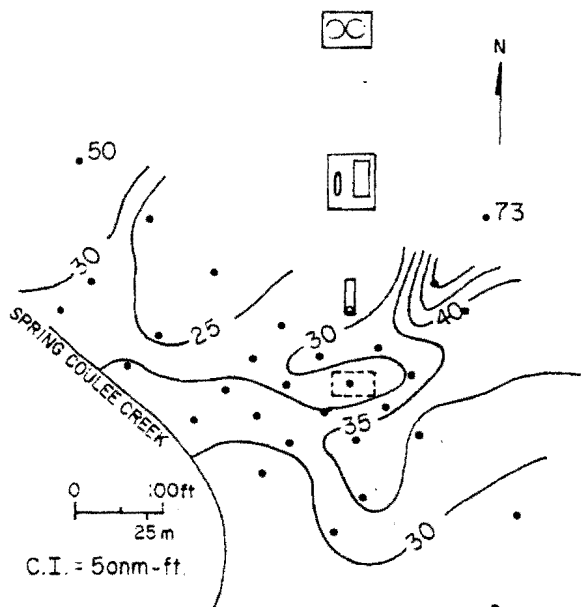
Figure 54. Apparent isoresistivity maps for electrode spacings of 24, 30, 40, and 50 feet (7.3, 9.1, 12.2, and 15.2 m) at the Winderl site.



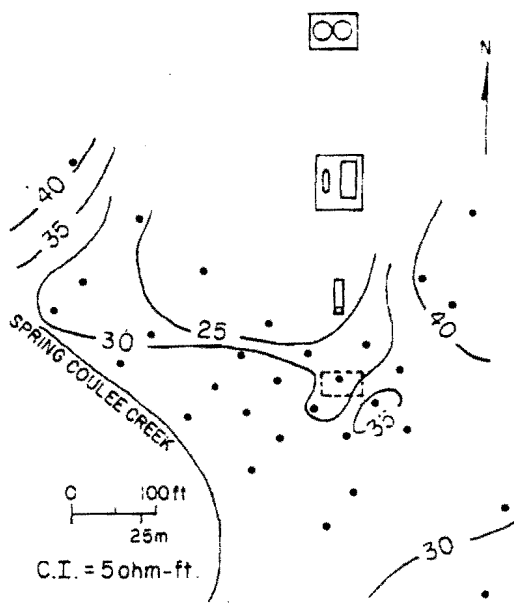
24 FOOT ELECTRODE SPACING



30 FOOT ELECTRODE SPACING



40 FOOT ELECTRODE SPACING



50 FOOT ELECTRODE SPACING

Figure 55. Apparent isoresistivity maps for electrode spacings of 60, 80, and 100 feet (18.3, 24.4, and 30.5 m) at the Winderl site.

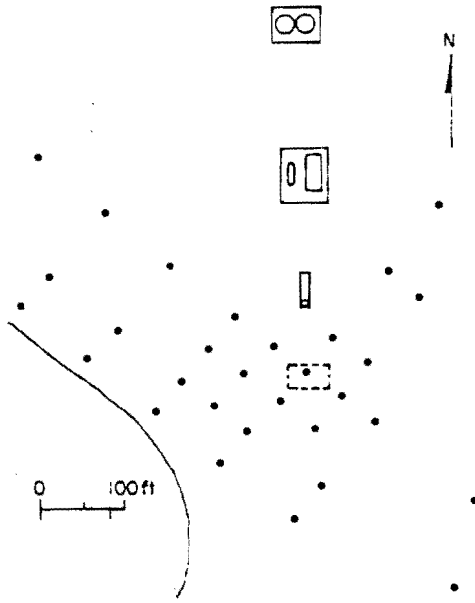
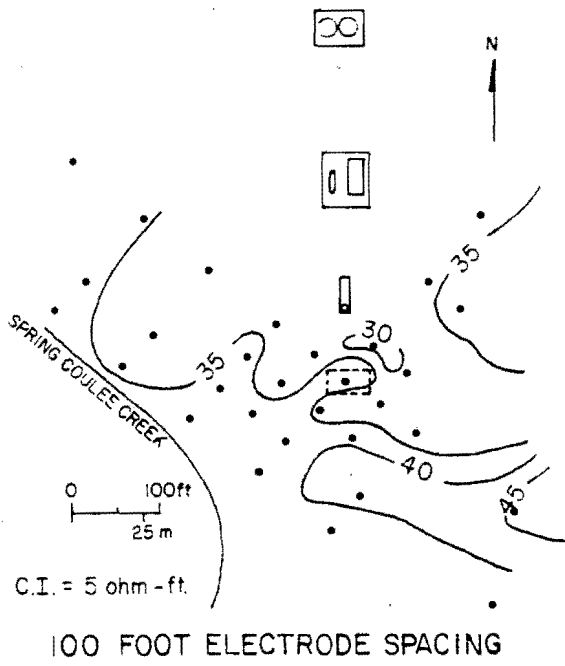
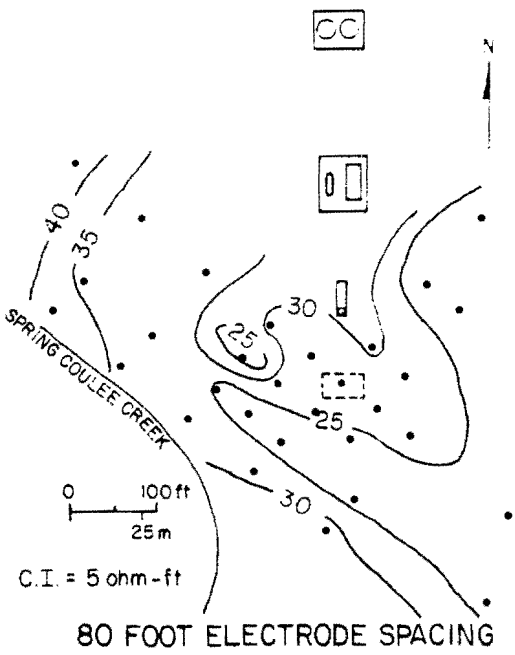
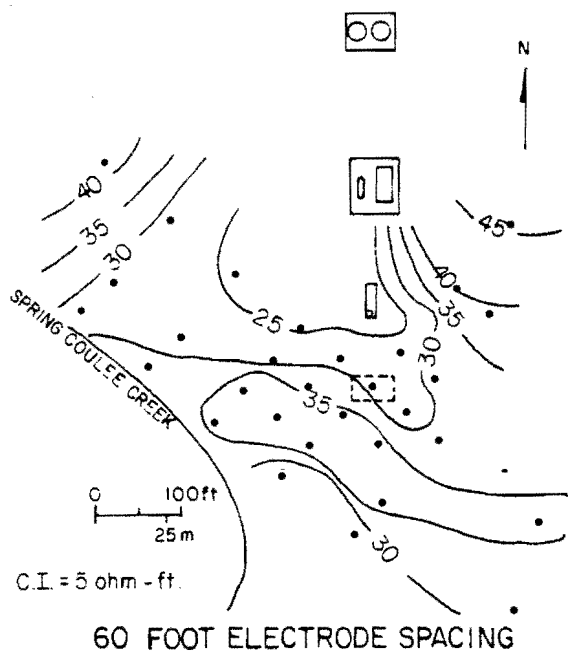
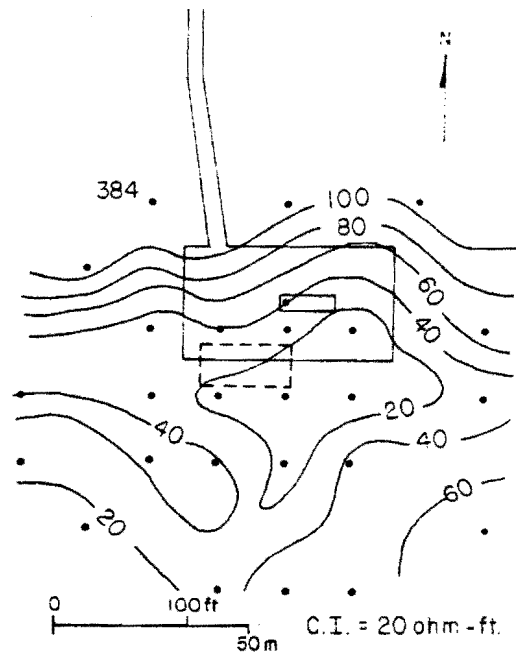
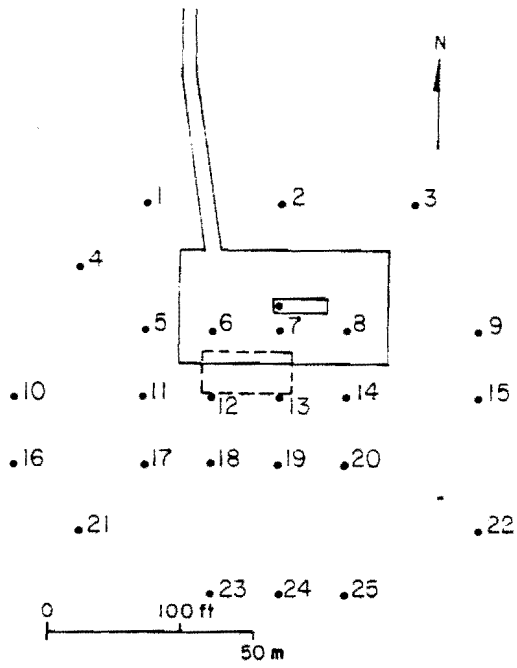
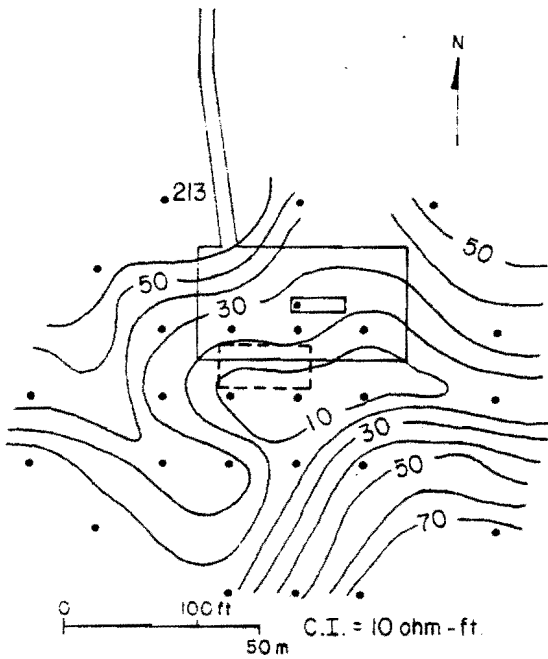


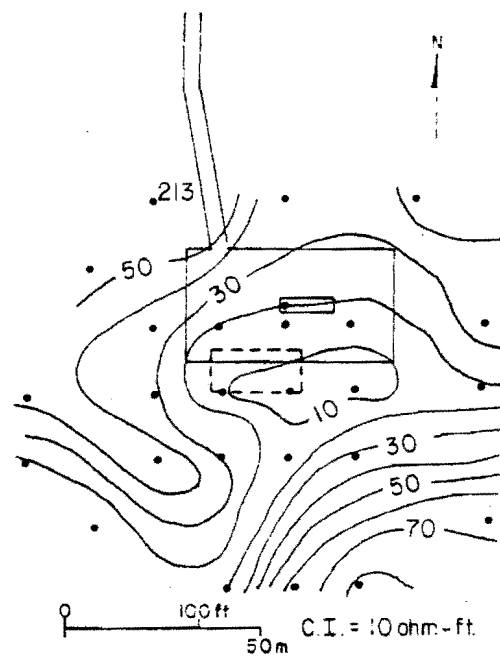
Figure 56. Resistivity station map and iso-resistivity maps of 3, 5, and 8 feet (0.9, 1.5, and 2.4 m) at the Fossum site.



3 FOOT ELECTRODE SPACING

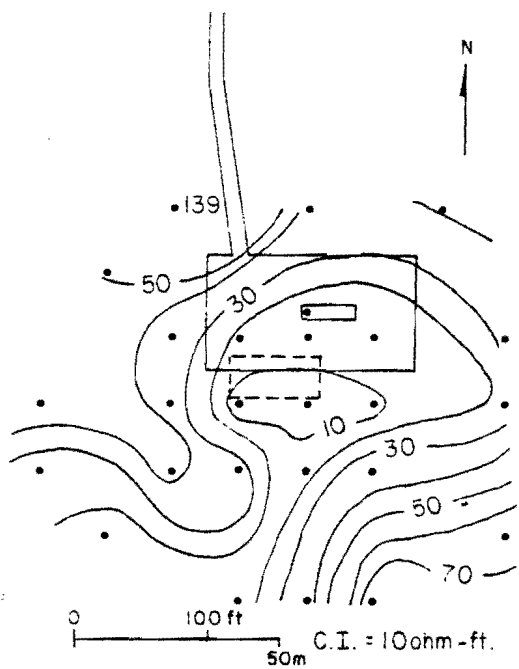


5 FOOT ELECTRODE SPACING

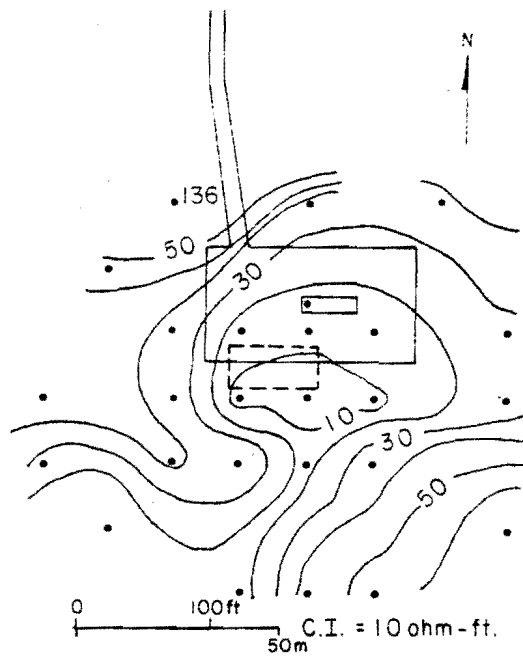


8 FOOT ELECTRODE SPACING

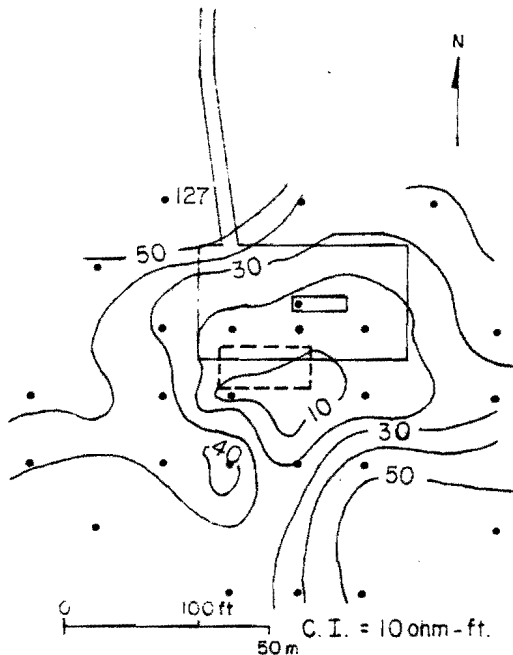
Figure 57. Isoresistivity maps for electrode spacings of 10, 12, 16, and 20 feet (3.1, 3.7, 4.9, and 6.1 m) at the Fossum site.



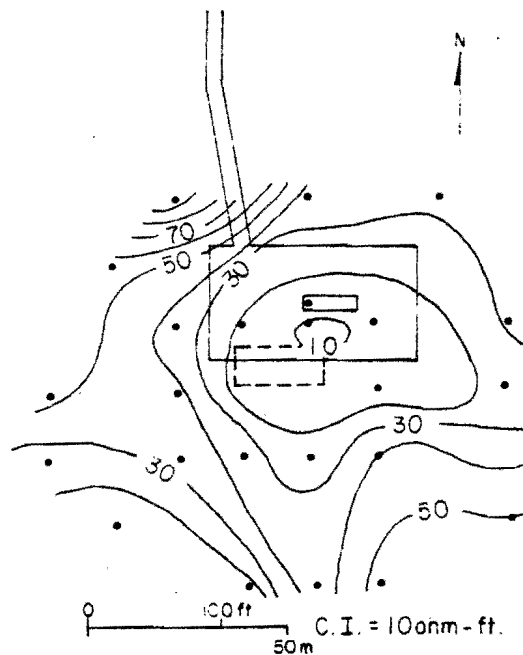
10 FOOT ELECTRODE SPACING



12 FOOT ELECTRODE SPACING

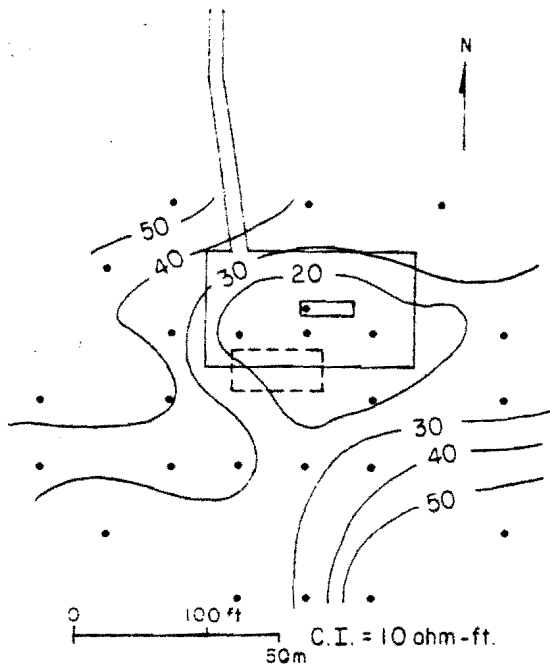


16 FOOT ELECTRODE SPACING

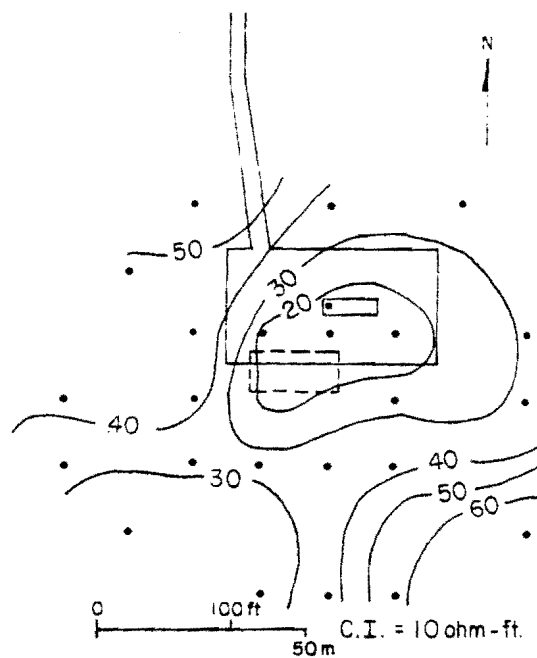


20 FOOT ELECTRODE SPACING

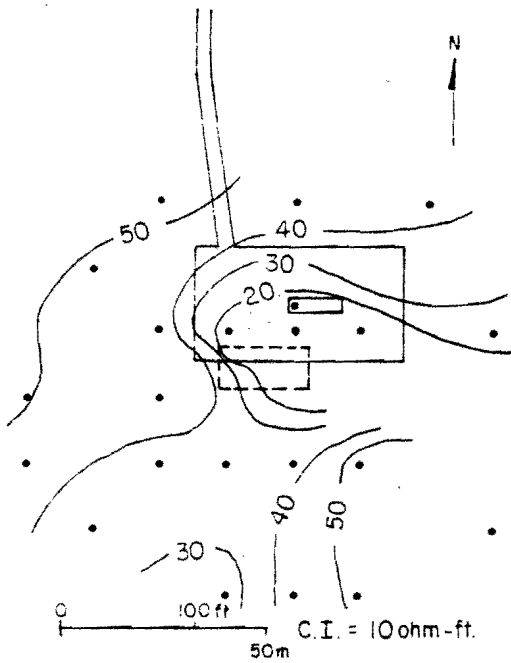
Figure 58. Isoresistivity maps for electrode spacings of 24, 30, 40, and 50 feet (7.3, 9.1, 12.2, and 15.2 m) at the Fossum site.



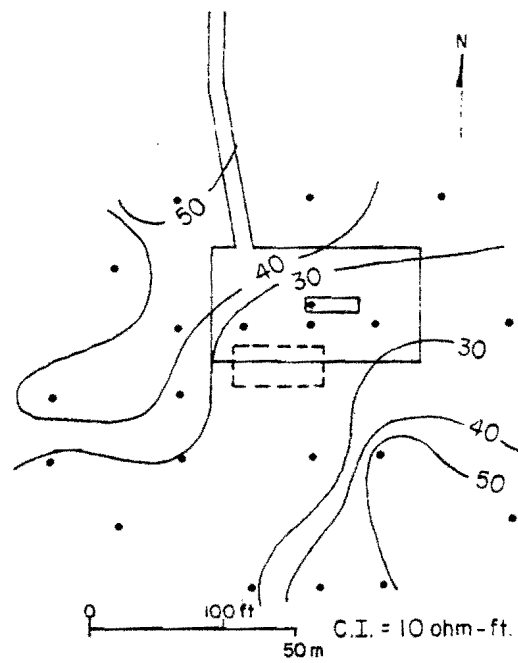
24 FOOT ELECTRODE SPACING



30 FOOT ELECTRODE SPACING



40 FOOT ELECTRODE SPACING



50 FOOT ELECTRODE SPACING

APPENDIX M
Groundwater and Pore Water Chemistry

Well Number	WP-1	WP-2	WP-3
Date	10-26-84	10-26-84	10-26-84
Temperature°C	9.5	9.0	9.5
Field pH	7.00	7.20	7.10
Field Conductivity µmhos/cm	2400	5400	3500
Lab pH @ 22°C	7.53	7.52	7.57
Lab Conductivity µmhos/cm	2653	8120	1624
TDS mg/L	2054	6179	1130
Hardness mg/L	700	1543	303
Alkalinity mg/L	279	171	189
Ca mg/L	172	447	74
Mg mg/L	66	104	28
Na mg/L	355	1124	221
K mg/L	25	40	16
SO ₄ mg/L	667	112	38
Cl mg/L	360	2605	401
NO ₃ mg/L	0.4	0.5	6.6
Fe µg/L	273	19	105
Mn µg/L	892	976	740
Cr µg/L	19.7	3.2	2.2
Pb µg/L	1.0	5	2.6

Well Number	WP-4	WP-5	WP-6
Date	10-26-84	10-26-84	10-26-84
Temperature°C	10.5	10.5	10.5
Field pH	7.25	7.20	6.65
Field Conductivity µmhos/cm	6000	5500	14500
Lab pH @ 22°C	7.72	7.71	7.40
Lab Conductivity µmhos/cm	8185	6370	46557
TDS mg/L	5462	4409	20335
Hardness mg/L	1089	753	7539
Alkalinity mg/L	421	268	114
Ca mg/L	204	211	2242
Mg mg/L	141	55	471
Na mg/L	1277	1111	3307
K mg/L	100	75	111
SO ₄ mg/L	134	132	261
Cl mg/L	2240	2061	10195
NO ₃ mg/L	0.5	4.3	---
Fe µg/L	113	61	792
Mn µg/L	903	530	7620
Cr µg/L	36	23	417
Pb µg/L	6.2	3.9	25

Well Number	WP-7	WP-8	WP-9
Date	10-26-84	10-26-84	10-26-84
Temperature°C	11.0	9.0	9.5
Field pH	6.85	7.40	7.25
Field Conductivity µmhos/cm	10900	2600	5500
Lab pH @ 22°C	7.45	7.42	7.41
Lab Conductivity µmhos/cm	16934	2891	8727
TDS mg/L	14203	2054	7978
Hardness mg/L	3910	726	2628
Alkalinity mg/L	192	140	136
Ca mg/L	1174	184	803
Mg mg/L	238	64	151
Na mg/L	2323	354	744
K mg/L	95	27	46
SO ₄ mg/L	313	505	387
Cl mg/L	6007	622	2734
NO ₃ mg/L	0.4	0.14	0.4
Fe µg/L	3225	18	129
Mn µg/L	6256	329	3519
Cr µg/L	23.1	14.7	19.8
Pb µg/L	32.8	1.5	1.4

Well Number	WP-10	WP-11	WP-12
Date	10-26-84	10-26-84	10-26-84
Temperature°C	9.5	9.5	10.0
Field pH	7.22	7.10	7.10
Field Conductivity µmhos/cm	5900	6100	8000
Lab pH @ 22°C	7.85	7.46	7.57
Lab Conductivity µmhos/cm	7817	8521	11596
TDS mg/L	4898	6113	8348
Hardness mg/L	800	1440	1170
Alkalinity mg/L	312	398	320
Ca mg/L	219	301	404
Mg mg/L	61	167	160
Na mg/L	1299	1259	1803
K mg/L	56	60	106
SO ₄ mg/L	142	467	132
Cl mg/L	2316	2659	3538
NO ₃ mg/L	7.2	0.5	0.4
Fe µg/L	31	28	125
Mn µg/L	1187	2421	1927
Cr µg/L	22.6	1.1	36.2
Pb µg/L	6.3	2.6	7.6

Well Number	WP-13	WP-14	WP-15
Date	10-26-84	10-26-84	10-26-84
Temperature°C	10.5	9.5	8.5
Field pH	6.35	7.15	7.20
Field Conductivity µmhos/cm	62000	2900	3400
Lab pH @ 22°C	7.00	7.51	7.7
Lab Conductivity µmhos/cm	85968	3086	3865
TDS mg/L	70492	2290	2732
Hardness mg/L	14198	789	898
Alkalinity mg/L	136	346	180
Ca mg/L	4415	187	233
Mg mg/L	771	78	77
Na mg/L	20013	463	522
K mg/L	618	26	32
SO ₄ mg/L	257	631	509
Cl mg/L	42105	505	872
NO ₃ mg/L	0.3	0.4	<0.1
Fe µg/L	12653	9	59
Mn µg/L	11177	1114	840
Cr µg/L	14.9	28.5	14
Pb µg/L	8.3	1.3	2.2

Well Number	WP-16	WP-17	WP-18
Date	10-26-84	10-26-84	10-26-84
Temperature°C	8.0	8.5	9.0
Field pH	6.70	7.10	7.15
Field Conductivity µmhos/cm	15100	4900	1825
Lab pH @ 22°C	7.46	7.54	8.05
Lab Conductivity µmhos/cm	46773	6204	1862
TDS mg/L	18669	3700	1526
Hardness mg/L	5229	845	565
Alkalinity mg/L	154	531	224
Ca mg/L	1720	193	135
Mg mg/L	227	88	55
Na mg/L	4022	1005	240
K mg/L	130	38	22
SO ₄ mg/L	185	137	756
Cl mg/L	8808	1746	74
NO ₃ mg/L	<0.1	1.2	0.4
Fe µg/L	7922	172	55
Mn µg/L	753	432	797
Cr µg/L	26	15	3.4
Pb µg/L	83	8.8	11.9

Well Number	WP-19	WP-20	WP-21
Date	10-26-84	10-26-84	10-26-84
Temperature °C	9.0	9.0	10.5
Field pH	7.15	7.00	7.00
Field Conductivity µmhos/cm	1550	4500	5400
Lab pH @ 22°C	7.50	7.45	7.64
Lab Conductivity µmhos/cm	1570	5511	7243
TDS mg/L	1318	3894	5134
Hardness mg/L	655	823	1297
Alkalinity mg/L	296	273	443
Ca mg/L	148	238	303
Mg mg/L	70	55	131
Na mg/L	251	831	985
K mg/L	18	29	105
SO ₄ mg/L	526	70	177
Cl mg/L	28	1641	2126
NO ₃ mg/L	0.4	1.0	1.6
Fe µm/L	127	9	256
Mn µm/L	1348	31	2491
Cr µm/L	8.9	9	16.7
Pb µm/L	1.6	1.4	4.9

Well Number	WP-22	WP-23	WP-24
Date	10-26-84	10-26-84	10-26-84
Temperature °C	10.5	8.0	7.5
Field pH	6.55	7.30	7.00
Field Conductivity µmhos/cm	33000	2300	6600
Lab pH @ 22°C	6.81	7.70	7.31
Lab Conductivity µmhos/cm	58034	2376	10318
TDS mg/L	34806	1861	7937
Hardness mg/L	14255	795	1978
Alkalinity mg/L	158	379	365
Ca mg/L	4028	171	472
Mg mg/L	1019	89	194
Na mg/L	6331	320	1312
K mg/L	377	25	50
SO ₄ mg/L	200	786	116
Cl mg/L	19412	172	3251
NO ₃ mg/L	0.8	<0.1	0.3
Fe µg/L	39920	13	
Mn µg/L	8641	1274	
Cr µg/L	635	25.3	
Pb µg/L	9.6	2.5	

Well Number	WP-25	WP-26	WP-27
Date	10-26-84	10-26-84	10-26-84
Temperature °C	7.5	8.0	8.0
Field pH	7.10	7.05	7.28
Field Conductivity µmhos/cm	11900	8900	1800
Lab pH @ 22°C	7.50	7.50	7.72
Lab Conductivity µmhos/cm	17941	14270	1938
TDS mg/L	13983	10732	1586
Hardness mg/L	2656	2652	636
Alkalinity mg/L	272	346	348
Ca mg/L	676	589	150
Mg mg/L	235	287	64
Na mg/L	3237	2003	238
K mg/L	118	377	21
SO ₄ mg/L	127	221	686
Cl mg/L	5350	4628	89
NO ₃ mg/L	3.3	<0.1	0.2
Fe µg/L	200		157
Mn µg/L	7800		566
Cr µg/L	52		20
Pb µg/L	15.7		2.1

Well Number	WP-28	WP-29	Creek
Date	10-26-84	10-26-84	10-26-84
Temperature °C	9.0	9.0	9.0
Field pH	7.10	7.20	7.9
Field Conductivity µmhos/cm	4600	3600	4000
Lab pH @ 22°C	7.36	7.52	7.46
Lab Conductivity µmhos/cm	7059	4010	5349
TDS mg/L	5675	3041	4146
Hardness mg/L	2058	613	1178
Alkalinity mg/L	88	200	153
Ca mg/L	627	173	221
Mg mg/L	119	44	152
Na mg/L	588	639	675
K mg/L	75	19	62
SO ₄ mg/L	168	53	339
Cl mg/L	2270	1284	1544
NO ₃ mg/L	0.1	8.0	0.4
Fe µg/L	31	129	90
Mn µg/L	2676	271	101
Cr µg/L	15.2	26.9	9.1
Pb µg/L	69.5	2.9	1.2

Well Number	Christianson	Stevans
Date	10-25-84	10-25-84
Temperature °C	10.5	12
Field pH	7.1	7.25
Field Conductivity µmhos/cm	1900	750
Lab pH @ 22°C	7.2	7.59
Lab Conductivity µmhos/cm	3259	1018
TDS mg/L	3433	749
Hardness mg/L	1201	411
Alkalinity mg/L	272	263
Ca mg/L	355	112
Mg mg/L	76	32
Na mg/L	169	119
K mg/L	14	23
SO ₄ mg/L	67	51
Cl mg/L	971	95
NO ₃ mg/L	1.4	35

Well Number	FP-1	FP-2	FP-3
Date	10-23-84	10-23-84	10-25-84
Temperature °C	7.00	6.0	9.5
Field pH	7.85	7.85	7.35
Field Conductivity µmhos/cm	2100	2200	4700
Lab pH @ 22°C	7.30	7.66	7.25
Lab Conductivity µmhos/cm	2230	2263	10080
TDS mg/L	1840	1868	7342
Hardness mg/L	753	621	2497
Alkalinity mg/L	411	328	346
Ca mg/L	156	137	495
Mg mg/L	88	68	306
Na mg/L	307	341	1280
K mg/L	23	23	64
SO ₄ mg/L	919	978	1276
Cl mg/L	14	20	2203
NO ₃ mg/L	<0.1	0.4	0.2
Fe µg/L	88	205	145
Mn µg/L	12	673	6913
Cr µg/L	6.6	19.5	18
Pb µg/L	2.9	5.0	2.7

Well Number	FP-4	FP-5	FP-6
Date	10-25-84	10-27-84	10-27-84
Temperature °C	8.5	6.0	7.0
Field pH	7.23	7.15	7.30
Field Conductivity µmhos/cm	7200	2200	2100
Lab pH @ 22°C	7.55	7.67	7.66
Lab Conductivity µmhos/cm	15494	2458	2436
TDS mg/L	12376	1994	2066
Hardness mg/L	2731	702	688
Alkalinity mg/L	200	375	311
Ca mg/L	838	155	150
Mg mg/L	155	76	76
Na mg/L	2472	357	366
K mg/L	87	21	23
SO ₄ mg/L	1054	1037	1062
Cl mg/L	5025	46	56
NO ₃ mg/L	0.4	---	<0.1
Fe µg/L	2141	132	114
Mn µg/L	8558	1639	1927
Cr µg/L	23	15.3	24
Pb µg/L	8.3	5.4	5.6

Well Number	FP-7	FP-8	FP-9
Date	10-23-84	10-23-84	10-25-84
Temperature °C	7.0	6.0	8.0
Field pH	7.48	7.79	7.46
Field Conductivity µmhos/cm	1100	900	2100
Lab pH @ 22°C	7.58	7.91	7.39
Lab Conductivity µmhos/cm	2339	1613	2593
TDS mg/L	1901	1276	2109
Hardness mg/L	748	505	755
Alkalinity mg/L	461	361	449
Ca mg/L	167	122	179
Mg mg/L	80	49	75
Na mg/L	336	201	399
K mg/L	21	21	23
SO ₄ mg/L	866	570	1076
Cl mg/L	27	30	52
NO ₃ mg/L	<0.1	0.4	0.4
Fe µg/L	151	152	116
Mn µg/L	667	1526	44
Cr µg/L	19.1	19.9	11.8
Pb µg/L	6.0	5.6	6.1

Well Number	FP-10	FP-11	FP-12
Date	10-25-84	10-25-84	10-25-84
Temperature °C	8.5	5.5	8.0
Field pH	7.62	7.10	7.50
Field Conductivity µmhos/cm	2100	2500	1975
Lab pH @ 22°C	7.63	7.67	7.64
Lab Conductivity µmhos/cm	2837	5424	2501
TDS mg/L	2389	4909	2078
Hardness mg/L	889	1515	628
Alkalinity mg/L	414	477	347
Ca mg/L	181	292	138
Mg mg/L	106	191	69
Na mg/L	399	864	417
K mg/L	26	35	22
SO ₄ mg/L	1228	2749	1054
Cl mg/L	58	146	51
NO ₃ mg/L	0.4	<0.1	---
Fe µg/L	172	4670	392
Mn µg/L	270	1122	526
Cr µg/L	5	13	44.5
Pb µg/L	6.9	4.0	5.6

Well Number	FL-1
Date	10-23-84
Temperature °C	7.2
Field pH	6.87
Field Conductivity µmhos/cm	1300
Lab pH @ 22°C	7.5
Lab Conductivity µmhos/cm	3151
TDS mg/L	3268
Hardness mg/L	1986
Alkalinity mg/L	271
Ca mg/L	419
Mg mg/L	228
Na mg/L	178
K mg/L	25
SO ₄ mg/L	1664
Cl mg/L	165
NO ₃ mg/L	0.2

Well Number	FL-6	FL-7
Date	10-24-84	10-24-84
Temperature °C	9	7
Field pH	7.3	7.48
Field Conductivity µmhos/cm	9000	1100
Lab pH @ 22°C	7.8	7.5
Lab Conductivity µmhos/cm	21579	45907
TDS mg/L	36839	23746
Hardness mg/L	15693	6583
Alkalinity mg/L	600	405
Ca mg/L	616	1060
Mg mg/L	3437	956
Na mg/L	3696	4235
K mg/L	97	137
SO ₄ mg/L	20236	3577
Cl mg/L	870	8732
NO ₃ mg/L	---	22.0
PO ₄ mg/L	89	198

Well Number	FL-9
Date	10-23-84
Temperature °C	8
Field pH	6.56
Field Conductivity µmhos/cm	<20000
Lab pH @ 22°C	6.5
Lab Conductivity µmhos/cm	90624
TDS mg/L	123684
Hardness mg/L	19006
Alkalinity mg/L	272
Ca mg/L	3797
Mg mg/L	2313
Na mg/L	38348
K mg/L	1497
SO ₄ mg/L	2231
Cl mg/L	73280
NO ₃ mg/L	
PO ₄ mg/L	89

Well Number	FL-11
Date	10-23-84
Temperature °C	7.5
Field pH	7.03
Field Conductivity µmhos/cm	4200
Lab pH	7.3
Lab Conductivity µmhos/cm	8586
TDS mg/L	7360
Hardness mg/L	3695
Alkalinity mg/L	391
Ca mg/L	502
Mg mg/L	593
Na mg/L	750
K mg/L	34
SO ₄ mg/L	2124
Cl mg/L	1678
NO ₃ mg/L	1.5

APPENDIX N
Saturated-Paste Extract Chemical Analyses

Sample	FS-2	FS-2	FS-2	FS-2
Depth	5 ft.	10 ft.	15 ft.	20 ft.
pH	7.7	7.8	7.8	7.1
EC mmhos/cm	27.91	8.64	7.48	7.53
Sat %	55	51	53	52
Ca mg/L	42.20	21.38	15.48	21.61
Mg mg/L	88.04	72.33	54.13	60.42
Na mg/L	212.28	40.39	39.23	35.30
SAR	26.0	5.9	6.6	5.5
HCO ₃ mg/L	1.10	2.01	2.75	1.80
Cl mg/L	236.59	2.35	3.77	1.88
SO ₄ mg/L	104.83	129.74	102.32	113.65

Sample	FS-3	FS-3	FS-3	FS-3	FS-3
Depth	5 ft.	10 ft.	15 ft.	20 ft.	30 ft.
pH	7.2	7.1	7.0	7.1	7.4
EC mmhos/cm	73.1	88.4	3.89	3.58	2.47
Sat %	81	54	53	51	45
Ca mg/L	94.23	133.16	16.30	17.65	9.04
Mg mg/L	68.92	48.86	13.19	11.30	5.10
Na mg/L	771.31	1004.41	16.79	13.68	12.85
SAR	85.0	105.0	4.4	3.6	4.8
HCO ₃ mg/L	1.32	5.49	1.68	2.14	2.98
Cl mg/L	845.85	1111.22	19.58	2.54	1.58
SO ₄ mg/L	87.29	69.72	24.82	37.95	22.43

Sample	FS-5	FS-5	FS-5	FS-5
Depth	5 ft.	10 ft.	15 ft.	20 ft.
pH	7.2	7.3	7.5	7.4
EC mmhos/cm	28.91	4.54	1.46	3.46
Sat %	52	47	51	50
Ca mg/L	59.04	18.80	4.12	18.92
Mg mg/L	105.39	14.84	2.82	11.59
Na mg/L	193.29	14.61	8.23	13.30
SAR	21.0	3.6	4.4	3.4
HCO ₃ mg/L	1.10	1.38	1.79	2.18
Cl mg/L	277.56	4.27	1.30	1.10
SO ₄ mg/L	79.06	42.60	12.08	40.53

Sample	FS-6	FS-6	FS-6	FS-6
Depth	5 ft.	10 ft.	15 ft.	20 ft.
pH	7.4	7.2	7.5	7.4
EC mmhos/cm	16.0	23.3	1.56	2.72
Sat %	49	52	46	51
Ca mg/L	42.63	76.49	4.69	12.77
Mg mg/L	36.19	64.67	3.67	9.63
Na mg/L	92.67	121.55	6.82	9.26
SAR	15.0	14.0	3.3	2.8
HCO ₃ mg/L	1.80	1.54	1.79	2.07
Cl mg/L	136.08	213.66	0.91	0.82
SO ₄ mg/L	33.61	47.61	12.48	28.77
Sample	FS-7	FS-7	FS-7	WP-9

Depth	5 ft.	10 ft.	15 ft.	18.5 ft.
pH	7.6	7.5	7.4	7.2
EC mmhos/cm	15.4	5.64	3.54	11.9
Sat %	52	48	52	56
Ca mg/L	26.44	27.85	18.80	35.58
Mg mg/L	15.96	28.45	13.84	18.10
Na mg/L	117.97	16.81	12.25	66.76
SAR mg/L	26.0	3.2	3.0	13.0
HCO ₃ mg/L	1.80	1.34	1.58	1.48
Cl mg/L	121.72	15.26	1.01	98.41
SO ₄ mg/L	36.85	56.51	42.30	20.55

APPENDIX 0
X-Ray Fluorescence Analyses

Hole Number	FS-1 (%)	FS-1 (%)	FS-1 (%)	FS-1 (%)	FS-1 (%)
Depth (in ft.)	3	5	6	8	10
Na ₂ O	0.69	0.83	0.79	0.86	0.76
MgO	5.76	5.11	4.99	4.62	4.59
Al ₂ O ₃	9.63	10.83	11.86	12.04	10.76
SiO ₂	51.17	60.69	61.34	62.63	58.24
P ₂ O ₅	0.13	0.15	0.15	0.14	0.15
K ₂ O	1.94	2.06	2.18	2.17	2.08
CaO	16.37	11.97	11.27	10.52	12.68
TiO ₂	0.57	0.57	0.65	0.63	0.62
MnO	0.07	0.11	0.09	0.09	0.12
Fe ₂ O ₃	4.18	4.32	4.71	4.76	4.72
TOTAL	90.51	96.66	98.04	98.47	94.73

Hole Number	FS-1 (%)	FS-1 (%)	FS-1 (%)	FS-1 (%)
Depth (in ft.)	12	15	20	25
Na ₂ O	0.79	0.85	0.89	0.84
MgO	4.46	4.42	9.17	3.86
Al ₂ O ₃	11.82	11.42	11.14	12.13
SiO ₂	62.14	63.59	63.72	64.92
P ₂ O ₅	0.16	0.14	0.14	0.16
K ₂ O	2.16	2.18	2.09	2.27
CaO	10.79	10.64	10.77	8.59
TiO ₂	0.63	0.64	0.57	0.68
MnO	0.30	0.05	0.09	0.09
FeiO ₃	4.73	4.48	4.16	4.71
TOTAL	97.99	98.42	97.77	98.25

Hole Number	FS-2 (%)	FS-2 (%)	FS-2 (%)	FS-2 (%)	FS-2 (%)
Depth (in ft.)	3	5	6	8	10
Na ₂ O	0.76	7.93	26.82	0.94	0.93
MgO	6.27	5.16	3.59	5.12	5.11
Al ₂ O ₃	10.97	9.84	7.04	11.93	11.59
SiO ₂	54.38	55.47	40.10	62.25	67.03
P ₂ O ₅	0.13	0.13	0.08	0.15	0.16
K ₂ O	2.20	1.82	1.19	2.18	2.16
CaO	14.32	10.40	7.00	10.32	16.79
TiO ₂	0.65	0.51	0.38	0.63	0.63
MnO	0.07	0.09	0.06	0.09	0.68
Fe ₂ O ₃	4.68	3.95	3.07	4.61	4.60
TOTAL	94.44	95.31	89.65		98.07

Hole Number	FS-2 (%)	FS-2 (%)	FS-2 (%)	FS-2 (%)
Depth (in ft.)	12	15	18.5	20
Na ₂ O	0.90	0.96	1.29	1.06
MgO	4.97	4.76	4.31	4.18
Al ₂ O ₃	11.76	11.72	8.57	13.59
SiO ₂	61.06	62.60	63.69	66.90
P ₂ O ₅	0.16	0.15	0.17	0.15
K ₂ O	2.20	2.19	1.89	2.27
CaO	10.95	9.97	9.13	6.93
TiO ₂	0.61	0.66	0.69	0.66
MnO	0.16	0.06	0.07	0.08
Fe ₂ O ₃	4.67	4.92	3.04	4.63
TOTAL	97.46	98.01	92.05	100.48

Hole Number	FS-3 (%)	FS-3 (%)	FS-3 (%)	FS-3 (%)	FS-3 (%)	FS-3 (%)
Depth (in ft.)	0.5	4	5	6	8	10
Na ₂ O	0.86	0.97	3.77	3.64	2.14	4.05
MgO	2.21	5.03	5.47	3.43	4.03	3.38
Al ₂ O ₃	10.96	10.75	9.73	12.93	10.61	8.98
SiO ₂	67.29	59.30	54.47	64.35	53.79	50.97
P ₂ O ₅	0.18	0.15	0.13	0.15	0.14	0.15
K ₂ O	2.40	2.08	1.91	2.27	2.06	2.06
CaO	2.48	12.24	12.68	5.16	10.86	13.66
TiO ₂	0.61	0.06	0.52	0.60	0.06	0.53
MnO	0.15	0.11	0.10	0.07	0.07	0.09
Fe ₂ O ₃	4.05	4.53	3.93	4.59	4.24	4.04
TOTAL	93.20	95.78	92.72	97.19	89.03	87.91

Hole Number	FS-3 (%)	FS-3 (%)	FS-3 (%)	FS-3 (%)	FS-3 (%)	FS-3 (%)
Depth (in ft.)	12.5	15	20	25	28	30
Na ₂ O	15.15	0.89	0.81	0.85	1.21	0.95
MgO	3.60	5.01	4.86	4.31	3.03	3.65
Al ₂ O ₃	9.07	10.91	11.31	12.29	9.33	13.94
SiO ₂	51.37	60.41	61.55	63.21	67.38	67.23
P ₂ O ₅	0.12	0.16	0.14	0.85	0.16	0.15
K ₂ O	1.55	2.12	2.15	2.23	1.97	2.34
CaO	7.94	11.33	11.85	10.07	7.38	6.58
TiO ₂	0.47	0.62	0.62	0.68	0.56	0.71
MnO	0.09	0.11	0.11	0.10	0.06	0.08
Fe ₂ O ₃	3.7	5.32	4.46	4.68	2.99	4.90
TOTAL	93.07	96.90	97.88	98.60	94.09	99.63

Hole Number	FS-3 (%)	FS-3 (%)	FS-3 (%)
Depth (in ft.)	35	40	45
Na ₂ O	0.94	0.95	0.94
MgO	3.52	3.73	3.86
Al ₂ O ₃	14.48	14.22	13.38
SiO ₂	67.31	66.74	66.41
P ₂ O ₅	0.16	0.15	0.16
K ₂ O	2.39	2.34	2.33
CaO	6.34	6.72	6.74
TiO ₂	0.70	0.71	0.72
MnO	0.08	0.09	0.08
Fe ₂ O ₃	5.05	4.94	4.81
TOTAL	100.97	100.59	99.45

Hole Number	FS-4 (%)	FS-4 (%)	FS-4 (%)	FS-4 (%)	FS-4 (%)
Depth (in ft.)	3	4	5	6	8
Na ₂ O	0.63	0.59	0.66	0.67	0.80
MgO	9.68	3.53	4.53	4.56	4.77
Al ₂ O ₃	9.75	8.58	10.26	10.16	11.79
SiO ₂	51.25	47.14	54.48	56.22	61.68
P ₂ O ₅	0.36	0.13	0.12	0.13	0.15
K ₂ O	1.91	1.69	1.91	1.98	2.11
CaO	17.47	21.52	16.46	15.4	11.37
TiO ₂	0.58	0.57	0.56	0.56	0.62
MnO	0.11	0.04	0.11	0.12	0.71
Fe ₂ O ₃	4.90	3.67	4.28	4.62	4.86
TOTAL	91.63	87.46	93.38	94.44	98.29

Hole Number	FS-4 (%)	FS-4 (%)	FS-4 (%)	FS-4 (%)
Depth (in ft.)	10	12	15	20
Na ₂ O	0.74	0.80	0.75	0.82
MgO	4.89	4.59	4.60	4.47
Al ₂ O ₃	11.64	12.41	11.46	11.64
SiO ₂	61.41	62.47	61.27	62.71
P ₂ O ₅	0.15	0.16	0.20	0.15
K ₂ O	2.70	2.25	2.19	2.23
CaO	11.19	10.44	11.01	10.74
TiO ₂	0.65	0.67	0.67	0.66
MnO	0.07	0.10	0.06	0.10
Fe ₂ O ₃	4.87	4.88	5.31	4.61
TOTAL	97.80	98.81	97.53	98.13

Hole Number	FS-5 (%)	FS-5 (%)	FS-5 (%)	FS-5 (%)	FS-5 (%)	FS-5 (%)
Depth (in ft.)	0.5	1.5	3	5	6	8
Na ₂ O	1.07	0.83	0.89	6.93	1.95	0.88
MgO	2.80	4.70	8.80	4.98	4.91	5.13
Al ₂ O ₃	10.49	7.94	9.51	10.28	10.76	12.07
SiO ₂	68.63	44.82	50.69	54.48	56.94	61.25
P ₂ O ₅	0.18	0.14	0.11	0.13	0.14	0.15
K ₂ O	2.35	1.55	1.80	1.85	1.94	2.19
CaO	1.76	0.65	15.64	11.98	11.84	11.13
TiO ₂	0.59	0.59	0.53	0.54	0.57	0.64
MnO	0.12	0.06	0.23	0.10	0.09	0.16
Fe ₂ O ₃	3.71	2.79	4.22	3.95	4.65	4.75
TOTAL	91.68	84.02	92.45	95.24	93.80	98.36

Hole Number	FS-5 (%)	FS-5 (%)	FS-5 (%)	FS-5 (%)	FS-5 (%)	FS-5 (%)
Depth (in ft.)	10	12	15	20	27.5	30
Na ₂ O	0.80	0.84	0.82	0.91	1.31	0.93
MgO	4.67	4.66	4.59	3.63	2.85	3.72
Al ₂ O ₃	11.40	11.96	12.00	12.15	9.65	13.04
SiO ₂	60.24	61.69	62.05	65.43	69.50	66.75
P ₂ O ₅	0.15	0.17	0.16	0.69	0.14	0.15
K ₂ O	2.15	2.20	2.21	2.25	2.02	2.29
CaO	12.26	10.92	10.77	8.37	6.37	7.34
TiO ₂	0.62	0.64	0.67	0.67	0.51	0.69
MnO	0.15	0.09	0.06	0.10	0.06	0.88
Fe ₂ O ₃	4.75	4.84	4.91	4.58	3.20	4.64
TOTAL	97.18	98.02	98.23	98.78	95.43	99.63

Hole Number	FS-6 (%)	FS-6 (%)	FS-6 (%)	FS-6 (%)	FS-6 (%)
Depth (in ft.)	1.5	4	5	6	8
Na ₂ O	0.65	0.76	1.09	1.60	1.99
MgO	3.35	4.73	5.12	5.08	4.60
Al ₂ O ₃	6.77	10.02	11.36	11.36	11.50
SiO ₂	12.87	53.01	50.79	58.39	59.82
P ₂ O ₅	0.16	0.12	0.14	0.13	0.14
K ₂ O	1.45	1.82	2.15	2.14	2.05
CaO	24.18	16.61	12.37	11.88	10.82
TiO ₂	0.53	0.56	0.59	0.51	0.61
MnO	0.08	0.10	0.17	0.13	0.07
Fe ₂ O ₃	2.78	4.60	4.94	4.88	4.46
TOTAL	82.82	92.32	97.72	96.16	96.07

Hole Number	FS-6 (%)	FS-6 (%)	FS-6 (%)
Depth (in ft.)	10	15	20
Na ₂ O	1.75	0.87	0.91
MgO	4.54	1.65	3.84
Al ₂ O ₃	11.29	11.88	13.57
SiO ₂	59.89	62.41	65.97
P ₂ O ₅	0.15	0.15	0.15
K ₂ O	2.00	2.19	2.33
CaO	10.94	10.83	6.93
TiO ₂	0.58	0.64	0.70
MnO	0.09	0.14	0.10
Fe ₂ O ₃	4.32	4.66	4.98
TOTAL	95.53	98.42	99.48

Hole Number	FS-7 (%)	FS-7 (%)	FS-7 (%)	FS-7 (%)	FS-7 (%)
Depth (in ft.)	0.5	1.5	3	5	6
Na ₂ O	0.85	1.11	0.87	1.20	1.05
MgO	2.32	2.86	5.89	4.32	5.06
Al ₂ O ₃	12.83	9.59	9.13	10.77	10.81
SiO ₂	69.86	72.09	52.23	62.60	59.94
P ₂ O ₅	0.10	0.13	0.14	0.14	0.15
K ₂ O	2.63	1.99	1.76	2.09	2.06
CaO	1.40	5.34	15.72	10.56	11.97
TiO ₂	0.65	0.39	0.58	0.59	0.61
MnO	0.10	0.07	0.06	0.10	0.09
Fe ₂ O ₃	5.03	3.51	3.49	4.42	5.10
TOTAL	95.75	97.08	89.86	97.78	96.84

Hole Number	FS-7 (%)	FS-7 (%)	FS-7 (%)	FS-7 (%)
Depth (in ft.)	8	10	12	15
Na ₂ O	1.15	0.80	0.76	0.80
MgO	4.80	5.04	9.84	9.53
Al ₂ O ₃	11.91	12.23	12.01	11.79
SiO ₂	61.94	61.15	61.32	61.81
P ₂ O ₅	0.15	0.16	0.16	0.16
K ₂ O	2.18	2.20	2.17	2.22
CaO	10.85	11.16	11.20	10.35
TiO ₂	0.65	0.65	0.65	0.66
MnO	0.10	0.07	0.11	0.30
Fe ₂ O ₃	4.70	4.81	4.84	5.15
TOTAL	98.44	98.28	98.10	97.79

Hole Number	WS-1 (%)	WS-1 (%)	WS-1 (%)	WS-1 (%)	WS-2 (%)	WS-2 (%)
Depth (in ft.)	2	3	6	7	2	5-8
Na ₂ O	1.04	1.06	2.57	1.23	1.44	1.10
MgO	5.39	5.31	5.05	5.47	3.63	5.07
Al ₂ O ₃	8.53	7.58	8.3	7.29	9.31	6.23
SiO ₂	54.53	50.76	51.89	47.49	68.58	58.72
P ₂ O ₅	0.23	0.17	0.16	0.23	0.16	0.09
K ₂ O	1.89	1.57	1.63	1.57	2.27	1.82
CaO	13.55	17.37	15.16	17.81	6.88	16.56
TiO ₂	0.19	0.46	0.45	0.44	0.32	0.16
MnO	0.12	0.15	0.11	0.17	0.14	0.14
Fe ₂ O ₃	4.06	3.99	3.83	3.92	3.08	2.34
TOTAL	89.84	88.44	89.18	85.64	95.83	90.26

Hole Number	WP-2 (%)	WP-9 (%)	WP-25 (%)
Depth (in ft.)	15	18.5	3-6
Na ₂ O	0.96	1.19	1.41
MgO	3.89	3.61	3.87
Al ₂ O ₃	13.80	13.23	7.43
SiO ₂	65.99	67.25	66.85
P ₂ O ₅	0.17	0.15	0.11
K ₂ O	2.33	2.29	1.68
CaO	7.03	6.47	9.68
TiO ₂	0.72	0.69	0.35
MnO	0.08	0.08	0.09
Fe ₂ O ₃	5.27	4.48	2.85
TOTAL	100.24	94.86	94.37

REFERENCES

REFERENCES

- Anderson, M.P., 1984, Movement of contaminants in groundwater: groundwater transport-advection dispersion, in *Groundwater Contamination: National Academy Press, Washington, DC*, p. 37-44.
- Anderson, S.B. and Bluemle, J.P., 1984, Oil exploration and development in the North Dakota Williston Basin-1983 update: North Dakota Geological Survey Miscellaneous Series no. 65, 34 p.
- Blatt, H., Middleton, G., and Murray, R., 1980, Origin of sedimentary rocks: Englewood Cliffs, NJ, Prentice-Hall, Inc., 634 p.
- Bluemle, J.P., compiler, 1971, Depth to bedrock preliminary map: North Dakota Geological Survey Miscellaneous Map no. 13, scale 1:500,000.
- Bluemle, J.P. 1983, Geologic and topographic bedrock map of North Dakota: North Dakota Geological Survey Miscellaneous map no. 25, scale 1:670,000.
- Bluemle, J.P., 1985, Geology of Bottineau County, North Dakota: North Dakota Geological Survey Bulletin /8, Part I (North Dakota State Water Commission County Groundwater Studies 35), 57 p.
- Cartwright, Keros, and McComas, M.R., 1968, Geophysical surveys in the vicinity of sanitary landfills in north-eastern Illinois: *Groundwater*, v. 6, p. 23-30.
- Cherry, J.A., Gillham, R.W., and Barker, J.F., 1984, Contaminants in groundwater, in *Groundwater Contamination: National Academy Press, Washington, DC*, p. 46-64.
- Clayton, Lee, Moran, S.R., and Bluemle, J.P., 1980a, Explanatory text to accompany the geologic map of North Dakota: North Dakota Geological Survey Report of Investigation no. 69, 93 p.
- Clayton, Lee, Moran, S.R., and Bluemle, J.P., and Carlson, C.G., 1980b, Geologic map of North Dakota: U.S. Geological Survey, scale 1:670,000.
- Dames and Moore, 1982, Analysis of hydrologic and environmental effects of drilling mud pits and produced water impoundments: Volume I- Executive summary and report: American Petroleum Institute, 109 p.
- Dewey, M.B., 1984, Effect of reserve pit reclamation on groundwater quality at selected oil well sites in eastern Montana and western North Dakota: Master's Thesis, University of Montana, Missoula, MT, 174 p.

- Drever, J.I., 1982, The geochemistry of natural waters: Englewood Cliffs, NJ, Prentice-Hall, Inc., 388 p.
- Fisher, Farley, project director, 1975, Conference on the Environmental Aspects of Chemical Use in Well Drilling, Houston, Texas, May, 1975, Proceedings: U.S. Environmental Protection Agency, EPA-560/1-75-004, 604 p.
- Freeze, R.A., and Cherry, J.A., 1979, Groundwater: Englewood Cliffs, NJ, Prentice-Hall, Inc., 604 p.
- Gatlin, Carl, 1960, Petroleum Engineering--Drilling and Well Completion: Englewood Cliffs, NJ, Prentice Hall Inc., 341 p.
- Gelhar, L.W., Mantogluo, A., Welty, C., and Reghfeldt, K.R., 1985, A review of field-scale physical solute transport processes in saturated and unsaturated porous media: Tennessee Valley Authority, prepared for the Electric Power Research Institute, EA-4190, Research Project 2485-5, Final Report, 100 p.
- Gerhard, L.C., and Anderson, S.B., 1981, Oil exploration and development in the North Dakota Williston Basin-1980 update: North Dakota Geological Survey Miscellaneous Series No. 59, 19 p.
- Greenhouse, J.P., and Harris, R.D., 1983, Migration of contaminants in groundwater at a landfill: a case study, 7. DC, VLF, and inductive resistivity surveys: Journal of Hydrology, vol 63, p 177-198.
- Griffin, R.A., Cartwright, Keros, Shimp, N.F., Steele, J.D., Ruch, R.R., White, W.A., Hughes, G.M., and Gilkeson, R.H., 1976, Attenuation of pollutants in municipal landfill leachate by clay minerals: Part I-Column leaching and field verification: Illinois State Geological Survey Environmental Geology Notes, no. 78, 34 p.
- Grisak, G.E., 1975, The fracture porosity of glacial till: Canadian Journal of Earth Science, V. 12, p. 513-515.
- Grisak, G.E., and Cherry, J.A., 1975, Hydrologic characteristics response of fractured till and clay confining a shallow aquifer: Canadian Geotechnical Journal, v. 12, p. 304-343.
- Grisak, G.E., Cherry, J.A., Vonhof, J.A., and Bluemle, J.P., 1976, Hydrogeologic and hydrogeochemical properties of fractured till in the interior plains region, in Legget, R.F., ed., Glacial Till: Royal Society of Canada Special Publication no. 12, Ottawa, p. .
- Grisak, G.E., Pickens, J.F., and Cherry, J.A., 1980, Solute transport through fractured media, 2 column study of fractured till: Water Resources Research, v. 16, no. 4, p. 731-739.
- Horslev, M.J., 1951, Time lag and soil permeability in groundwater observations: Waterways Experiment Station, Corps of Engineers, U.S. Army Bulletin 36, Vicksburg, Mississippi, 147 p.

- Javandel, I., Doughty, C., and Tsang, C.F., 1984, Groundwater transport: Handbook of mathematical models, American Geophysical Union, Washington, DC, 228 p.
- Jenne, E.A., 1968, Control of Mn, Fe, Ni, Cu, and Zn concentration in soils and waters: Significant role of hydrous Mn and Fe oxides. Trace inorganics in water, American Chemical Society Publication 73, pp. 475-488.
- Jensen, R.E., 1972, Climate in North Dakota: Fargo, North Dakota, North Dakota State University, 48 p.
- Kehew, A.E., and Clayton, Lee, 1980, Late Wisconsinan catastrophic floods and the development of the Souris Pembina spillway system, in Teller, J.T., and Clayton, Lee, eds., Glacial Lake Agassiz: Geological Association of Canada Special Paper 26, p. 187-209.
- Krauskopf, K.B., 1979, Introduction to geochemistry (2nd ed.): New York, McGraw-Hill, 617 p.
- Moran, S.R., Harris, K.L., Deal, D.E., and Bluemle, J.P., 1985, Geologic map of Bottineau County, North Dakota, scale 1:127,000, in Bluemle, J.P., Geology of Bottineau County, North Dakota: North Dakota Geological Survey Bulletin 78, Part I (North Dakota State Water Commission County Groundwater Studies 35) Plate 1.
- Mosely, H.R., 1983, Summary and analysis of American Petroleum Institute onshore drilling mud and produced water environmental studies: American Petroleum Institute, 75 p.
- Murphy, E.C., 1983, The effect of oil and gas well drilling on shallow groundwater in western North Dakota: Master's Thesis, University of North Dakota, Grand Forks, North Dakota, 242 p.
- Murphy, E.C., and Kehew, A.E., 1984, The effect of oil and gas well drilling on shallow groundwater in western North Dakota: North Dakota Geological Survey Report of Investigation 82, 156 p.
- Pettyjohn, W.A., and Hutchinson, R.D., 1977, Groundwater resources of Renville and Ward counties, North Dakota: North Dakota Geological Survey Bulletin 55, Part III (North Dakota State Water Commission County Ground-water Studies 11), 41 p.
- Randich, P.G., and Kuzniar, R.L., 1984, Ground-water resources of Bottineau and Rollete counties, North Dakota: North Dakota Geological Survey Bulletin 78, Part III (North Dakota State Water Commission Ground-water Studies 35), 41 p.
- Reed, P.C., Cartwright, Keros, and Osby, Donald, 1981, Electrical resistivity surveys near brine holding ponds in Illinois: Illinois State Geological Survey Geology Notes 95, 30 p.

- Sandoval, F.M., and Power, J.F., 1977, Laboratory methods recommended for chemical analysis of mined-land spoils and overburden in western United States: U.S. Department of Agriculture, Agriculture Handbook No. 525, 31 p.
- Simpson, J.P., 1975, Drilling fluid principles and operations, in Fisher, Farley, project director, Conference on the Environmental Aspects of Chemical Use in Well Drilling, Houston, Texas, May, 1975, Proceedings: U.S. Environmental Protection Agency, EPA-560/1-75-004, p. 61-71.
- Soiltest Inc., 1968, Earth resistivity manual: Evanston, Illinois, Soiltest Inc., 52 p.
- Stevenson, R.J., 1985, Personal communication, Director of the Natural Materials Analytical Laboratory, University of North Dakota, Grand Forks, North Dakota, April, 10.
- Tillotson, Stephen, 1986, Personal communication, Environmental Scientist, North Dakota State Department of Health-Division of Hazardous Waste Management, January 22.
- Zhody, A.R., 1975, Automatic interpretation of Slumberger sounding curves using modified Dar Zarrouk functions: U.S. Geological Survey Bulletin 1313-E, 39 p.
- Zhody, A.R., and Bisdorf, R.J., 1975, Computer program for the forward calculation and automatic inversion of Wenner sounding curves: U.S. Department of Commerce National Technical Information Service publication no. PB-247, 47 p.